Fall 1-31-2003

Study of vapor/gas permeation using thin immobilized liquid membrane

Gordana Obuskovic
New Jersey Institute of Technology

ABSTRACT

STUDY OF VAPOR/GAS PERMEATION USING THIN IMMOBILIZED LIQUID MEMBRANE

by
Gordana Obuskovic

To improve liquid membrane selectivity and stability for removal of vapor and gases from a gas stream, a thin immobilized liquid membrane (ILM) has been studied. Low vapor pressure liquid solvent/solutions were immobilized in part of the micropores of a hydrophilic, hydrophobic or ceramic hollow fiber substrate. To prepare such thin ILMs, three approaches were used: evaporation of the a volatile solvent; acrylic acid-grafted hollow fibers providing a thin hydrophilic layer; pressurization technique.

For removal of volatile organic compound (VOC), a thin ILM of silicone oil incorporated in the micropores of a hydrophobic hollow fiber with a silicone rubber coating yielded a highly VOC-enriched permeate and increased separation factor. The same ILM was stable over an extended period (6 months - 2 years) demonstrating the potential utility of such an ILM-based hollow fiber device for VOC-N_2/air separation. A mathematical model was successfully developed to describe the VOC-N_2 permeation-separation in a hollow fiber permeator having this special type of membrane containing a thin ILM.

Grafting method used for the preparation of a thinner ILM resulted in various hollow fibers having different hydrophilic layer thickness. These fibers were used to study the effect of various glycerol-based and aqueous liquid

membranes immobilized in the thin hydrophilized part of the fiber. Glycerol-based ILMs resulted in low CO_2 permeances in the range of $1*10^{-6}$ $cm^3/cm^2*s*cmHg$ for enclosed atmosphere application; aqueous based ILMs has much better performance.

A pressurization technique was used to prepare a thin ILM in porous hydrophilic and ceramic substrates. It was shown that when appropriate asymmetric hollow fibers substrates were used, increase in CO_2 permeance was achieved.

STUDY OF VAPOR/GAS PERMEATION USING THIN IMMOBILIZED LIQUID MEMBRANE

by

Gordana Obuskovic

A Dissertation
Submitted to the Faculty of
New Jersey Institute of Technology
In Partial Fulfillment of the Requirements for the Degree of
Doctor of Philosophy in Chemical Engineering

Otto H. York
Department of Chemical Engineering

January 2003

STUDY OF VAPOR/GAS PERMEATION USING THIN IMMOBILIZED LIQUID MEMBRANE

Gordana Obuskovic

Dr. Kamalesh K. Sirkar, Dissertation Advisor **Date**
Distinguished Professor of Chemical Engineering, NJIT

Dr. Piero Armenante, Committee Member **Date**
Distinguished Professor of Chemical Engineering, NJIT

Dr. Dana Knox, Committee Member **Date**
Associate Professor of Chemical Engineering, NJIT

Dr. Gordon Lewandowski, Committee Member **Date**
Distinguished Professor of Chemical Engineering, NJIT

Dr. Chao Zhu, Committee Member **Date**
Assistant Professor of Mechanical Engineering, NJIT

BIOGRAPHICAL SKETCH

Author: Gordana Obuskovic

Degree: Doctor of Philosophy

Date: January, 2003

Undergraduate and Graduate Education:

- Doctor of Philosophy in Chemical Engineering,
  New Jersey Institute of Technology, Newark, NJ, 2003
- Master of Science in Chemical Engineering,
  New Jersey Institute of Technology, Newark, NJ, 1996
- Bachelor of Science in Chemical Engineering,
  Belgrade University, Belgrade, Serbia, Yugoslavia, 1992

Major: Chemical Engineering

Publications and Presentations:

Obuskovic G., T.K. Poddar and K.K. Sirkar, Flow swing membrane-absorption permeation, *Ind. Eng. Chem. Res.*, 37 (1998) 212.

Chen H., G. Obuskovic, S. Majumdar and K.K. Sirkar, Immobilized glycerol-based liquid membranes in hollow fibers for selective CO_2 separation from CO_2-N_2 mixtures, *J. Membr. Sci.*, 183 (2001) 75-88.

Obuskovic G., S. Majumdar and K.K. Sirkar, Highly VOC-selective hollow fiber membranes for separation by vapor permeation, *J. Membr. Sci.*, In press.

I dedicate this thesis to
my sister Nina who inspired me to start and finish my Ph.D.
To my nephew and niece, Shon and Nicole
and most of all to my parents.

ACKNOWLEDGMENT

I would like to express my deepest appreciation to Dr. Kamalesh Sirkar, for his support, guidance, giving valuable suggestions and comments throughout this research. Special thanks to Dr. Piero Armenante, Dr. Dana Knox, Dr. Gordon Lewandowski and Dr. Chao Zhu for participating as members of my committee.

I would like to thank Dr. Majumdar not only for his friendship but also for giving his expertise regarding the experimental and mathematical modeling part of this work. Thanks to Dr. Kovvali for his friendship and criticism. I truly enjoyed and I am still missing his "caustic tongue". Thanks are due to all members of the Membrane Separation and Biotechnology group for their friendship and help whenever was needed.

Special thanks to my sister Nina, who gave me not only moral but also the financial support throughout my graduate studies. Also, to my brother-in-law Joey, for his endless help whenever needed. Thanks to my Chuchi, for his patience, belief and love he had for me.

Also to my parents for their support, understanding and encouragement. Tanks to the rest of my family and anyone else who helped and participated in any way during my Ph.D. studies.

TABLE OF CONTENTS

TABLE OF CONTENTS
(Continued)

Chapter **Page**

TABLE OF CONTENTS
(Continued)

Chapter **Page**

TABLE OF CONTENTS
(Continued)

Chapter **Page**

TABLE OF CONTENTS
(Continued)

LIST OF TABLES

LIST OF TABLES
(Continued)

Table **Page**

LIST OF TABLES
(Continued)

Table **Page**

LIST OF FIGURES

LIST OF FIGURES
(Continued)

Figure **Page**

LIST OF FIGURES
(Continued)

Figure **Page**

CHAPTER 1

INTRODUCTION

Volatile organic compounds (VOCs) are quite harmful to the environment and they can be toxic at the same time. It is well known that VOCs have important roles in the tropospheric chemistry of ozone and aerosols and the creation of smog. On the other hand, greenhouse gases, notably carbon dioxide (CO_2), have been linked to global warming. Carbon dioxide emission has been increasing remarkably, mostly because of the combustion of fossil fuels such as coal, petroleum and natural gas. Therefore, the environmental protection agency (EPA) has made more stringent emission standards for major VOCs; CO_2 emissions control is also being considered. Hence, many applications need innovative, reliable and cost effective technologies that can fulfill such requirements. Also, removal of CO_2 from the enclosed atmospheres has an important function in a life support system, not only for space applications (e.g. extravehicular activities, space suit application) but also for earth applications in enclosed spaces (e.g. submarines, control rooms).

Membranes appear as an attractive alternative solution to conventional separation processes. They are drawing more and more attention, their market is growing rapidly and their application has expanded to a variety of industries as new membrane materials are produced. Gas separation membranes have emerged as a viable alternative to commercial gas separation technologies (e.g. absorption, adsorption, condensation, distillation etc).

Like any other chemical engineering process, they have their advantages and disadvantages. Membrane devices are modular in nature and a large membrane area can be packed in a small volume. Therefore, they have a smaller footprint than conventional processes. An added advantage is the simplicity of the system and the absence of the moving parts. Still, membranes are sometimes expensive, can be easily fouled and stability can be a problem.

Membranes are thin films which separate the feed gas stream into a permeate stream and a retentate stream. The quality of the separation is determined by the selectivity. A common definition for membrane selectivity is called the separation factor α_{ij} between species i and j and it is given by

$$\alpha_{ij} = \frac{c_i'' / c_j''}{c_i' / c_j'} \tag{1.1}$$

where the single prime and the double prime denote the retentate and the permeate phases respectively (Ho and Sirkar, 1992). Usually the achieved selectivities of the membranes are insufficient to achieve the desired purities. Consequently, there is constant need for membranes that can give higher selectivities without drastic flux reduction. Since the species flux is affected by the membrane thickness, a very thin membrane will result in a significant increase in the transport of the preferentially permeating component across the membrane.

The usefulness of a given membrane system is also very much dependent on the membrane stability. For instance, the instability of a liquid membrane is due to evaporation of the solvent/solution. Therefore, less volatile solvents are needed to overcome the instability problem. On the other hand, some chemicals

can have a very harmful effect and can permanently damage the polymeric membrane materials.

Gas separation membranes are based on solution-diffusion mechanism. The penetrant first dissolves in the polymer surface and then, diffuses through the polymer material. Therefore, membrane permeability of a species is defined as a product of the species solubility and diffusivity in the membrane. Highly selective and permeable gas separation membranes are needed in order for the membrane to be commercialized. One way of improving the membrane selectivity is to incorporate certain solvents that might contain a reactive species in addition, in which a species of interest preferentially dissolves or reacts with the reactive species, the carrier. If the transport mechanism in addition to solution-diffusion includes the reversible reaction with the species of interest, it is called the facilitated transport mechanism and such a membrane is called a facilitated transport membrane (FTM).

This study will focus on existing membrane materials and possible modifications of the same in order to improve the membrane selectivity and stability for environmental and/or specific gas separation applications. In particular, removal of VOCs and CO_2 from nitrogen or air streams based on thin immobilized liquid membranes and the effect of the incorporated thin layer of solvent/solution into the porous polymeric or ceramic matrix on VOC/CO_2 separations are investigated.

Most commonly used membranes for the VOC separation are composite membranes, e.g., membrane which has a thin layer of silicone rubber

superimposed onto the porous polymeric support. In order to enhance the VOC separation using a composite membrane, a thin layer of a solvent, such as silicone oil, which has a high solubility for the VOCs and virtually no solubility for N_2 or air is incorporated in a porous polymeric support. In this way, N_2 flux will be drastically reduced compared to the VOC flux across a thin composite membrane enhancing the membrane selectivity. Furthermore, due to the extremely low vapor pressure of silicone oil, liquid membrane stability is improved as well. Solvent evaporation technique will be used for the preparation of such a thin ILM.

Carbon dioxide separation membranes are an environmentally friendly alternative to traditional amine treatment processes. This study will focus on facilitated transport membranes for specific applications where a highly selective and stable CO_2 liquid membrane is needed. When low volatility solvent and/or carriers are used, membrane stability is drastically improved (Chen et al, 1999, 2000, 2001). An added advantage will be the reduced thickness of the ILM for further CO_2 flux enhancement. A novel approach to reduce the immobilized liquid membrane (ILM) thickness (Kovvali, 2000) will be explored on different hollow fiber membrane substrates using a low volatility solvent/solution in the form of an ILM.

1.1 Preparation of a Thin ILM

In order to obtain the desirable fluxes of the reacting and non-reacting species for various applications, thin ILMs were prepared instead of fully immobilized liquid membrane. Various approaches of thin liquid membrane formation will be

mentioned here. Figure 1.1 illustrates the basic concepts of thin liquid membrane formation used in this study:

- partial evaporation of mixed or pure solvents
- plasma graft method
- pressurization technique.

The partial evaporation technique was used to prepare the thin silicone-based liquid membrane in a hollow fiber having a thin layer of silicone rubber plasma polymerized on the outer surface of the fiber. This thin ILM was used to study the removal of VOCs from the nitrogen streams. The ILM thickness was reduced by evaporation of hexane from the hexane-silicone oil mixture incorporated in the porous structure of the hollow fiber. This thinner ILM gave an increased selectivity by drastically reducing the nitrogen flux and marginally reducing the VOC flux. The substrate was microporous polypropylene hollow fiber. This fiber has a thin layer of plasmapolymerized silicone rubber placed on the outside diameter (OD) of the fiber. The partial evaporation approach and the technique of thin ILM preparation is considered in Chapter 2. This silicone oil-based ILM was also tested for stability and water vapor permeation. In addition, a mathematical model was developed to predict the hollow fiber permeator behavior for VOC removal containing the thin ILM in the pores (Chapter 2 and Appendix F).

For carbon dioxide removal two different approaches were used to create thin glycerol-based or glycerol carbonate-based liquid membranes:

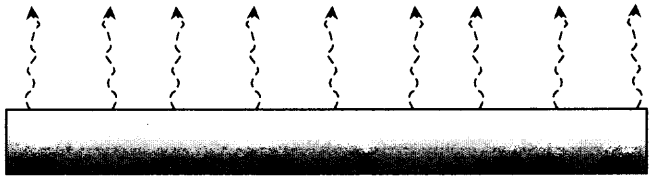

a) Partial evaporation method for pure or mixed solvent.

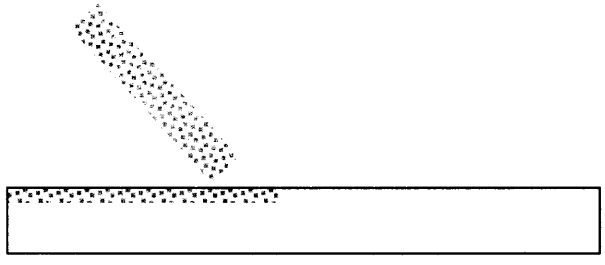

b) Plasma graft method for hydrophobic membrane with hydrophilic monomer.

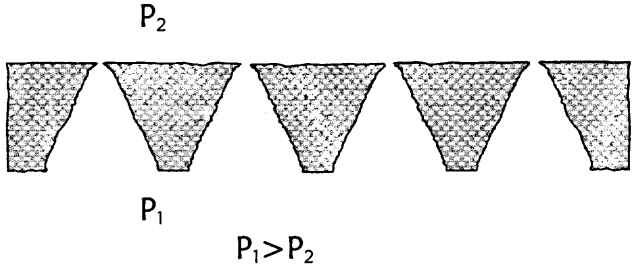

c) Pressurization technique for expulsion of the liquid from the pores of an asymmetric membrane.

Figure 1.1 Different methods for preparation of the thin ILMs.

- plasma grafted hollow fiber membrane having glycerol-Na-glycinate based ILM immobilized in a thin hydrophilic (e.g. acrylic acid grafted) part
- pressurization technique for the expulsion of the liquid from the pores of an asymmetric hollow fiber membrane using glycerol-Na- glycinate and glycerol carbonate based ILMs.

Preparation of the thin glycerol-Na-glycinate based ILMs in a grafted hollow fibers is described in the first part of Chapter 3. A thin hydrophilic film is crated by the plasma graft technique and it is placed on the O.D. of the fiber. Grafted layer thicknesses varied based on the grafting conditions. The thickness of the ILM is expected to be the same as the thickness of the grafted layer, which is much smaller than if the ILM were formed throughout the substrate, the full ILM. By changing the grafting conditions, six different batches of fibers having various thickness of the AA grafting were formed (Appendix E).

The second part of Chapter 3 describes the preparation of the thinner ILMs by the pressurization technique in asymmetric hollow fibers. Two types of asymmetric structures were used:

- polymeric asymmetric hollow fiber having an integrated skin on the inner surface diameter (I.D.)
- ceramic tube having a skin layer placed on the inner diameter.

By gradually increasing the pressure across the membrane, more and more solvent or solution is displaced form the pore resulting in a thinner ILM. If sufficiently high transmembrane pressure is applied, an ILM with the thickness equal to thickness of the skin of the asymmetric hollow fiber is likely to be produced.

The organization of this thesis will be as follows. Chapter 2 will focus on VOC separation using the thin ILM prepared by solvent evaporation technique. Chapter 3 deals with CO_2 separation using thin and stable ILMs prepared using AA-grafted hollow fibers, asymmetric and ceramic membranes. The literature review, experimental details, results and discussion sections and conclusions on VOC and CO_2 separations are provided in each chapter accordingly. The experimental sections summarize the preparation of thin ILMs using various techniques along with the equipment and procedure for experimental measurements. To predict the VOC outlet concentrations a mathematical model is developed. Derivation of the mathematical equations along with the determination of the parameters is provided in Chapter 2. Finally, conclusions and recommendations for future investigation are provided in Chapter 4.

CHAPTER 2

VOC REMOVAL FROM A GASEOUS STREAM WITH OR WITHOUT AN IMMOBILIZED LIQUID MEMBRANE IN STEADY STATE OR CYCLIC MODE OF OPERATION

2.1 Introduction

Separation processes are essential to a variety of industries for purification of raw materials, recovery and purification of the products or removal of contaminants from their gaseous or liquid waste streams. The control of volatile organic compounds (VOCs) in waste gas streams from manufacturing industries is becoming very important due to environmental concerns. Volatile organic compounds are carbon-based substances, with certain properties, such as the tendency to react with nitrogen oxides in the presence of sunlight to create ozone as the primary component of the smog. This can occur after the VOC evaporates into the ambient atmosphere. More stringent emission standards for specific emission sources (e.g. combustion plant, pharmaceutical and chemical industries, dry cleaning etc.) require best available techniques to be used to reduce or eliminate discharges and to keep emissions down. The complexity of the task has allowed the progress to take place at a slow pace. Removal of VOCs from gaseous industrial and waste streams is necessary either to meet these stringent emission standards or to recover and/or reuse valuable organics.

Volatile organic compound emission control techniques are basically classified into two groups: (1) process and equipment modifications to control VOC emission; (2) add-on control techniques for recovery and/or destruction of VOCs. Vapor emission control is generally achieved by carbon adsorption, absorption, condensation and incineration. Selection criteria depend on nature and concentration of the organic pollutant in the gas stream to be removed, flow rate of the stream, need for recovery of the contaminants, specific site characteristics and the value of the organic pollutant.

Adsorption processes are used in situations where high purification of a gas mixture is needed. Carbon adsorption is suitable when dealing with dilute mixtures of VOCs in air (5000 ppmv or less) (Simmons et al., 1994), gases with humidity less than 50% and gas flow rates ranging from medium to high. Regeneration of the adsorbed material from the carbon is guided by economics. The energy demand for adsorption process is high and there is a risk of self-ignition because the adsorption process is exothermic.

Absorption is suitable for high to medium gas flow rates and pollutant concentrations. This system is also bulky and flooding and loading can be a problem due to changes in gas flow rates. Condensation is a process with very high energy demand because oversaturation of the VOCs is achieved by chilling of the large volume of the waste gas stream. Usually this process requires concentrations above 5% and low to medium flow rates. The amount of VOC that can be recovered from the waste stream depends on the inlet VOC

concentration, the boiling point of the VOC and the temperature and pressure of the waste stream.

Incineration is also used as one of VOC emission control techniques; it can treat wide ranges of concentrations and gas flow rates but VOCs cannot be recovered. This process is rather expensive and it can produce more toxic air emissions and not easily disposable wastes.

Most of the existing techniques for VOCs-emission control and recovery have proved to be unsatisfactory in terms of safety, performance, operating costs and facility space. A review of the available options to control VOC emission (destruction based and recovery based) with their advantages and limitations is given in Khan and Ghoshal (2000).

Therefore, it would be useful if a membrane device could be economically used to purify the feed gas mixture to the same extent achieved using commercialized processes. None of the membrane separation processes on its own can alter or break down the pollutants, but they have the ability to separate, fractionate and concentrate contaminants. In some cases membrane processes combined with traditional separation techniques allows the reduction of VOC emissions to satisfy most rigorous emissions standards. In the last ten years, membrane technology is becoming a viable VOC pollution abatement technique due to improved quality of synthetic membrane materials, simplicity of the process and compactness of the devices; further membrane capital costs are generally lower. However, membrane separation processes operated

conventionally in a steady-state fashion are known to be efficient for bulk gas separation only (Beaver et al., 1988).

Polymeric membranes used for recovery and removal of organic solvents from the gaseous streams have to be chemically and mechanically stable and their selectivity and permeability will determine the efficiency of the gas separation process. Based on the flux and selectivity, membranes can be classified broadly into four classes: (1) porous, (2) nonporous, (3) asymmetric and (4) composite.

Porous membranes separate gases based on the relative sizes of the molecules and exhibit high fluxes but low selectivity. Different mechanisms are involved in the transport of gases across porous membrane e.g. convective flow, Knudsen diffusion. Which mechanism is going to take place depends on the ratio of the pore radius, r, to the mean free path, λ, of the molecules.

Transport through a nonporous membrane is governed by the solution-diffusion mechanism achieving high selectivities but low fluxes. Solution-diffusion mechanism depends on both solubility and diffusion of the components through the membrane material. The permeability, P_i, of a species "i" can be expressed as the product of the diffusion coefficient, D_i, and the solubility coefficient, S_i. The diffusion coefficient reflects the capability of the molecules to pass through the membrane material and the solubility coefficient relates to the ability of a solute to dissolve into the membrane material. In polymeric materials, diffusivity decreases as the molecular size increases since larger molecules interact much more with the polymer chains than smaller molecules do; solubility increases as the condensability of the solute increases. Therefore, the selectivity, α_{ij}, of the

membrane material depends on the balance between these two coefficients for any pair (i,j) of gases.

A membrane will separate the components based on their relative permeation rates through the membrane material. In glassy polymers (e.g. polysulfone or polyimide) diffusion coefficient is most important. On the other hand for rubbery membranes e.g. polydimethylsiloxane (PDMS), the solubility coefficient is most important.

Glassy polymers are usually prepared as asymmetric (skinned) membranes by solution precipitation procedure developed by Loeb and Sourirajan (1964). These membranes are composed of two distinctive regions made of the same material, a thin dense semipermeable skin, and a much less dense non-selective layer. Separation is accomplished in the thin dense skin whereas the less dense layer provides a mechanical and physical support to the skin. A limited number of polymers that can be used to make anisotropic membranes with useful gas fluxes and selectivities are known. Surface modifications are sometimes employed to increase the gas separation capabilities. These methods include UV treatment, plasma treatment, plasmapolymerization, fluorination and fluorooxidation.

Silicone rubber membranes have been found to have the unusual ability to separate certain gases from mixtures as it is described in Kammermeyer's patent (1960). As mentioned earlier, rubbery membranes also have a high solubility for organic compounds and therefore, they are more desirable for VOC removal from gas streams. The amount of gas that can permeate through a membrane of a given area is inversely dependent upon the membrane thickness in addition to being

directly proportional to the gas partial pressure drop across the membrane (e.g. driving force); therefore, Robb (1967) tried to prepare ultrathin defect-free organosiloxane films. Since a rubbery material made in the form of an asymmetric membrane would collapse under high pressures used in gas separations, silicone membranes are fabricated as a composite membrane where a thin selective layer of silicone rubber is placed on a strong microporous support by a variety of techniques including plasma polymerization.

Another approach to develop gas separation membrane involves preparing a composite membrane having a superimposed membrane supported on an anisotropic porous support wherein the superimposed membrane provides the desirable separation. These porous supports provide low resistance to gas passage and yet have a pore size small enough to prevent the rupture of the superimposed membrane. Many studies have been done with dense membranes superimposed on a microporous support (Klass and Landahl, 1971; Yasuda, 1973). On the other hand, Henis and Tripodi (1980) prepared a composite membrane using different porous supports (e.g. polysulfone, polyetherimide, polyimide, polypropylene etc.), where separation properties were essentially determined by the properties of the dense region of the microporous layer as opposed to the membrane coating material which penetrates the micropores (Henis and Tripodi, 1981).

Based on previous experiences with multicomponent or composite membranes, a commercialized VOC separation membrane has been developed Henis and Tripodi, 1981); it has a thin nonporous skin on the porous substrate. If

the membrane is in a form of a hollow fiber, this nonporous thin silicone coating is placed on the outer side of a porous polymeric support.

One of the techniques which is recognized as a unique method of preparing uniform, ultrathin (~1 μm), defect-free silicone containing polymeric films is plasma polymerization technique. Generally thin film composite membranes of PDMS exhibit high selectivity for VOC/N_2 separation. Plasma-based polymers can be made from different types organosilicon monomers like: diethoxydimethylsilane (DEDMS), hexamethyldisiloxane (HMDS), octamethyltrisiloxane (OMTS) or poly(dimethylsiloxane) (PDMS) (Yamamoto et al. 1983). Most of the membrane-based VOC researches have used PDMS membranes (Cha et al., 1997; Bhaumik et al., 2000; Gales et al., 2002). A disadvantage of these composite membranes is that it is hard to produce ultra-thin, defect-free PDMS films since the material is very sticky. Also, certain organic solvents, when present in high concentration in the feed gas, may cause the silicone rubber to swell giving higher nitrogen flux through the coating. This may result in lower selectivity and less concentrated permeate side composition. Recently, an attempt was made to overcome the problem of PDMS composite membranes by preparing hexamethyldisiloxane (HMDS) composite membrane by plasma polymerization technique (Sohn et al., 2000). Although they were successful in preparing very stable and more resistant films to many different solvents, the selectivities of new HMDS plasma polymerized films were lower than the PDMS membranes for the same pair of gases.

Most VOC separation studies were carried out using a composite silicone rubber PDMS coated membrane on different porous polymeric supports, e.g., PDMS/polysulfone (Kimmerle et al., 1988; Paul et al., 1988), PDMS/polyetherimide (Fouda et al. 1993; Leeman et al., 1996; Gales et al., 2002), PDMS/polypropylene (Cha et al., 1997; Bhaumik et al., 2000; Poddar et al., 1996b). Separation takes place in the thin permselective layer by the solution-diffusion mechanism; the porous support provides mechanical strength and should not offer considerable transport resistance. PDMS membranes have not only high permeability coefficients for vapors but also high selectivity for VOCs over air/N_2. Evaluated selectivities for composite PDMS membranes with microporous polypropylene hollow fiber substrate were in the range of 15-60 for certain VOCs (like methanol or toluene) for relatively low inlet feed gas composition and moderate flow rates (Cha et al., 1997).

There are many potential membrane applications to fulfill specific industrial needs where conventional methods can not meet the standards. For instance, very good separation of gases is required in petrochemical and refinery operations. It is not sufficient to recover 90-95% of the organic, but the vapor must be recovered as a pure product with less than 5-10% or less of other component.

There are many applications where membranes selectively remove water vapor from the VOC-laden gas streams either for dehydration of air or natural gas, to control humidity or to recover moisture for drinking purposes. For the purpose of water recovery, it was demonstrated that Cuprophan membrane made

of regenerated cellulose could efficiently remove water vapor while blocking air and VOCs (Cha et al., 1996). There are some applications where VOCs should be preferentially removed over water vapors due to various needs. For instance, if VOCs are condensed for recovery purposes, presence of water in a condenser is undesirable due to development of ice, which can block the device.

Another example is in the paper industry where methanol is an unwanted byproduct of Kraft pulping and is released in low concentrations along with water vapor. Commercially used PDMS membranes will not be very efficient in this case, since thin PDMS coating is highly water permeable (Watson and Baron, 1996) and therefore, methanol/water selectivity of such a material will be low. Therefore, a new process was developed in which methanol was selectively removed from the feed stream with minimal transport of water using water vapor as a purge stream (Klug et al., 2001).

The ability to increase membrane selectivity, produce more concentrated permeate side stream and develop a system that can deal with water vapor if present in a feed gas stream will be an added advantage. One possibility is to incorporate an appropriate solvent in the porous membrane substrate, which will act as an immobilized liquid membrane (ILM) having a high solubility for VOCs, virtually no solubility for N_2 and a low vapor pressure and very low solubility for water vapor. Therefore, highly VOC-selective essentially nonvolatile solvents, e.g., silicone oil or Paratherm® oil, are solvents of choice since they have all the desired properties mentioned above.

When silicone oil is immobilized in part of the pore thickness (thin ILM), the membrane selectivity for VOC removal is likely to be enhanced by a substantial reduction of the N_2 flux and only a marginal reduction in the VOC flux thereby yielding a more concentrated permeate side composition. Pressure difference between the feed and the vacuum sides create the partial pressure driving force needed for the removal of the VOCs. In this case, the ILM functions as a supplementary selective membrane in addition to the silicone coating on the outer side of the hollow fiber which also prevents liquid membrane expulsion. Water practically has no solubility in these oils, thus they can be utilized for water vapor/VOC separation as well. Suitable applications of silicone oil and Paratherm® oil for VOC removal have already been demonstrated in membrane-based regenerative absorption process (Poddar, 1995; Poddar et al., 1996a; Poddar et al., 1996b; Xia et al., 1999; Majumdar et al., 2001). Such a process requires two membrane devices, one for stripping and the other for the absorption of VOCs.

An attempt was made to apply hollow fiber contained liquid membrane (HFCLM) configuration (Majumdar et al., 1988) to VOC separation. A hollow fiber membrane module for VOC removal was prepared with two sets of fibers (Obuskovic et al., 1998) where one set of fibers is used for absorption and another set for the desorption process with the silicone oil in between these two fiber sets. This contained liquid membrane (CLM) configuration combined with two sets of fibers provides an opportunity for both processes (absorption/desorption) to take

place in a single membrane device. Needless to say that pumping of the viscous absorbent liquid through the system is eliminated in this configuration. The idea of incorporating a liquid membrane in the pore structure of the membrane substrate will substantially decrease the liquid membrane thickness, enhance the VOC selectivity by reducing N_2 flux substantially and VOC flux marginally, simplify the membrane device and make the desorption process easier.

In addition, cyclic membrane processes of different types have been studied previously for a variety of applications in order to improve gas purification. Existing cyclically-operated membrane-based separation processes are operated either by cyclic pulsing of the gas pressure on the upstream side of the membrane (Paul, 1971) or by cyclically introducing a feed gas flow into microporous hollow fiber membranes having adsorbent particles (Gilleskie et al., 1995) or an aqueous absorbent liquid (Bhaumik et al., 1996) on the shell side. The adsorbent particle or the absorbent liquid adsorbs/absorbs specific species from the feed gas mixture. Regeneration of the adsorbent/absorbent media is achieved by a variety of demanding multistep procedures borrowed from pressure swing adsorption (PSA) processes.

Since a membrane for selective removal of organic vapors from the air acts as an absorbent for species which is preferentially removed (e.g. VOCs), incorporating the operational principle of (PSA) processes into a membrane device can possibly produce two highly purified streams. Therefore, a cyclic process will be applied to the hollow fiber permeators which are constructed somewhat like a shell-and-tube heat exchanger. The principle of this cyclic membrane process is as

follows: a VOC-containing gas stream is cyclically introduced into the bores of the hollow fibers while vacuum is constantly maintained on the shell side of the module to insure a continuous driving force for the VOC removal and regeneration of the membrane. Since only feed gas flow is cyclically introduced, this process will be named Flow Swing Membrane Permeation (FSMP) process.

In this process, the feed gas mixture is cyclically introduced into the feed channel inlet of the membrane module, while, on the permeate side, conditions were maintained for the permeation of the feed gas species (e.g. VOCs) from the feed side to the permeate side by applying a vacuum. For a short period of time, say 10 or 20 seconds, which is called the absorption or adsorption time t_{abs}, the feed gas flows through the feed gas channel (e.g. bore of the hollow fiber). Figure 2.1 illustrates the principle of FSMP process where a VOC present is removed by selective permeation through the silicone coated fiber from the nitrogen feed gas stream.

During the short period of time, the front end of the feed gas is highly purified since the membrane acts as the absorber for the VOC species. During that time, permeate side is maintained under vacuum so that the VOC species is passed over to the permeate side. After the absorption part of the cycle is over, the feed flow into the feed channel is stopped for a short period of time (e.g. 10 or 20 seconds) which is called the regeneration time, t_{reg}. During the regeneration time, the membrane feed channel end is closed and no retentate stream is withdrawn. However, the VOC present in the remaining feed gas in the feed channel will be preferentially removed by permeation through the membrane. The gas remaining

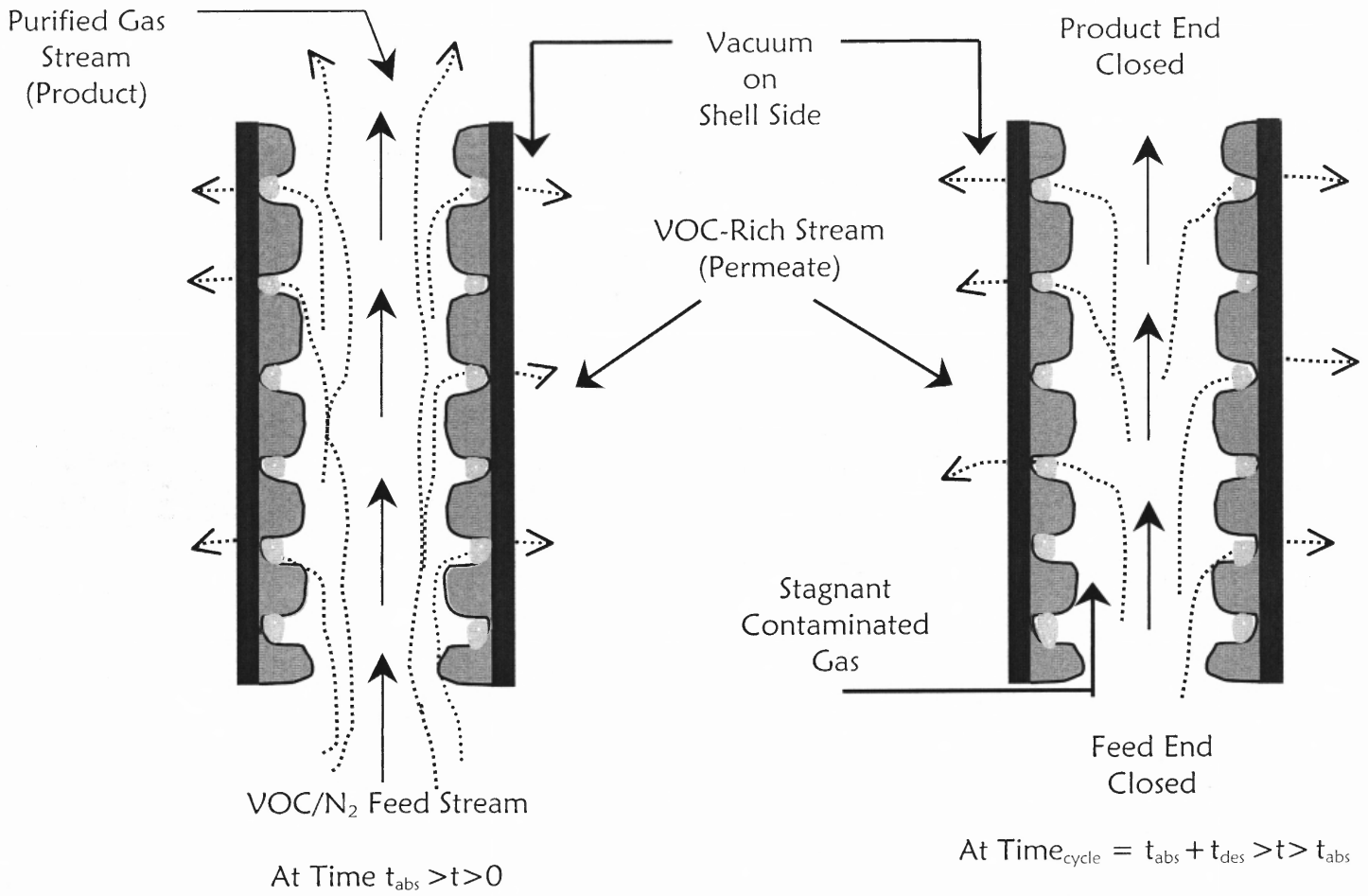

Figure 2.1 Principle of FSMP process.

in the feed channel will be highly purified in nitrogen or air. The pressure on the feed side will be marginally reduced from the feed gas pressure due to selective permeation. When the feed gas is reintroduced into the membrane feed channel after the regeneration time is over, the gas that is pushed out first as the retentate stream at the exit is highly purified in nitrogen, and the absorption part of the new cycle starts again.

To obtain a steady output, two membrane device in parallel are used, where absorption and regeneration of the feed gas mixture and retentate is alternatively taking place between these two modules. The sum of the absorption time and the regeneration time for each membrane device should equal the cycle time T_{cycle} ($= t_{abs} + t_{reg}$) of the process.

This process will assure that the membrane does not get saturated and it will prevent breakthrough of the VOC into the product end. Unlike the pressure swing adsorption process, this system will operate at nearly constant pressures on both sides. If the membrane is highly selective, the permeate stream can be highly purified too. Such a system can replace activated carbon beds effectively for gas purification. The distinct advantages of this cyclic membrane process will be:

1. no drastic changes of pressure on either side of the membrane (unlike PSA processes);
2. simplified regeneration of the absorbent and/or membrane.

To improve the membrane selectivity for VOCs and achieve better purification, two strategies are pursued here:

1. immobilize a non-volatile solvent in part of the thickness or the full thickness of the membrane pores;
2. cyclic mode of operation.

In this study, the use of hollow fiber membrane modules with or without an appropriate immobilized liquid membrane (ILM) in steady state, as well as in cyclic mode of operation, is studied for effective removal of volatile organic compounds (VOCs) from gas streams possibly containing water vapor.

2.2 Experimental

2.2.1 Types of Experiments

1. For the determination of the thin ILM thickness and the nitrogen permeance across the thin ILM, Modules 1 and 2 were used where the tube side was pressurized with pure nitrogen and the permeation flow rate was measured on the shell side with one end closed.
2. For the determination of the VOC permeance across the thin ILM, Module 2 was used to measure the extent of removal of each of the VOCs, e.g. toluene, methanol and acetone, individually. Feed VOC/N_2 mixture was passed through the tube side while a vacuum was applied on the shell side.

3. The extent of removal of each of VOCs, e.g. toluene, methanol and acetone, was studied individually with various feed flow rates using Module 1 with or without a thin ILM incorporated in the porous structure; feed VOC concentration was varied in different experiments. The feed gas containing a VOC was introduced through the tube side of the hollow fiber membrane module.

4. For determination of water vapor permeance, Module 2 was used with a full ILM. The extent of removal of methanol from the feed gas stream containing water vapor using Module 2 with a full ILM incorporated in the porous structure was studied; feed inlet methanol concentration was 292 ppmv and the humidity level was varied in different experiments.

5. The extent of the removal of a VOC was studied in FSMP with different concentrations, feed flow rates and cycle times. The experiments were carried out using Module 1 having a thin ILM incorporated in the porous structure. Feed gas stream was cyclically introduced into the bore of the hollow fiber module.

6. The extent of the removal of VOCs was studied in FSMP with different concentrations, feed flow rates and cycle times. The experiments were carried out using two identical modules where the feed gas stream was alternately introduced into the bore of one of the hollow fiber modules.

2.2.2 Chemicals, Gases, Membranes and Modules

Different volatile organic compounds (VOCs) (e.g. methanol, acetone and toluene) were used to study the basic performance of the hollow fiber membrane module. Initial experiments were done using the bare membrane without any ILM, followed by experiments where a highly VOC-selective essentially nonvolatile solvent, e.g., Silicone oil (Kramer Chemicals, Inc., Paterson, NJ) was immobilized in part of the pore thickness creating a thin immobilized liquid membrane (ILM). Some properties of the Silicone oil are given in Table 2.1. These experiments were carried out to develop a better understanding of the effect and benefit of the thin ILM for removal and recovery of the VOCs. Also a set of experiments were done with another membrane module containing uncoated microporous polypropylene hollow fibers using the same VOC gas mixtures and pure nitrogen in order to estimate the VOC permeances and the thin ILM thickness.

The VOC/N_2 gas mixture and pure gases used in this study are listed below (Matheson, E. Rutherford, NJ:

1. Certified gas mixture containing a VOC/nitrogen balance:

   Acetone 11, 000 ppmv; Methanol 10, 000 ppmv; Methanol 9, 200 ppmv; Methanol 292 ppmv; Toluene 1, 953 ppmv; Toluene 215 ppmv.

2. Pure gases:

   nitrogen zero, helium zero, hydrogen zero, air zero.

Module 1 used for these experiments, had one set of 300 microporous hydrophobic polypropylene hollow fibers having a thin nonporous

Table 2.1 Properties of Silicone Oil Used for the Preparation of ILM

Properties*	**Silicone Oil**
Molecular Weight	3,200 (avg)
Density	0.98@77°F
Viscosity	50cs@77°F
Vapor Pressure	< 5mmHg@77°F
Flash Point	605°F
Solubility in Water	Insoluble (< 0.1%)
Appearance	Colorless, clear liquid
Other Properties	nontoxic

- Dow Corning product information sheet for Fluid 200® 50 cSt.

plasmapolymerized silicone coating on the outside surface of the hollow fibers (Celgard® X-10, ID/OD: 240μm/290μm). Module 1 was obtained from Applied Membrane Technology, Inc., (AMT, Minnetonka, MN). Detailed characteristics of the module are given in Table 2.2. This module was used and studied for the separation of organic vapors from dry air streams with or without the ILM configuration. In the case where an ILM configuration was studied, the microporous support was impregnated with the suitable nonvolatile liquid absorbent (e.g. Silicone oil) in order to increase the membrane selectivity for VOC removal.

Module 2 was prepared in the laboratory from the same type of the Celgard® fibers as in Module 1. This module has 120 microporous hydrophobic polypropylene hollow without a silicone coating (Celgard® X-10, ID/OD: 240 μm/290 μm). The fibers were obtained from Hoechst Celanese (Charlotte, NC). Characteristics of the Module 2 are given in Table 2.2. This module was used to determine VOC and nitrogen permeances through the ILM and thereby the thin ILM thickness needed to simulate membrane performance in Module 1 via the mathematical model.

Module 2 was also used to determine the water vapor permeance through the fully immobilized liquid membrane. The same module was used to study the extent of methanol removal from a humid nitrogen stream with full ILM configuration.

Table 2.2 Geometrical Characteristics of Different Hollow Fiber Modules Used

Module No.	Type of fiber	Fiber ID (cm)	Fiber OD (cm)	Effective length (cm)	No. of fibers	Mass transfer area (cm^2)*
1	Celgard X-10*** with a silicone skin	0.024	0.029	20.5	300	510.0
2	Celgard X-10** without silicone skin	0.024	0.029	18.5	120	191.0
3	Celgard X-10*** with a silicone skin	0.024	0.029	20.0	150	273.0
4	Celgard X-10*** with a silicone skin	0.024	0.029	20.0	150	273.0
5	Celgard X-10*** with a silicone skin	0.024	0.029	21.0	150	287.0

* Calculation based on outer diameter of the fiber
** Hoechst Celanese, Charlotte, NC
*** AMT Inc., Minnetonka, MN

2.2.3 Experimental Setup for the Separation of VOCs from VOC/N_2 Mixtures in the Steady State Mode of Operation with or without an ILM

The experimental setup used to study the removal of VOCs from VOC/N_2 mixtures using PDMS coated hollow fiber membrane module in steady state mode of operation with or without the ILM configuration is shown in Figure 2.2. The same setup was also used when VOC permeances through the thin ILM were determined. For all cases, different feed gas mixtures were passed through the tube side of the membrane module while vacuum was constantly applied on the shell side to create the driving force for VOC removal. The inlet VOC concentration in the feed gas mixture was varied from very low to very high.

Different concentrations of VOCs in VOC/N_2 mixtures were achieved either by directly purchasing a gas cylinder containing a mixture of the desired concentration from Matheson Gas Products (Matheson, E. Rutherford, NJ), or by mixing pure nitrogen with such a VOC/nitrogen mixture to decrease the VOC concentration or by bubbling nitrogen through the liquid VOC to produce very high VOC concentrations. The flow rate of each gas stream was controlled by an electronic mass control flow meter (Matheson, E. Rutherford, NJ). The purified feed gas exiting the membrane module was sent to a gas chromatograph (GC) (HP 5890 series II, Hewlett-Packard, Paramus, NJ) for analysis. The same connection existed for the permeate side analyses in the case where an oil-less vacuum pump (KNF Neuberger Inc., Trenton, NJ) was used. In this case the composition of the permeate side was determined by direct GC analysis. If an oil-lubricated vacuum pump (HyVac® Products, Inc., Norristown, PA) was used, the

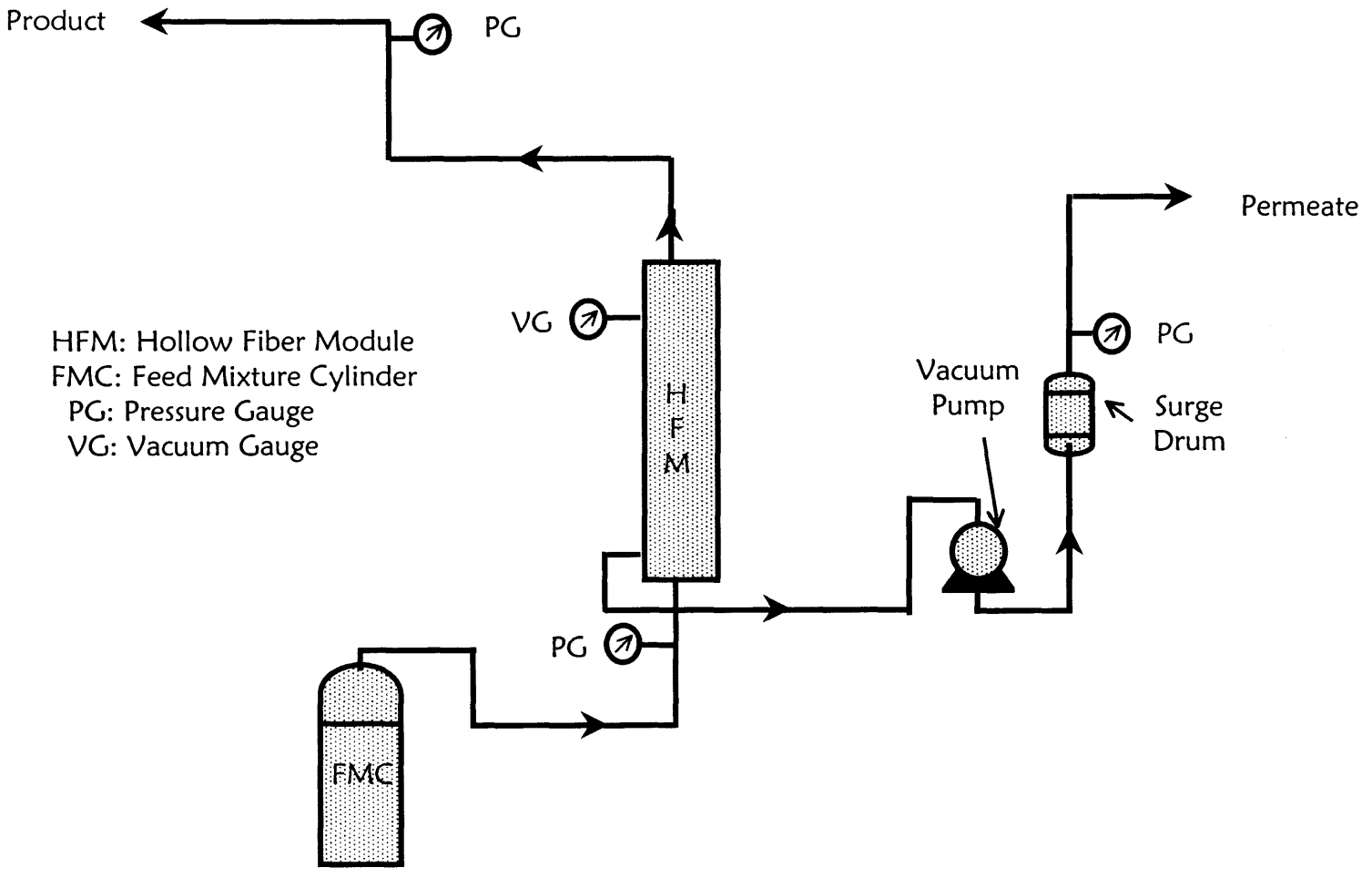

Figure 2.2 Experimental setup for VOC removal with or without ILM in steady state mode of operation.

permeate side composition was calculated based on material balance since it was suspected that the lubricant could absorb some VOCs from the permeate stream and direct GC analysis would not be very accurate.. The GC (HP 5890 series II), had a flame ionization detector (FID) for VOC analysis. The GC conditions used are listed below:

- HP column Hayesep Q (10/100 mesh): l=6 ft
- HP Molecular Sieve 13X (60/80 mesh): l=6 ft
- carrier gas: helium (He)
- columns temperature: 70 °C
- injector temperature: 200 °C
- detector temperature: 200 °C

Some experiments were done to study selective removal of VOCs from humid nitrogen streams. To humidify the incoming VOC-containing gas stream, pure nitrogen was passed through a bubbler filled with pure water. This humidified nitrogen stream was then blended with a dry VOC-N_2 mixture prior to contacting the membrane. In order to determine if any water was permeating through the membrane, two humidity probes (model MP 32 UT, Vaisala, Woburn, MA) were used to measure the humidity levels at the inlet and at the outlet of the membrane module. The humidity and temperature indicator (model HMI 32, Vaisala, Woburn, MA) was used to monitor the temperature and humidity level of the gas streams. Inlet and outlet VOC concentrations of a gas mixture were determined by GC (HP 5890 series II, Hewlett-Packard, Paramus,

NJ) analysis. The setup using a humidified feed gas mixture is shown in Figure 2.3. All connecting lines used for this experiment were 1/8-inch soft copper tubing (McMaster Carr, New Brunswick, NJ). The inlet feed pressure and the permeate vacuum level were measured with pressure gauges (Matheson, E.Rutherford, NJ).

2.2.4 Preparation of the Thin ILM

The nonvolatile liquid absorbent Silicone oil (viscosity 50 cSt, Kramer Chemicals, Inc., Paterson, NJ) was immobilized in part of the length of the pores of a microporous hollow fiber substrate. As mentioned earlier, these fiber have a thin silicone coating (~1 μm) on the outer side of the hollow fiber; therefore, the immobilized liquid membrane (ILM) was incorporated in the hollow fiber support pores using the lumen side coating procedure.

In order to prepare a thin ILM, a mixture of 30% Silicone oil and 70% hexane was pumped through the bore of the hollow fiber module for 1 hour using a Micropump (model 7144-04, Cole-Palmer, Chicago, IL). Subsequently, the module was drained and any residual liquid present on the lumen side was removed by purging with a dry gas stream (e.g., nitrogen) for 1 – 2 hr. To assure complete evaporation of the solvent, vacuum was applied on the shell side of the module overnight. The ILM was then ready for testing.

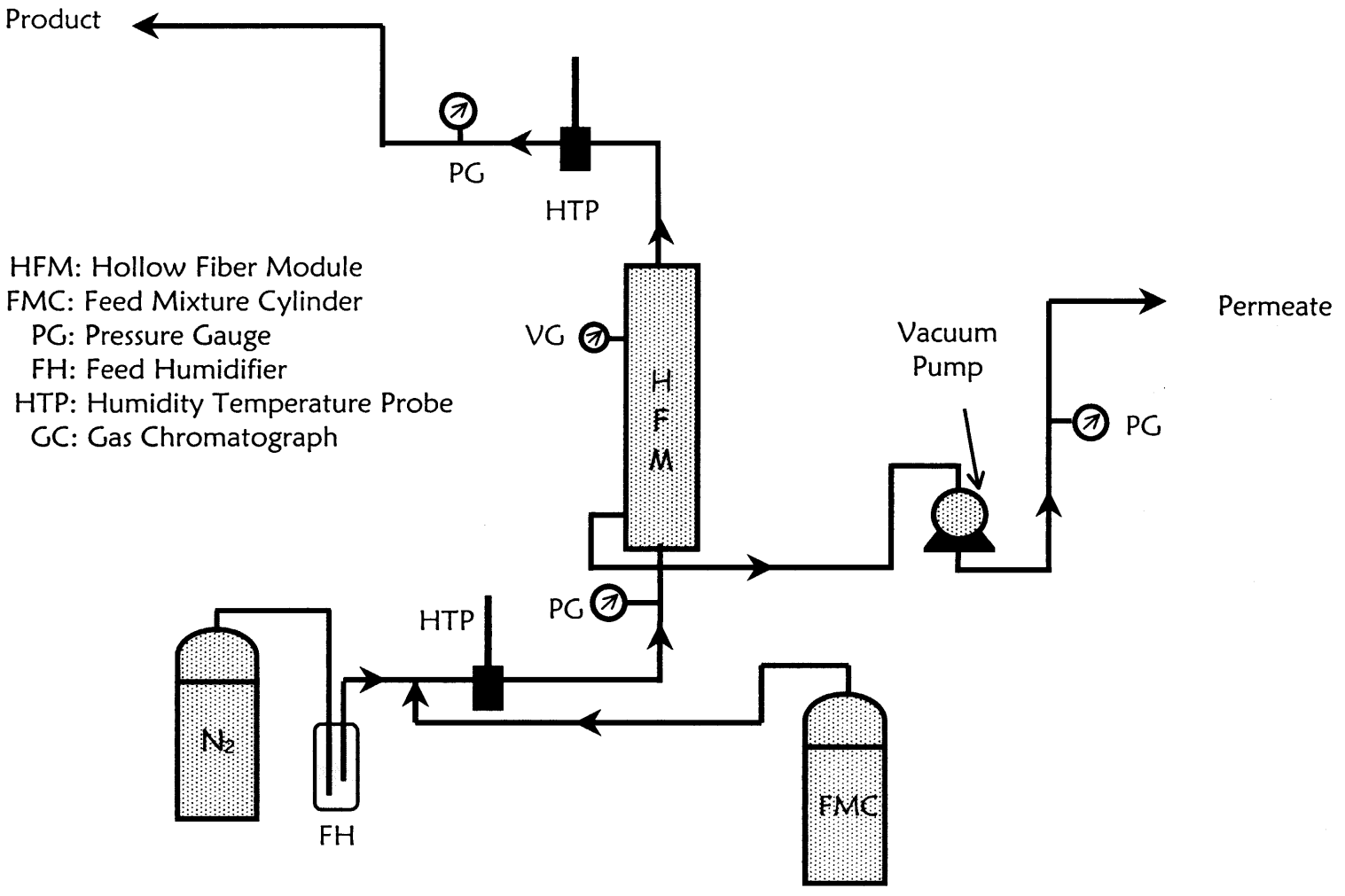

Figure 2.3 Experimental setup for VOC removal from humidified gas stream in steady state mode of operation.

2.2.5 GC Calibration for VOCs

Calibration curves for acetone, methanol and toluene were prepared for the desired ranges of VOC concentrations. Different concentrations of a VOC containing gas (N_2) stream were prepared by diluting a VOC/N_2 gas stream of known concentration with a pure N_2 gas stream. For each calibration range, at least 4 to 5 different concentrations were utilized. When preparing calibration for the lower range of VOC concentrations (e.g. 0.1% - 1%) a certified mixture of VOC/N_2 gas mixture was purchased from Matheson Gas Products (Matheson, E.Rutherford, NJ). The highest available concentration of a VOC (N_2 balance) in a cylinder from Matheson was ~1%. Sample GC calibration curves for low and higher ranges of concentrations are shown in Figures 2.4 and 2.5 for methanol in N_2.

To prepare calibrations in a much higher concentration range (Figure 2.6), liquid VOC (e.g. methanol HPLC grade) (Fisher Scientific, Springfield, NJ) was placed in a surge drum vessel (bubbler) and pure N_2 stream was bubbled through the liquid VOC at a low flow rate. This unknown highest methanol concentration was determined by GC (HP 5890 series II, Hewlett-Packard, Paramus, NJ) analysis. In order to determine this high concentration, the VOC containing gas stream was diluted with pure N_2 till the composition of the mixed gas stream came in the range of the calibration curve made for methanol concentration of upto 1% shown in Figure 2.5. This known VOC concentration (e.g. 1%) was purchased from Matheson Gas Products (Matheson, E.Rutherford, NJ) as a

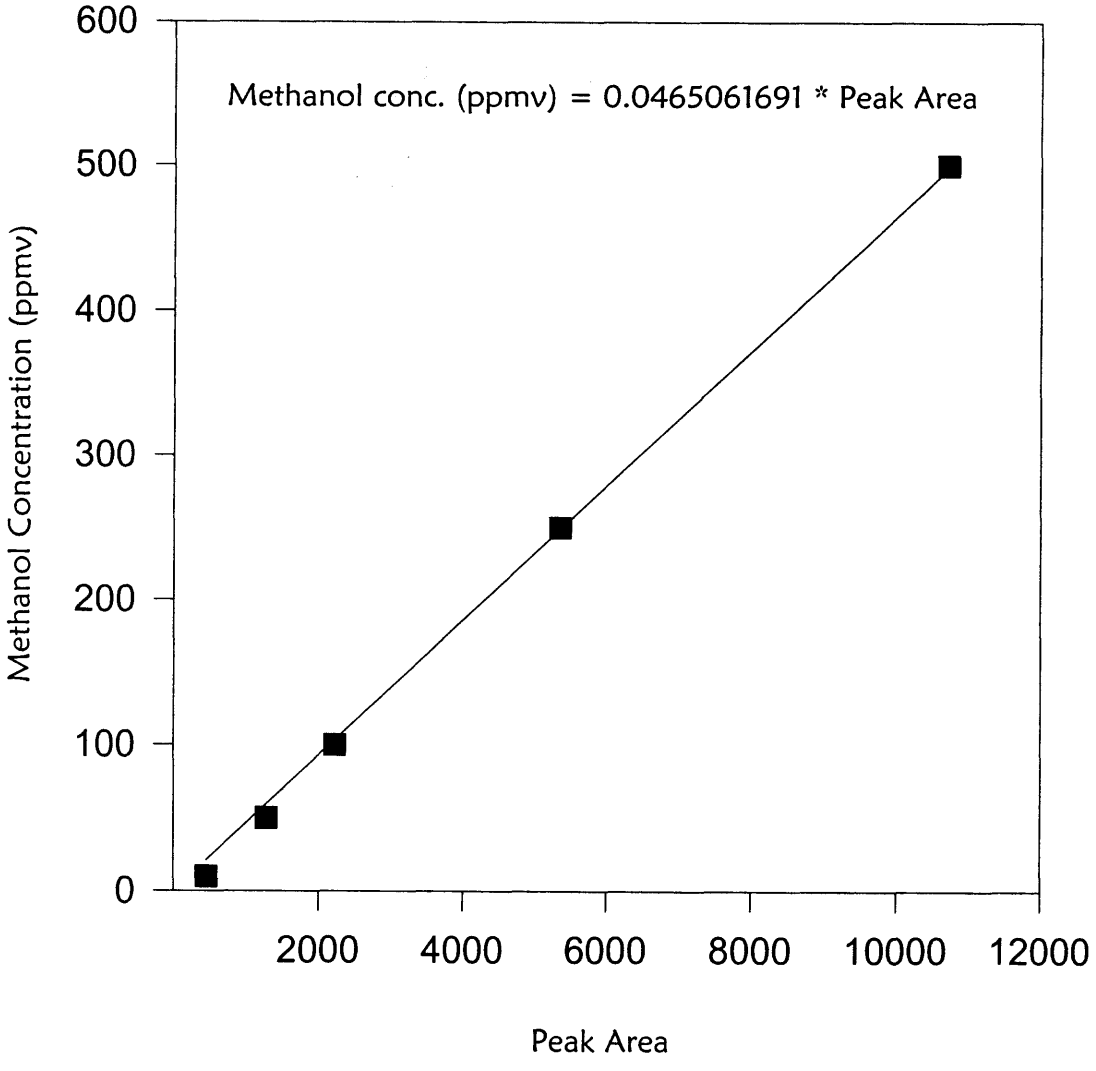

Figure 2.4 GC calibration for low concentration of Methanol in N_2.

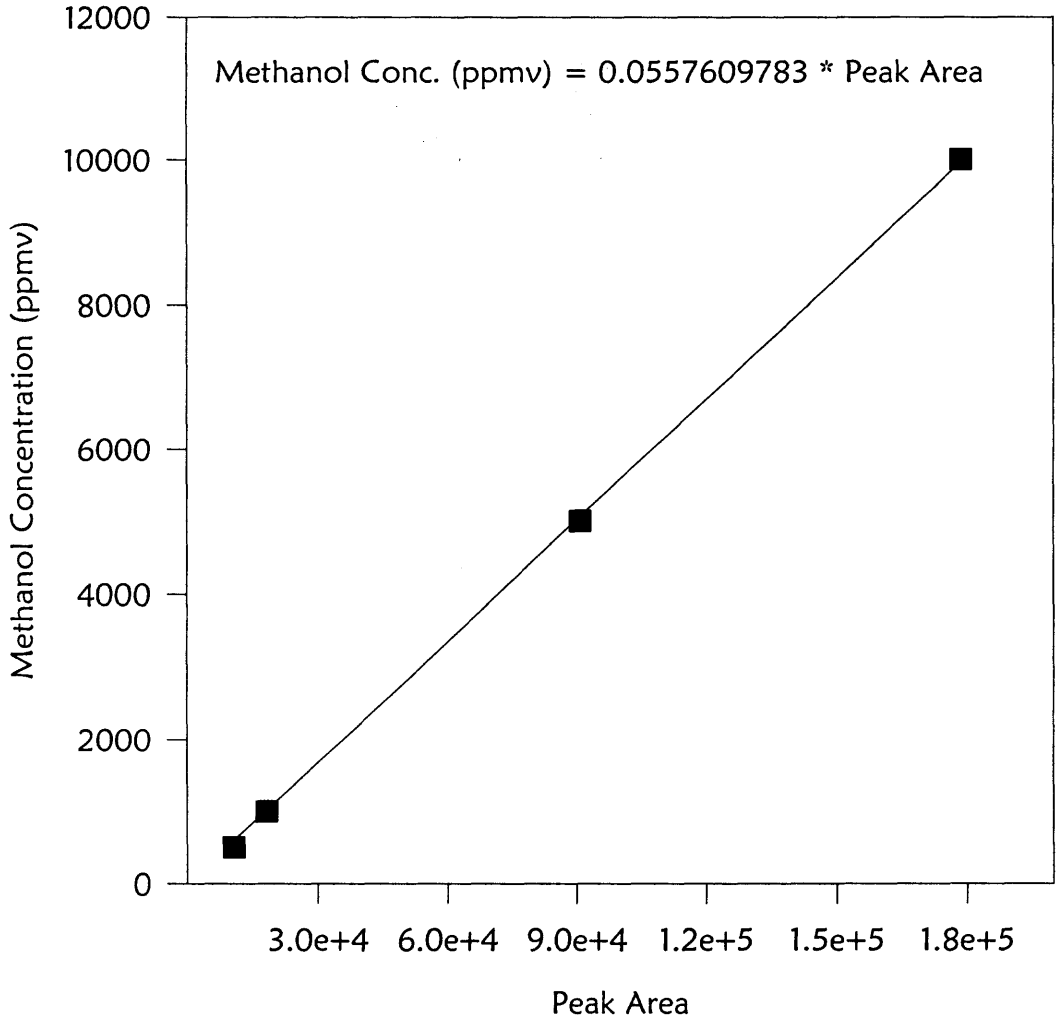

Figure 2.5 GC calibration for intermediate range of concentrations of Methanol in N_2.

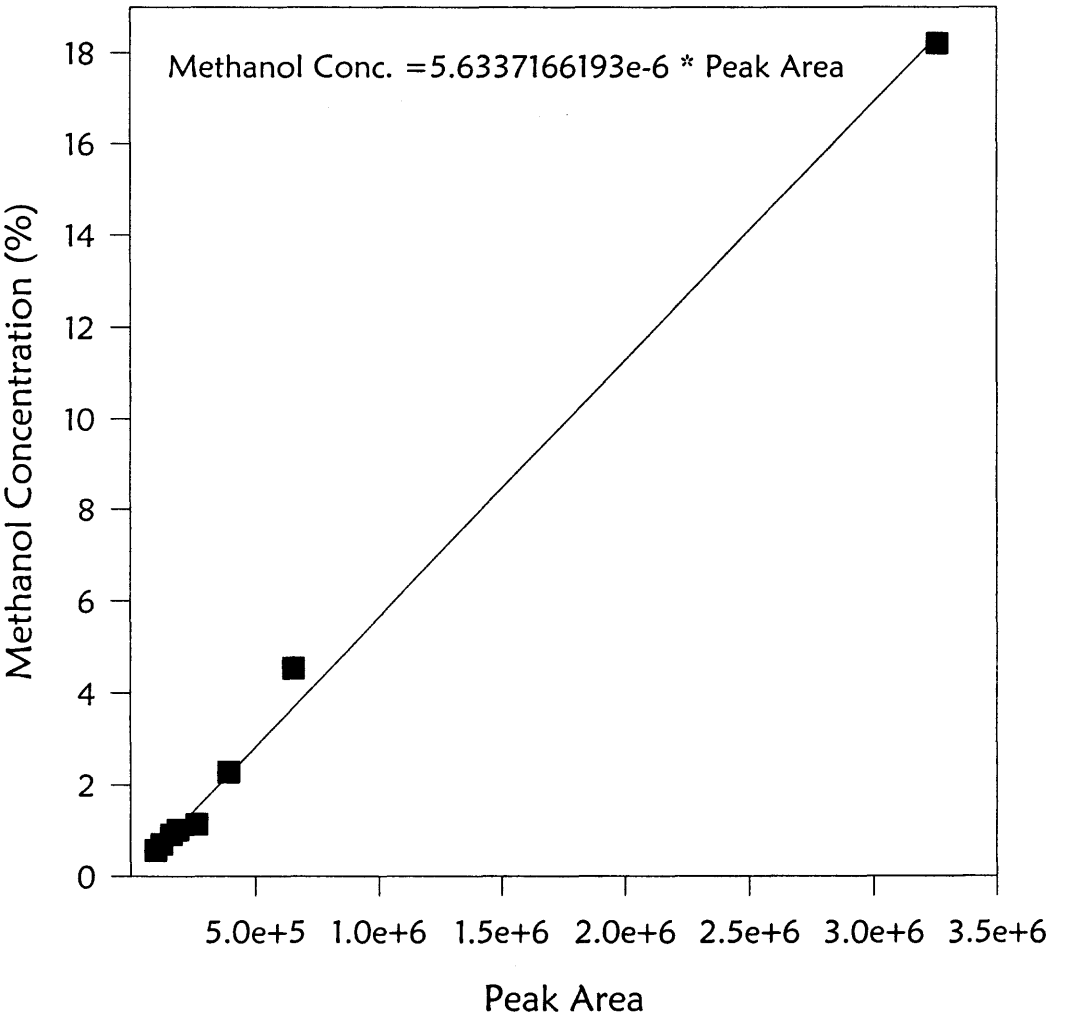

Figure 2.6 GC Calibration for very high concentrations of Methanol in N_2.

certified standard mixture and then diluted with nitrogen stream in appropriate ratio to obtained different calibration points. Other concentrations of the methanol diluted gas streams were recalculated knowing the gas flow rates of pure N_2 and the high concentration methanol gas stream from the bubbler.

2.2.6 Experimental Setup for Cyclic Mode of Operation for the VOC Removal

For the FSMP process, two membrane modules were employed. As shown in Table 2.2, Modules 3 and 4 have a set of 150 fibers each; these microporous polypropylene hollow fibers (Hoechst Celanese, SPD Charlotte, NC; X-10 (0.03 μm pore size)) have a thin plasmapolymerized nonporous silicone coating on the outside diameter (prepared by AMT Inc., Minnetonka, MN). The experimental setup for the unsteady state (e.g. cyclic) mode of operation is shown in Figure 2.7. The mixture of VOC and nitrogen (Matheson, E.Rutherford, NJ was fed through the fiber bores of one of the hollow fiber modules for a short period of time; then the feed gas flow was stopped by a three-way solenoid valve (3-WSV) (Components and Control, Carlstad, NJ) at the inlet and the outlet of the first module. At the same time, the feed flow was redirected into the bores of the fibers of the second module for a short period of time (e.g. absorption time) after which the settings of the three-way solenoid valves (3-WSV) will be switched so that the inlet and the outlet of the second module were closed for a desorption period of cycle.

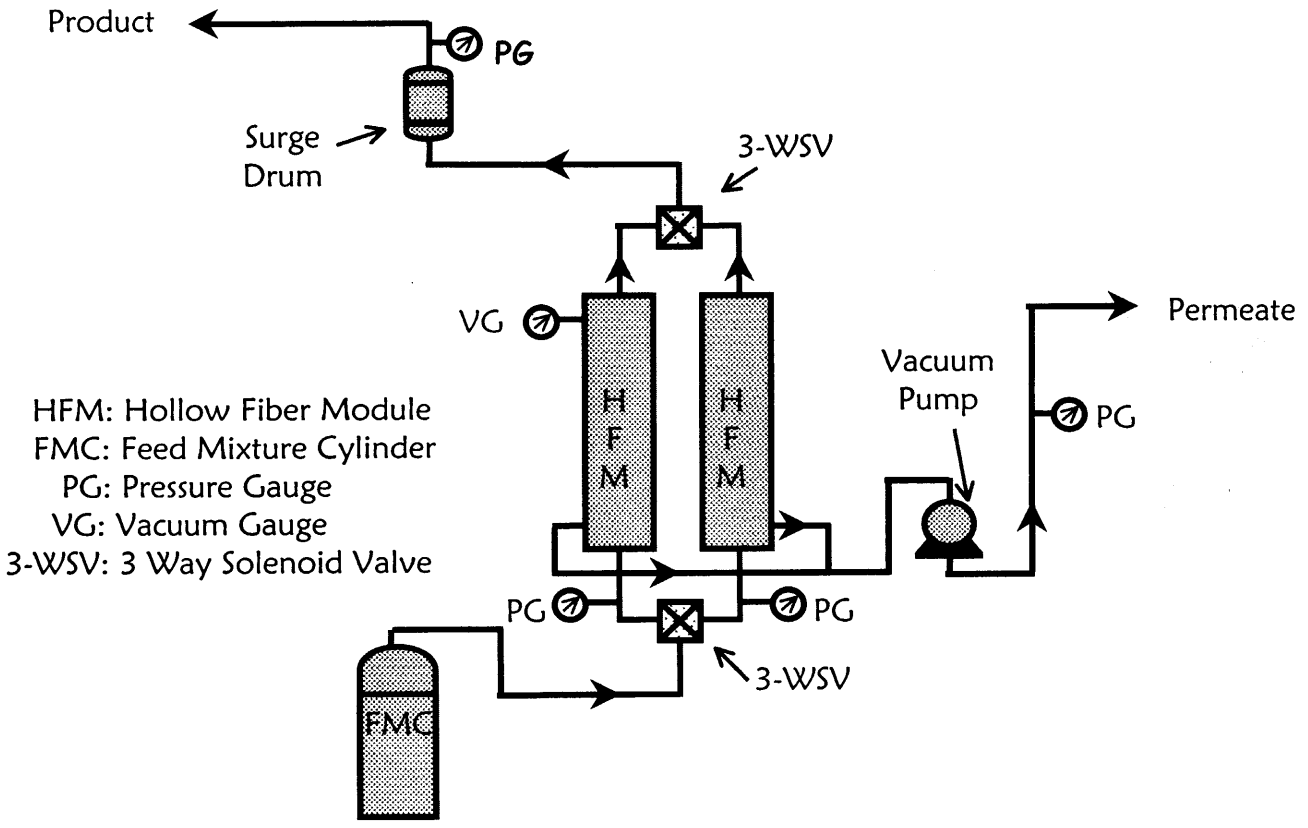

Figure 2.7 Experimental setup for VOC removal using FSMP process.

Both three-way solenoid valves at the inlet and at the outlet of these two modules connected in parallel were controlled by a single timer so they can work in perfect synchronization. The feed inlet gas flow rate was controlled by an electronic mass flow-metering valve (Matheson, E. Rutherford, NJ). On the shell side of both hollow fiber modules, vacuum was applied. During the part of the cycle meant for the absorption from the flowing feed stream, the VOC permeated through the silicone coating of the hollow fibers selectively over N_2/air into the shell side where a continuous vacuum was applied in both hollow fiber modules to create a driving force for the VOC removal. The purified gas was collected at the outlet of both modules where a small surge vessel was placed in order to avoid any pulsation of the product flow due to the cyclic process; the purified gas mixture was analyzed with a gas chromatograph (HP 5890 series II, Hewlett-Packard, Paramus, NJ).

All connecting lines used for the experiment were 1/8-inch soft copper tubing (McMaster Carr, New Brunswick, NJ). Any fluctuation of the feed inlet gas pressure was measured with pressure gauges (Matheson, E. Rutherford, NJ). All gas mixtures used for these experiments were obtained from Matheson (E. Rutherford, NJ). The VOC concentration in the permeate was calculated from a material balance.

2.2.7 Calculation of Nitrogen Permeance (Q/δ) and Determination of the ILM Thickness Needed to Simulate Results from the Mathematical Model

In order to model mathematically the steady state system containing a thin ILM in the pores of the hollow fibers, certain parameters (e.g. thickness of the oil, nitrogen gas permeance through the oil etc.) have to be determined earlier. To estimate the thickness of oil in the pores, the following three quantities, namely, the N_2 permeance through the coated membrane $(Q/\delta)_c$ containing no oil in the pores, N_2 permeance through the composite membrane $(Q/\delta)_{ov}$ (e.g. silicone oil and PDMS coating) and the N_2 permeance through the oil $(Q/\delta)_l$ were determined.

In order to find out the N_2 permeance through the oil, $(Q/\delta)_l$, a new module (Module 2) was prepared using Celgard X-10 hollow fibers without any PDMS coating. The pores in the fibers of this module were filled completely with Silicone oil by pumping the oil through the bore of the hollow fiber module for some time using a Micropump (model 7144-04, Cole-Palmer, Chicago, IL) in order to prepare a full ILM in the pores of the hollow fibers. Afterward, the module was drained and any residual liquid present in the module was removed by using a dry purge gas stream (e.g., nitrogen) for 1 – 2 hr through the shell and tube side of the hollow fiber module. The nitrogen permeation rate was measured for all cases in the same manner described below. One end of the tube side of the hollow fiber module was connected to the N_2 cylinder and the other end was closed. Nitrogen in the bore side was pressurized to various pressures monitored with a pressure

gauge (Matheson, E.Rutherford, NJ). On the other side of the membrane, one end of the shell side of the hollow fiber was closed; at the other end, the N_2 permeation rate was measured using a bubble flow meter.

To determine the thin ILM thickness, nitrogen permeances for all three cases were calculated in a manner given below. Detailed sample calculations are given in Appendix A.

Effective surface area (A) based on the logarithmic mean diameter (d_{lm})of the fiber is given by

$$A = \pi d_{lm} L N \tag{2.1}$$

Where the logarithmic mean diameter is

$$d_{lm} = (d_0 - d_i)/\ln(d_0/d_i) \tag{2.2}$$

Knowing the nitrogen permeate flow rate (Q_p) measured according to the technique described above, nitrogen permeate molar flow rate (F_p) is calculated:

$$F_p = \frac{P Q_p}{R T} \tag{2.3}$$

Nitrogen permeation flux:

$$N_{N_2} = \frac{F_p}{A} \tag{2.4}$$

Module average nitrogen permeance:

$$\left(\frac{Q}{\delta}\right) = \frac{N_{N_2}}{(P_F - P_p)} \tag{2.5}$$

Note that $\left(\frac{Q}{\delta}\right)_c$ is for a bare membrane with PDMS coating on the outer diameter and $\left(\frac{Q}{\delta}\right)_l$ for the noncoated fully immobilized or coated partially immobilized liquid membrane. We can estimate the liquid membrane thickness (δ_l) knowing all parameters for the overall permeation equation:

$$\frac{1}{\left(\frac{Q}{\delta}\right)_{OV}} = \frac{1}{\left(\frac{Q}{\delta}\right)_c \times \frac{d_o}{d_{lm}}} + \frac{1}{\left(\frac{Q}{\delta}\right)_l} \qquad (2.6)$$

In order to estimate the thin ILM thickness, the above equation was solved knowing all the parameters except $(Q/\delta)_l$. Now this $(Q/\delta)_l$ is really equal to $\left(\frac{Q_l \varepsilon_m}{\tau_m \delta_l}\right)_l$ (Chen et al. 2000) . Knowing the nitrogen permeate flow rate measured with Module 2 and the full ILM thickness δ_l=25μm, one can estimate $\left(\frac{Q_l \varepsilon_m}{\tau_m \delta_l}\right)_l$ and thereby $\left(\frac{Q_l \varepsilon_m}{\tau_m}\right)_l$ for nitrogen through Silicone oil. Once $\left(\frac{Q_l \varepsilon_m}{\tau_m}\right)_l$ was determined, equation (2.6) was solved for δ_l, and the thin ILM thickness was determined knowing that $(Q/\delta)_l$ in equation (2.6) for the overall permeation is really $\left(\frac{Q \varepsilon_m}{\tau_m \delta_l}\right)_l$.

2.3 Gas Permeation Model for a Silicone Coated Hollow Fiber Module Containing a Thin ILM

A mathematical model for binary gas separation in a conventional permeation mode in a hollow fiber module containing silicone coated fibers is available in Cha et al. (1997). This modeling analysis considered a strong dependence of the VOC permeance (i.e. Q_i/δ) of the silicone coating on the partial pressure of VOC. In the present thesis, a mathematical model has been developed to simulate the experimental results for the silicone-coated hollow fiber containing permeator having a thin layer of silicone oil incorporated in the porous structure (thin ILM) under the operational conditions. The model incorporates the type of dependence of the VOC permeance of the silicone coating on the VOC partial pressure employed by Cha et al. (1997).

The polymeric membrane consists of a thin layer of around 1μm of PDMS coating developed on the outer side of the microporous polypropylene hollow fiber by a plasma polymerization technique. The manufacturer (AMT Inc., Minnetonka, MN) provided an approximate estimate of the thickness of the PDMS coating. In addition, this membrane has a thin layer of silicone oil immobilized in the porous structure whose thickness was estimated in a manner described earlier for the purpose of obtaining results from the mathematical model.

The following assumptions were employed while developing the model for the separation of the VOC/N_2 mixtures using this composite hollow fiber permeator:

1. The permeability coefficient of a VOC through the silicone (PDMS) coating depends on the feed side VOC partial pressure.
2. The pressure on the permeate side is constant along the module.
3. Hagen-Poiseuille law governs the gas pressure drop in flow through the fiber lumen.
4. Axial diffusion is insignificant compared to bulk gas convection.
5. The end effects inside the permeator are negligible.
6. The deformation of the hollow fiber under pressure is negligible.

2.3.1 Estimation of the Parameters for the Mathematical Model

To model this system, the permeances (i.e. Q_i/δ) of the VOC and N_2 through the thin ILM have to be determined. Figure 2.8 shows the cross section of a pore of the hollow fiber having a thin ILM immobilized within the pore along with a silicone coating on the outer surface. In order to find the VOC permeance, the condition at the interface of the ILM and the silicone coating (e.g. P'x'), has to be determined first. Permeation rate equations 2.7 - 2.10 of the VOC and N_2 through the skin and ILM are given below for a length dl of a single hollow fiber of outside diameter d_0:

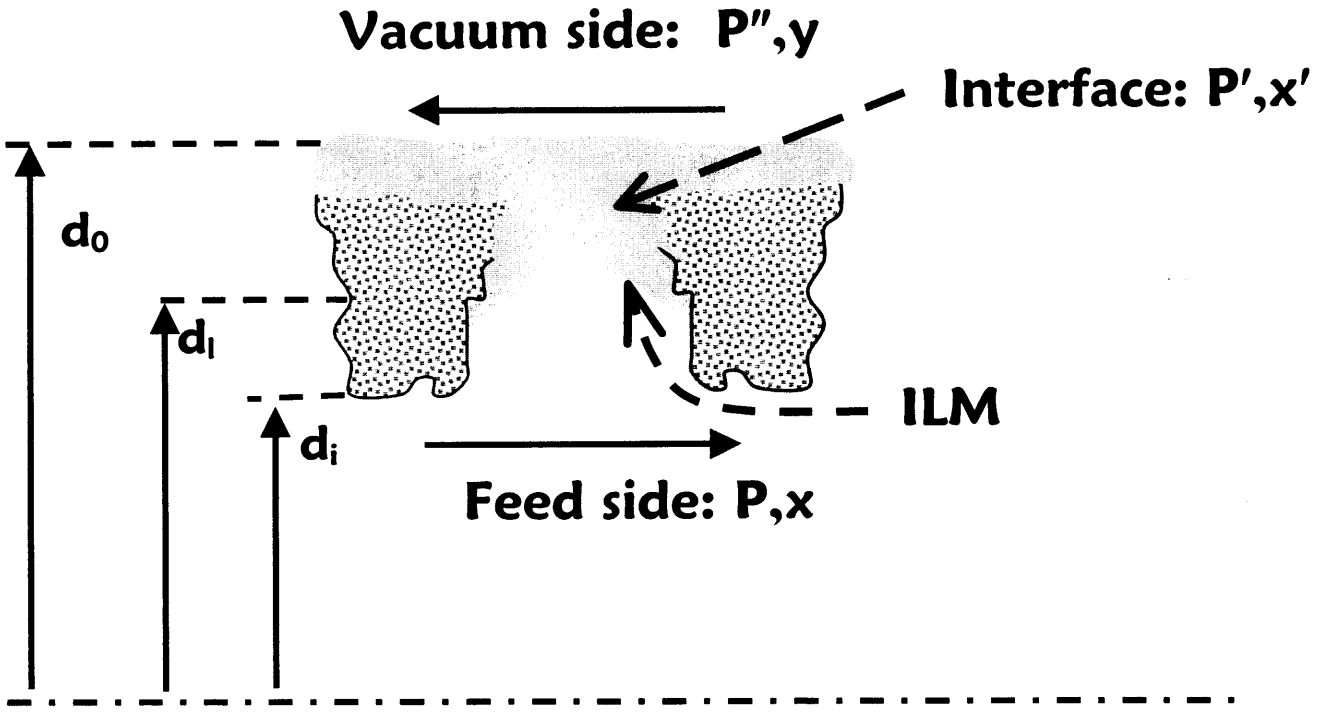

Figure 2.8 Cross section of a hollow fiber pore having a thin ILM.

1. Permeation rate of the VOC across the silicone skin:

$$W_{VOC} = \pi d_0 dl\left(\frac{Q_{C_{VOC}}}{\delta_C}\right)[P'x' - P''y] \tag{2.7}$$

2. Permeation rate of N_2 across the silicone skin:

$$W_{N_2} = \pi d_0 dl\left(\frac{Q_{C_{N_2}}}{\delta_C}\right)[P'(1-x') - P''(1-y)] \tag{2.8}$$

3. Permeation rate of VOC across the oil ILM:

$$W_{VOC} = \pi d_{lm} dl\left(\frac{Q_{I_{VOC}}}{\delta_I}\right)[Px - P'x'] \tag{2.9}$$

4. Permeation rate of N_2 across the oil ILM:

$$W_{N_2} = \pi d_{lm} dl\left(\frac{Q_{I_{N_2}}}{\delta_I}\right)[P(1-x) - P'(1-x')] \tag{2.10}$$

where the logarithmic mean diameter (d_{lm}) is defined by equation (2.2). Adding equations (2.7) and (2.9):

$$\frac{W_{VOC}}{\pi d_{lm} dl}\left[\frac{1}{\frac{Q_{C_{VOC}}}{\delta_C}\frac{d_0}{d_{lm}}} + \frac{1}{\frac{Q_{I_{VOC}}}{\delta_I}}\right] = (Px - P''y) \tag{2.11}$$

The overall permeation equation for VOC across the skin and the thin ILM can be written as:

$$W_{VOC} = \pi d_{lm} dl \left(\frac{Q}{\delta}\right)_{OV_{VOC}} [Px - P''y] \tag{2.12}$$

From equations (2.11) and (2.12):

$$\frac{W_{VOC}}{\pi d_{lm} dl}\left[\frac{1}{\frac{Q_{C_{VOC}}}{\delta_C}\frac{d_0}{d_{lm}}} + \frac{1}{\frac{Q_{I_{VOC}}}{\delta_I}}\right] = \frac{W_{VOC}}{\pi d_{lm} dl \left(\frac{Q}{\delta}\right)_{OV_{VOC}}} \tag{2.13}$$

Therefore, the expression for the overall VOC permeance from equation (2.13) is:

$$\frac{1}{\alpha_{OV_{VOC}}} = \frac{1}{\frac{Q_{C_{VOC}}}{\delta_C}\frac{d_0}{d_{lm}}} + \frac{1}{\frac{Q_{I_{VOC}}}{\delta_I}} = \frac{1}{\left(\frac{Q}{\delta}\right)_{OV_{VOC}}} \tag{2.14}$$

Similarly adding equations (2.8) and (2.10) and following the same procedure, an expression for the overall N_2 permeance can be derived:

$$\frac{1}{\beta_{OV_{N_2}}} = \frac{1}{\frac{Q_{C_{N_2}}}{\delta_C}\frac{d_0}{d_{lm}}} + \frac{1}{\frac{Q_{I_{N_2}}}{\delta_I}} = \frac{1}{\left(\frac{Q}{\delta}\right)_{OV_{N_2}}} \tag{2.15}$$

Therefore, the overall VOC permeation equation may be represented as:

$$W_{VOC} = \pi d_{lm} dl \alpha_{OV_{VOC}} [Px - P''y] \tag{2.16}$$

For N_2 the overall permeation equation is:

$$W_{N_2} = \pi d_{lm} dl \beta_{OV_{N_2}} [P(1-x) - P'(1-x')] \tag{2.17}$$

The same equation (2.16) can also be written in the following manner:

$$W_{VOC} = \pi d_{lm} dl \frac{[Px - P''y]}{\left[\frac{1}{\frac{Q_{C_{VOC}}}{\delta_C}\frac{d_0}{d_{lm}}} + \frac{1}{\frac{Q_{l_{VOC}}}{\delta_l}}\right]} \tag{2.18}$$

As mentioned earlier (Cha et al., 1997), a strong dependence of the VOC permeance through the silicone coating on the feed side partial pressure of VOC is given as

$$\frac{Q_{C_{VOC}}}{\delta_C} = a * \exp(bP'x') \tag{2.19}$$

An expression for P'x' can be derived from equation (2.9) as

$$P'x' = Px - \frac{W_{VOC}}{\pi d_{lm} dl \left(\frac{Q_{l_{VOC}}}{\delta_l}\right)} \tag{2.20}$$

Substituting the expression for P'x' given by equation (2.20) into equation (2.19),

$$\frac{Q_{C_{VOC}}}{\delta_C} = a \exp\left[b\left(Px - \frac{W_{VOC}}{\pi d_{lm} dl \left(\frac{Q_{l_{VOC}}}{\delta_l}\right)}\right)\right] \tag{2.21}$$

If the expression for VOC permeance through the silicone coating given by equation (2.21) is introduced into equation (2.18), one obtains

$$W_{VOC} = \pi d_{im} dl \frac{[Px - P''y]}{\left[\frac{1}{a\exp\left[b\left(Px - \frac{W_{VOC}}{\pi d_{im} dl\left(\frac{Q_{l_{VOC}}}{\delta_l}\right)}\right)\right]\frac{d_0}{d_{im}}} + \frac{1}{\frac{Q_{l_{VOC}}}{\delta_l}}\right]} \qquad (2.22)$$

If equation (2.22) is solved for W_{VOC}, than from equation (2.20) one can determine P'x'. To solve the above equation (2.22), the unknown parameters like "a" and "b" which are constants for the VOC permeance through the silicone skin and the VOC permeance through the thin layer of silicone oil (e.g. $\frac{Q_{l_{VOC}}}{\delta_l}$) have to be estimated based on the experimental results.

Therefore, the first step was to determine parameters "a" and "b" in the expression used to described the VOC permeance through the silicone coating (Q_i/δ_c) for all three VOCs (e.g. methanol, toluene and acetone). This was done by simulating the experimental results obtained using the bare membrane having a thin silicone skin on the outer diameter of the fiber using the mathematical model developed and verified by Cha et al. (1997). These two parameters for each VOC

were adjusted in such a way that the experimental and simulated data were at their closest proximity. Estimated values of "a" and "b" for all three VOCs for this silicone coated membrane (Module 1) are tabulated in a table in section 2.4 and compared with the "a" and '"b" values obtained by Cha et al. (1997).

VOC permeance for each of the three organic vapors (e.g. toluene, methanol and acetone) individually studied here was estimated based on the extent of removal of each VOC with various feed flow rates using Module 2 whose fibers were without a PDMS coating and whose pores were fully immobilized with the silicone oil. From this set of experiments, an effective permeability, $\left(\frac{Q_i \varepsilon_m}{\tau_m}\right)$, where the true permeability Q_i is ($Q_i = S_i \times D_i$), for all three VOCs was estimated knowing the full ILM thickness (δ_l= 25μm). The feed gas containing a VOC was introduced through the tube side of the membrane Module 2 while vacuum was applied to the shell side. These experimental results were used to calculate all three VOC permeances. The procedure for parameter estimation is given below and detailed calculations can be found in Appendix B. Experimental results acquired after immobilization of the thin ILM can also be used to estimate the overall permeance and permeance through the thin ILM for all three VOCs used following the same procedure as mentioned in Appendix B.

Note that through the ILM: $\left(\frac{Q_i}{\delta}\right)_l = \left(\frac{Q_i \varepsilon_m}{\tau_m \delta_l}\right)_l$.

Based on the experimental results, the VOC permeate flux can be calculated from the permeate flow rate and the permeate composition using the following equation

$$N_{VOC} = \frac{F_P y_{VOCf}}{A} \tag{2.23}$$

where F_P (gmol/s) is the molar VOC-containing permeate flow rate

$$F_P = F_{in} - F_{out} \tag{2.24}$$

and y_{VOC_i} is the mole fraction of the VOC in the permeate.

$$y_{VOC_i} = \frac{F_{in}x_{in} - F_{out}x_{out}}{F_P} \tag{2.25}$$

Similarly, the molar permeate flux of nitrogen N_{N_2} (gmol/cm^2 s) is

$$N_{N_2} = \frac{F_P y_{N_{2P}}}{A} \tag{2.26}$$

where $y_{N_{2P}}$ is the mole fraction of nitrogen in the permeate:

$$y_{N_{2P}} = 1 - y_{VOC_i} \tag{2.27}$$

To analyze the performance of the module, the percent removal of VOC (%), the module average permeances and the separation factor α were calculated follows:

$$\%\ \text{Removal} = \frac{F_P y_{VOC_i}}{F_{in}x_{in}} \times 100 \tag{2.28}$$

The module average permeance of VOC, $\frac{Q_{OV_{VOC}}}{\delta_{OV}}$ (gmol/s cm^{2}cmHg), is

$$\frac{Q_{OV_{VOC}}}{\delta_{ov}} = \frac{N_{VOC}}{\Delta P_{lm}} \tag{2.29}$$

The above equation uses the logarithmic mean partial pressure driving force (ΔP_{lm}) expressed as

$$\Delta P_{lm} = \frac{(P_{VOC_f} - p_{VOCf}) - (P_{VOC_w} - p_{VOC_w})}{\ln\left(\frac{(P_{VOC_f} - p_{VOCf})}{(P_{VOC_w} - p_{VOC_w})}\right)} \tag{2.30}$$

where the permeate side partial pressure p_{VOC} and the feed side partial pressure P_{VOC} are given as

$$p_{VOC} = pY_{VOC} \tag{2.31}$$

$$P_{VOC} = PX_{VOC} \tag{2.32}$$

The partial pressures of VOC were calculated based on the VOC composition on both sides at the inlet ("f") and the outlet ("w") of the module. Since the permeate side VOC composition is unknown at the closed end of the module ("w"), as a first estimate, this composition (y_{VOC_w}) is considered to be zero. Using this approximation, one can estimate the module average permeances and determine the separation factor (α) between the VOC and N_2 from

$$\alpha = \alpha_{VOC\text{-}N_2} = \frac{\frac{Q_{OV_{VOC}}}{\delta_{OV}}}{\frac{Q_{OV_{N_2}}}{\delta_{OV}}} \tag{2.33}$$

Once the average module VOC permeance across the fully immobilized silicone oil, $\frac{Q_{VOC_l}}{\delta_l}$, is estimated, knowing the full liquid membrane thickness, δ_l=25μm, one can estimate the VOC permeability, e.g. $\left(\frac{Q_{l_{VOC}}\varepsilon_m}{\tau_m}\right)$, for all three

VOCs studied here. Knowing the thin ILM thickness that was determined previously δ_l=5μm (Appendix A), the permeance across the thin ILM thickness e.g. $\left(\frac{Q_l \varepsilon_m}{\tau_m \delta_l}\right)$ was estimated.

Knowing the VOC permeance through the silicone coating $(Q/\delta)_c$ and the permeance across the thin silicone layer $(Q/\delta)_l$ one can easily calculate the overall permeance $(Q/\delta)_{ov}$ (e.g. silicone coating and thin ILM), using equation (2.6). Using these values of the VOC permeances, the experimental data were simulated using the mathematical model developed and described below. In the case where there was a significant difference between the simulated and experimental results, VOC permeances (e.g. $(Q/\delta)_l$ and $(Q/\delta)_{ov}$) were reevaluated in the following manner.

Using the cross flow condition equation, one can recalculate the VOC permeate composition at the closed end $\left(y_{VOC_w}\right)$ and correct the logarithmic mean partial pressure driving force (ΔP_{lm}) using the equation below (Sengupta and Sirkar, 1986).

$$\frac{y_{VOC_w}}{\left(1-y_{VOC_w}\right)} = \frac{\alpha\left(x_{VOC_w} - \gamma\, y_{VOC_w}\right)}{\left(\left(1-x_{VOC_w}\right) - \gamma\left(1-y_{VOC_w}\right)\right)} \qquad (2.34)$$

where γ denotes the pressure ratio between the permeate and the feed side, $\frac{p}{P}$, and α is the separation factor defined previously via equation (2.33). To estimate the VOC composition at the closed end, one uses the α value calculated at the first step using the assumption (e.g. y_{VOCw}=0). Once the new value of the VOC in the

permeate composition at the closed end was obtained, logarithmic mean partial pressure driving force and the VOC permeance were recalculated. The same procedure of reevaluation of the parameters was followed till the simulated and experimental results came to the closest proximity.

Another approach to estimating the needed parameters is based on the experimental results acquired after immobilization of the thin ILM used to calculate overall permeance for all VOCs used. Knowing the VOC permeance through the silicone coating $(Q/\delta)_c$ and the overall permeance $(Q/\delta)_{ov}$ (e.g. silicone coating and thin ILM), one could easily calculate the VOC permeance through the liquid layer $(Q/\delta)_l$ using equation (2.6). Procedure for parameter estimation and for the correction of the driving force given in detail in Appendix B can be used for both parameter estimation approaches mentioned before.

A summary of the parameters used for the mathematical model is provided in the results section and detailed calculations can be found in Appendix B. Experimental results for the VOC runs using Module 2 used to determine VOC permeances are also given in the results section.

2.3.2 Governing Differential Equations for the Hollow Fiber Permeator

A schematic diagram where the VOC/N_2 feed stream and the permeate stream flow countercurrently is shown in Figure 2.9. The overall material balance between the feed inlet end and any location at a distance l from the closed end of the permeate side leads to

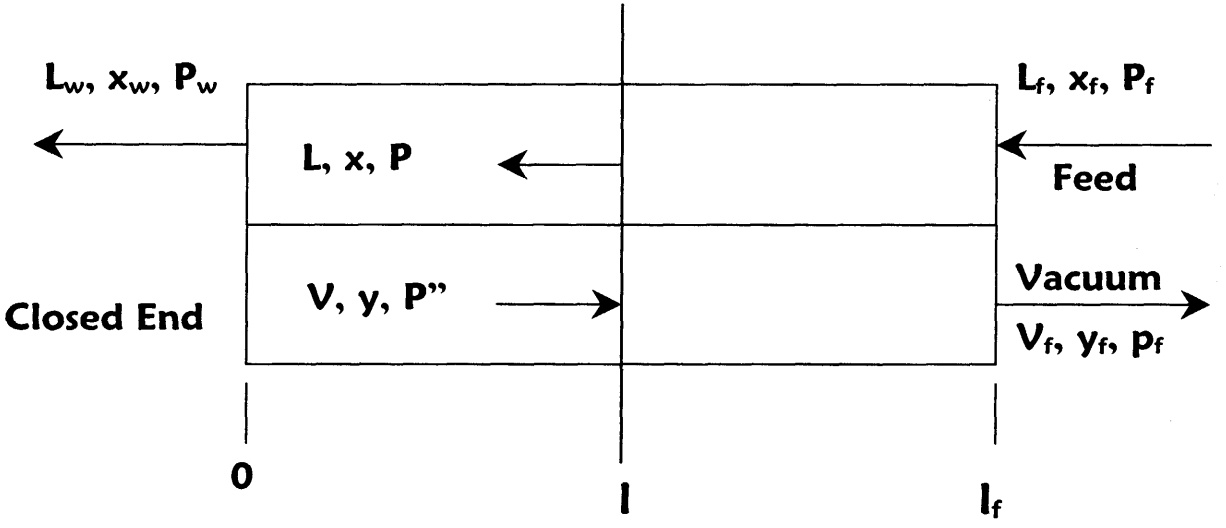

Figure 2.9 Schematic of a hollow fiber permeator for modeling vacuum mode of operation.

$$L - V = L_f - V_f \tag{2.35}$$

The mass balances for VOC and nitrogen can be written as

$$VOC: \quad Lx - Vy = L_f x_f - V_f y_f \tag{2.36}$$

$$N_2: \quad L(1-x) - V(1-y) = L_f(1-x_f) - V_f(1-y_f) \tag{2.37}$$

If the axial coordinate l is positive in the direction of permeate gas flow, the governing differential equations for permeation of the two species are

$$VOC: \quad \frac{d(Lx)}{dl} = \pi d_{lm} \alpha_{OV_{VOC}} (Px - P''y) = \frac{d(Vy)}{dl} \tag{2.38}$$

$$N_2: \quad \frac{d[L(1-x)]}{dl} = \pi d_{lm} \beta_{OV_{N_2}} [P(1-x) - P''(1-y)] = \frac{d[V(1-y)]}{dl} \tag{2.39}$$

Note that equations (2.14) and (2.15) give the overall permeance expressions for VOC and N_2 at any location l of the hollow fiber. The equation governing the pressure drop in the bore of the fiber is

$$\frac{dP}{dl} = \frac{128RTL\mu_f}{\pi P d_i^4} \tag{2.40}$$

Rearranging the above equations, one can develop the following set of differential equations to represent mathematically the permeation behavior of the permeator

$$\frac{dL}{dl} = \pi d_{lm} \alpha_{OV_{VOC}} (Px - P''y) + \pi d_{lm} \beta_{OV_{N_2}} [P(1-x) - P''(1-y)] \tag{2.41}$$

$$\frac{dV}{dl} = \pi d_{lm} \alpha_{OV_{VOC}} (Px - P''y) + \pi d_{lm} \beta_{OV_{N_2}} [P(1-x) - P''(1-y)] \tag{2.42}$$

$$\frac{dx}{dl} = \frac{\left[\pi d_{lm} \alpha_{OV_{VOC}} (Px - P''y)(1-x) + \pi d_{lm} \beta_{OV_{N_2}} x[P(1-x) - P''(1-y)]\right]}{L} \tag{2.43}$$

$$\frac{dy}{dl} = \frac{\left[\pi d_{lm} \alpha_{OV_{VOC}} (Px - P''y)(1-y) + \pi d_{lm} \beta_{OV_{N_2}} y[P(1-x) - P''(1-y)]\right]}{V} \tag{2.44}$$

Equations (2.41) to (2.44) have to be solved simultaneously along with the boundary conditions

at $l=0$, $y=y_w$, $V=V_w$

at $l=l_f$, $x=x_f$, $L=L_f$, $P=P_f$ (2.45)

When vacuum is applied to the permeate side in countercurrent flow, at the location $l=0$, the permeate flow $V_w = 0$. The permeate side VOC mole fraction, y_w, at this location cannot be specified explicitly and it has to be determined from equations (2.38) and (2.39) by using the boundary conditions at $l=0$. The VOC mole fraction y_w in the vacuum mode has been shown to be (Guha et al., 1992):

$$y_w = \frac{A - (A^2 - B)^{\frac{1}{2}}}{C} \tag{2.46}$$

where

$$A = \beta_{OV_{N_2}} P_w + \left(\alpha_{OV_{VOC}} - \beta_{OV_{N_2}}\right)\left(P_w + P''_w\right)$$

$$B = 4\alpha_{OV_{VOC}} P_w P''_w x_w \left(\alpha_{OV_{VOC}} - \beta_{OV_{N_2}}\right)$$

$$C = 2P''_w \left(\alpha_{OV_{VOC}} - \beta_{OV_{N_2}}\right)$$

The IMSL subroutine BVPFD was used to solve numerically the set of nonlinear ordinary differential equations (2.41) to (2.44) using boundary conditions (2.45). Initial estimate for each dependant variable at the selected grid point was generated by solving the set of differential equations as an initial value problem, assuming cocurrent flow using the IMSL subroutine IVPRK (Majumdar, 1986; Guha, 1989).

2.4 Results and Discussion

2.4.1 Experimental Results for Steady State Removal of VOCs with or without a Thin ILM

The results for removal of volatile organic compounds (VOCs) via steady state vapor permeation with or without a thin silicone oil-based immobilized liquid membrane (ILM) are presented and discussed here. Module 1 obtained from

Applied Membrane Technology (AMT Inc., Minnetonka, MN) was used for all steady state type of experiments.

For this set of experiments, the nitrogen gas stream containing the VOC was passed through the tube side of the hollow fiber module while a high or medium vacuum (~1-30 torr) was applied to the shell side. The feed gas flow rate was varied in the range of 50-600 cc/min; the acetone and toluene concentrations used ranged from ~ 20 ppmv to ~1% and for methanol from ~68 ppmv to ~ 13%.

Measurements of nitrogen permeate flow rate in order to determine the permeance of nitrogen through the silicone skin $(Q/\delta)_c$, the overall N_2 permeance $(Q/\delta)_{OV}$ across the silicone skin and the thin ILM and nitrogen permeance through the oil $(Q/\delta)_l$ in this composite membrane were carried out with Module 1 and Module 2. Table 2.3 shows the results of the nitrogen permeate flow rate measurements for different feed pressures. When Module 2 was used with fully immobilized liquid membrane in the pores of the hollow fiber, no permeate flow was observed for pressures below 20 psig. Based on these measurements, the thickness of the thin ILM immobilized in the hollow fiber Module 1 was determined. The thin ILM thickness was found to be 4.7μm, which is about 25% of the thickness. A sample calculation is provided in Appendix A.

Table 2.4 illustrates the flux and percent removal of different VOCs for changing feed flow rates in Module 1 without any ILM incorporated in the porous structure. As one can see, the percent removal varied along with a change of the

Table 2.3 Gas Permeance Measurements for Hollow Fiber Module Containing no ILM, with Thin and Full ILM

Module No.	Feed pressure (psig)	N_2 permeate flow rate (cc/min)	N_2 permeance ($cm^3/s\ cm^2$ cmHg)	CO_2 permeate flow rate (cc/min)	CO_2 permeance ($cm^3/s\ cm^2$ cmHg)
Module 1 no ILM	15	42.0	1.65 E-5	513	2.28 E-4
Module 1 no ILM	10	27.0	1.59 E-5	N.A.	N.A.
Module 1 no ILM	5	13.7	1.61 E-5	N.A.	N.A.
Module 1 thin ILM	15	3.1	1.22 E-6	N.A.	N.A.
Module 1 thin ILM	10	2.2	1.30 E-6	N.A.	N.A.
Module 1 thin ILM	5	1.3	1.53 E-6	N.A.	N.A.
Module 2 full ILM	20	0.3	2.36 E-7	N.A.	N.A.
Module 5 no ILM	15	12.7	8.8 E-6	150.0	1.12 E-4
Module 5* no ILM	10	8.8	9.2 E-6	101.0	1.13 E-4
Module 5 no ILM	5	4.7	9.8 E-6	51.0	1.12 E-4

* Separation factor between CO_2 and N_2: $\alpha = 12.2$

Separation factor is defined as: α = permeance CO_2/permeance N_2

Table 2.4 Flux and Percent Removal* of VOCs from Nitrogen at Different Feed Flow Rates** and VOC Concentrations

VOC	Feed Composition (ppmv)	Feed Flow Rate (cc/min)	Product Flow Rate (cc/min)	Product Composition (ppmv)	Permeate Composition (ppmv)	Permeate Pressure (torr)	VOC Flux (gmol/ s cm^2)	VOC Percent Removal (%)
Methanol	10 000	100	64	73	24 000	33.8	13.5 E-10	99.5
Methanol	10 000	150	115	104	36 410	33.3	22.2E-10	99.2
Methanol	10 000	200	160	115	44 370	33.4	29.6 E-10	99.1
Toluene	1 953	150	108	5	6 740	32.3	3.9 E-10	99.8
Toluene	1 953	250	206	67	10 890	33.3	6.4 E-10	97.2
Acetone	11 000	100	63	~ 0	29 440	32.5	14.9 E-10	99.9
Acetone	11 000	100	62	~ 0	25 690	32.6	14.9 E-10	99.9
Acetone	11 000	150	109	82	37 280	32.8	22.9 E-10	99.4
Acetone	11 000	200	160	428	47 410	32.7	28.9 E-10	96.9
Acetone	11 000	207	174	515	53 220	32.9	29.7 E-10	96.1

* Feed pressure in all experiments was atmospheric
** Module 1 without any ILM

feed flow rate and the type of VOC used. As expected, the percent removal decreases as the feed gas flow rate increases (Figure 2.10). The permeate fluxes for acetone and methanol were almost in the same range; however, toluene permeate fluxes were much lower since toluene inlet concentration was only ~ 2000 ppmv compared to the inlet concentrations (~1.0%) of the other two VOCs (Figure 2.10). On the other hand, the nitrogen flux is basically independent of the gas flow rate, but the VOC fluxes increase as the flow rate is increased giving higher selectivities (Table 2.4). As one can see, the purification of the gas stream depends on the feed inlet flow rate and the type of the VOC to be removed. For this set of steady state experiments, high percent removal (96 - 99 %) was accomplished for all VOCs regardless of the flow rate. Even at a flow rate of 250 cc/min, around 97% of toluene was removed. This corresponds to a flow rate of 0.84 cc/min/fiber. The permeate side vacuum was between 32 and 33 torr. In this case where a bare membrane was used, it appears that the silicone skin on the outer side of the hollow fibers was rather thin and therefore, higher vacuum levels could not be achieved.

The same module (Module 1) was used to study the effect of immobilizing silicone oil in part of the pores of the hollow fiber in order to marginally reduce the VOC fluxes and improve the separation factor considerably. The thin ILM preparation was previously described and it can be found in section (2.2.4). The nitrogen permeate flow rate was cut down from ~ 37 cc/min to ~ 3-4 cc/min. In order to study the benefit of the thin ILM, experimental conditions used were the same as in the experiments with bare membrane (Module 1). Table 2.5 shows the

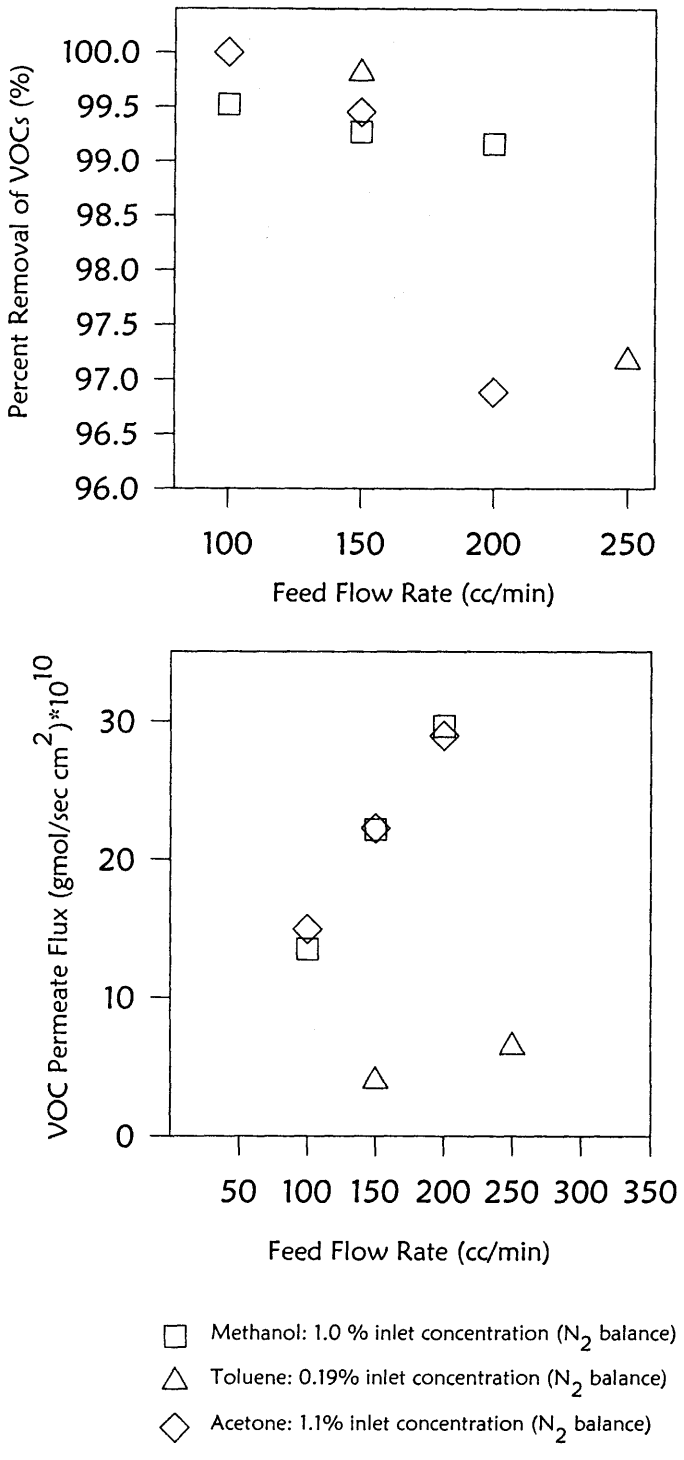

Figure 2.10 Dependence of percent removal of VOCs and VOC flux on feed gas flow rate for the membrane without ILM.

Table 2.5 Flux and Percent Removal of VOCs from Nitrogen at Different Flow Rates and VOC Concentrations with ILM

VOC	Feed Composition (ppmv)	Feed Flow Rate (cc/min)	Product Flow Rate (cc/min)	Product Composition (ppmv)	Permeate Composition (ppmv)	Permeate Pressure (torr)	VOC Flux (gmol/ s cm^2)	VOC Percent Removal (%)
Methanol	9 200	100.8	95.5	2 930	86 120	19.1	8.8 E-10	69.8
Methanol	9 200	150	144.8	4 290	100 050	17.9	10.3 E-10	55.0
Methanol	9 200	200	195	4 500	110 420	17.9	13.1 E-10	52.0
Toluene	1 953	152	147	490	26 310	17.9	3.0 E-10	75.7
Toluene	1 953	200	194	720	27 830	17.4	3.4 E-10	64.0
Toluene	1 953	252	248	890	28 510	17.4	3.6 E-10	55.0
Acetone	11 000	100	94	2590	80 820	19.2	11.5 E-10	77.6
Acetone	11 000	100	95	3 690	74 510	30.0*	10.2 E-10	68.0
Acetone	11 000	146	141	4 030	91 940	18.3	14.4 E-10	64.5
Acetone	11 000	187	182	5 710	95 940	18.4	13.6 E-10	49.0
Acetone	11 000	205	200	5 920	123 270	18.0	14.4 E-10	47.5

flux and the percent removal for the hollow fiber module (Module 1) after immobilization of the silicone oil. The change in nitrogen flux and the separation factor before and after immobilization of silicone oil in the porous structure are shown in Figure 2.11. As one can see, the nitrogen flux was reduced 7-8 times whereas the VOC flux was marginally reduced. The separation factor, which is defined as a ratio of VOC permeance to the permeance of nitrogen is plotted as a function of the feed gas flow rate. As one can see, the separation factor increased 5 to 20 times depending on the type of the VOC and the feed gas flow rate. The highest increase in separation factor was obtained for toluene, whose separation factor increased approximately 19 times.

Another benefit of having the ILM incorporated in the porous structure is, that 2-5 times more concentrated permeate side stream is produced since the nitrogen flux was reduced (Figure 2.12). The permeate side composition for the case of methanol, acetone and toluene is plotted versus the gas flow rate; as the gas flow rate increases, the permeate side composition increased too, since the feed composition increased throughout the permeator length. It is known that for the silicone membrane, the VOC permeability will increase as the VOC concentration increases.

The separation performance of the thin ILM was studied also using low concentrations of methanol or toluene by varying the feed gas flow rates and the inlet concentrations. Table 2.6 provides a summary of how the methanol flux and the percent removal varies with the flow rate when the inlet feed concentration was ~ 292 ppmv. As one can see, high percent removal (~99.9 %)

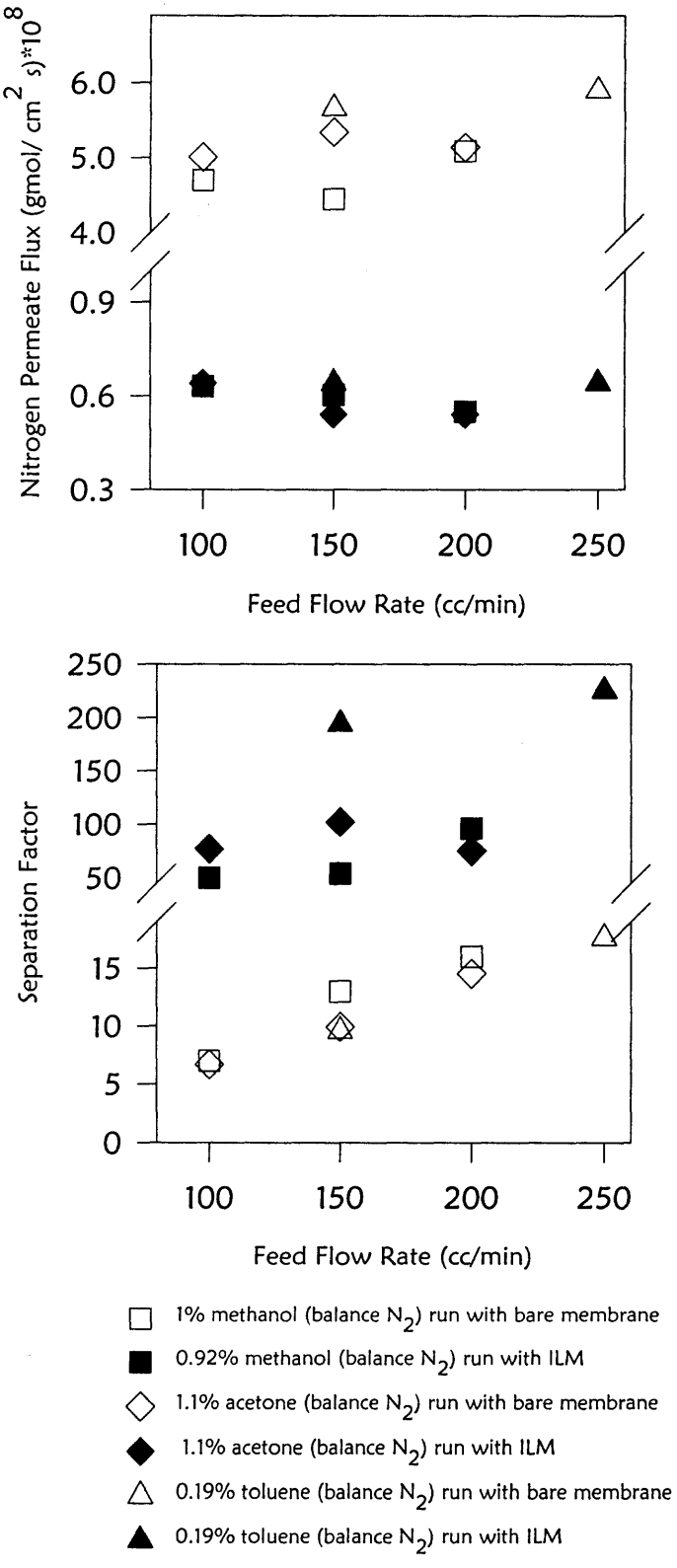

Figure 2.11 Effect of silicone oil immobilization on the variation of Nitrogen flux and separation factor (Module 1).

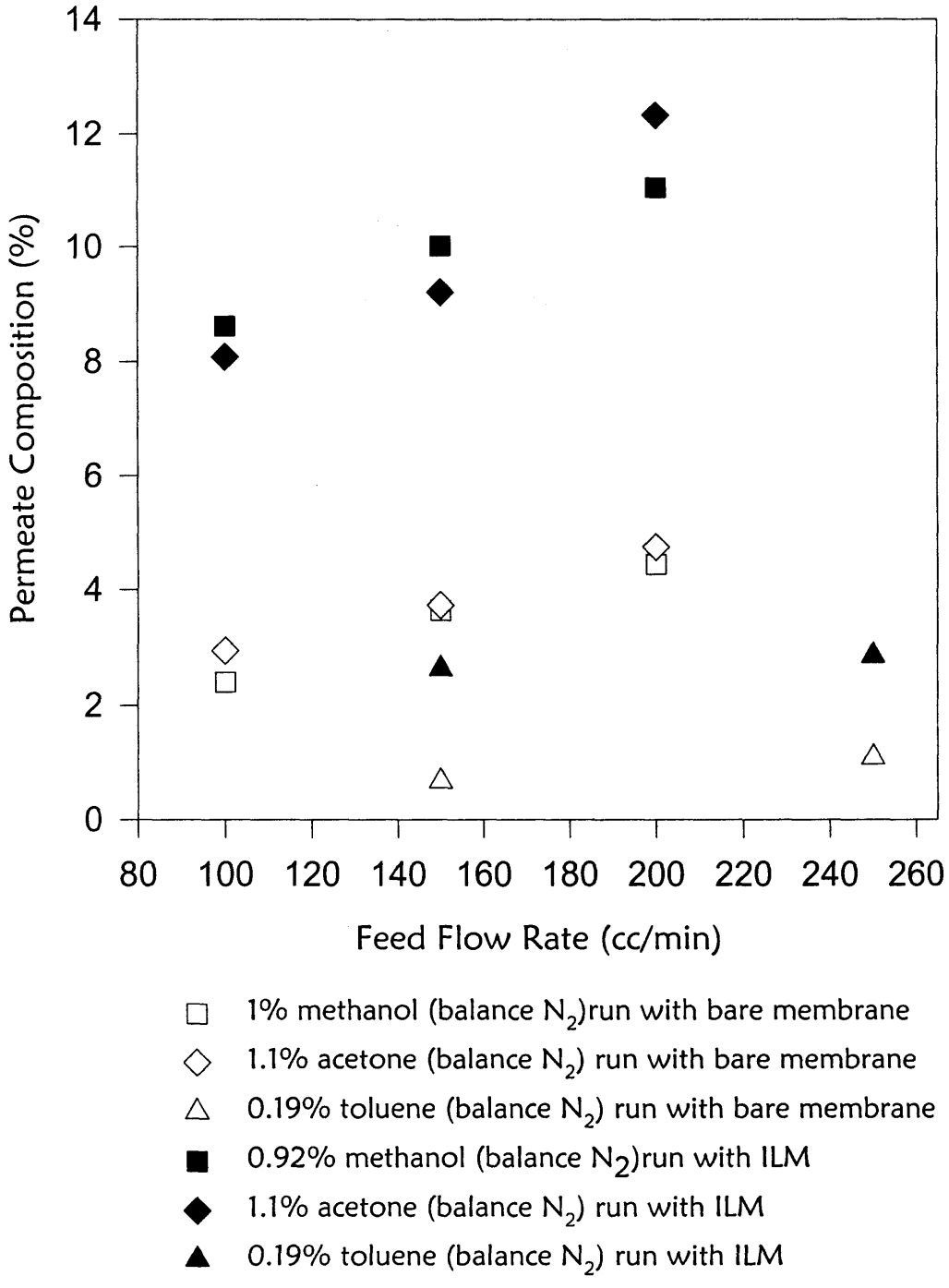

Figure 2.12 Effect of silicone oil immobilization on the permeate side composition (Module 1).

Table 2.6 Flux and Percent Removal of Low Concentration of Methanol from Nitrogen at Different Flow Rates*

VOC	Feed Composition (ppmv)	Feed Flow Rate (cc/min)	Product Flow Rate (cc/min)	Product Composition (ppmv)	Permeate Composition (ppmv)	Permeate Pressure (torr)	VOC Flux (gmol/ s cm^2)	VOC Percent Removal (%)
Methanol	292	51.1	48	~ 0	4 810	1.0	2.01 E-11	99.9
Methanol	292	103	99	56	6 590	7.0	3.31 E-11	81.0
Methanol	292	104	101	51	7 230	1.1	3.43 E-11	83.0
Methanol	292	152	148	99	8 720	3.0	4.02 E-11	67.0
Methanol	292	217	213	132	8 630	7.6	4.80 E-11	55.7
Methanol	292	299	295	167	9 740	10.1	5.12 E-11	43.0
Methanol	292	488	484	229	7 920	3.0	4.30 E-11	22.0
Methanol	292	600	596	234	8 950	3.0	4.86 E-11	20.0

* Module 1 with ILM

can be achieved when the flow rate was around 50 cc/min. It is observed that at the given inlet methanol concentration, percent removal of methanol decreased with an increase in feed flow rate, e.g. for 600 cc/min it came down to 20% (Figure 2.13). This module was also tested for the performance and percent removal of methanol in the case where high to moderate flow rates (~600 -300 cc/min) and lower inlet concentrations (from ~180 to 68 ppmv) were used (Table 2.7). Highest percent removal (~99.99%) was achieved when the inlet gas flow rate was reduced to 100 cc/min and the inlet methanol concentration of 68 ppmv. Generally, it can be concluded, that the percent removal of VOC decreases as the feed inlet gas flow rate increases (Table 2.7).

Table 2.8 summarizes the results of low inlet concentrations of toluene at different gas flow rates. For a feed composition of ~215 ppmv, the percent removal decreases as the feed gas flow rate increases from 100 to 300 cc/min (Figure 2.13). Even though lower inlet concentrations and higher gas flow rates were used, toluene percent removal still stayed quite high (~ 86%). If one compares the methanol and toluene results for the inlet feed gas composition of the approximately same level (~200 ppmv), it is obvious that better purification and removal was obtained for toluene since toluene has a much higher solubility in silicone oil than the other VOCs used in this study (Poddar et al., 1996; Xia et al., 1999).

For the case of the higher inlet methanol concentration in a feed gas, the latter was varied from 13.7% to 8.9%, depending on the pure nitrogen gas flow rate and the blending ratio. As mentioned earlier, a high concentration of

Table 2.7 Flux and Percent Removal of Various Low Inlet Concentration of Methanol from Nitrogen at Different Flow Rates for the Membrane Containing Thin ILM*

VOC	Feed Composition (ppmv)	Feed Flow Rate (cc/min)	Product Flow Rate (cc/min)	Product Composition (ppmv)	Permeate Composition (ppmv)	Permeate Pressure (torr)	VOC Flux (gmol/ s cm^2)	VOC Percent Removal (%)
Methanol	182.5	595	590	133	6 640	3.0	4.05 E-11	27.5
Methanol	112	605	601	62	7 270	3.0	4.14 E-11	45.0
Methanol	90	294	290	47	3 350	3.0	1.73 E-11	48.0
Methanol	78.6	202	198	29	2 620	7.6	1.38 E-11	64.0
Methanol	67.8	102	98	~ 0	1 820	7.6	0.94 E-11	99.9

* Module 1 with ILM

Table 2.8 Flux and Percent Removal of Low Concentration of Toluene from Nitrogen at Different Flow Rates for the Membrane Containing Thin ILM*

VOC	Feed Composition (ppmv)	Feed Flow Rate (cc/min)	Product Flow Rate (cc/min)	Product Composition (ppmv)	Permeate Composition (ppmv)	Permeate Pressure (torr)	VOC Flux (gmol/ s cm^2)	VOC Percent Removal (%)
Toluene	215	106	103	~ 0	6 520	1.6	3.01 E-11	99.9
Toluene	215	209	205	7.0	12 740	1.3	5.90 E-11	96.8
Toluene	215	311	307	25	15 170	1.2	8.04 E-11	88.5
Toluene	54	423	419	7.4	5 390	2.5	2.68 E-11	86.4
Toluene	23	323	320	~ 0	2 410	3.0	0.99 E-11	99.9

* Module 1 with ILM

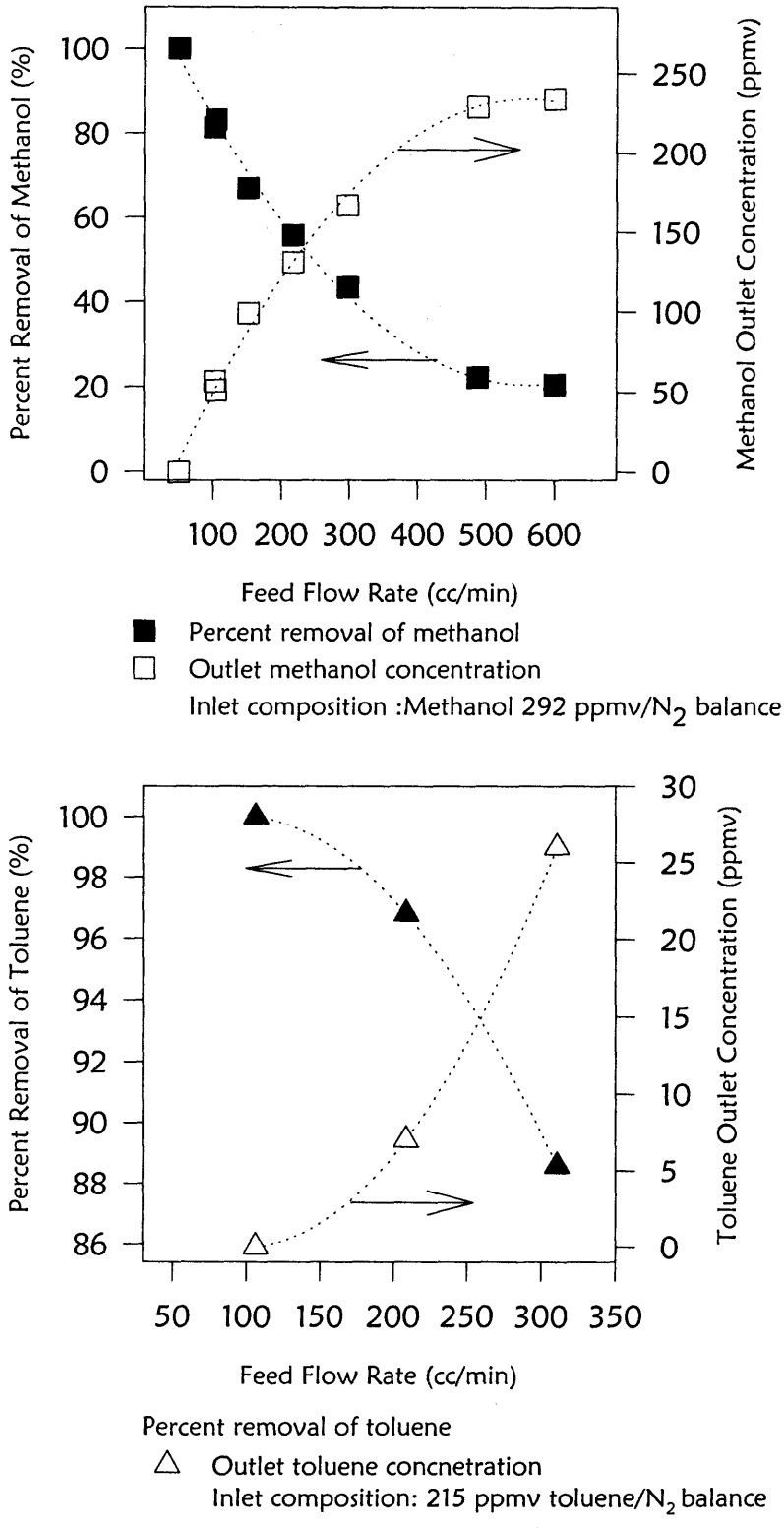

Figure 2.13 Dependence of percent removal and outlet concentration of Methanol and Toluene on flow rate with thin ILM (Module 1).

methanol was obtained by passing pure nitrogen at a certain flow rate through the liquid methanol. Lower inlet VOC concentrations in the same range of feed gas flow rate were obtained by blending the VOC-containing nitrogen gas stream with pure nitrogen gas stream in a certain ratio. The experimental results for high inlet concentration of methanol are presented in Table 2.9. It can be seen that at the flow rate of around 50 cc/min, 98% removal was achieved for the inlet feed composition of 8.9% and 10.9%. Percent removal of methanol was reduced to 77% at a higher nitrogen flow rate, although it had a somewhat higher inlet feed gas concentration (~12.9%).

So far, ILMs were found unstable for the commercial application usually due to evaporation of the immobilized liquid or due to the inability of the ILMs to withstand the transmembrane pressure difference. Therefore, in order to show the stability of this system, an extended time stability run (upto six months) was performed with the Module 1 having a thin ILM. The shell side of this module was constantly exposed to the vacuum. The vacuum level was varied from 33 torr to 1.0 torr depending on whether an oilless or an oil lubricated vacuum pump was used. Nitrogen flow rate was first set at 50 cc/min and later reduced to ~ 20 cc/min. The nitrogen permeate flow rate was estimated occasionally to ensure ILM stability by measuring the product flow rate. Once a week, an acetone-containing feed gas mixture having a composition of around 1% acetone/N_2 balance mixture was used in the experiment to determine the module performance for VOC removal. Results of this longterm stability run are plotted in Figure 2.14. The results summarized in Table 2.10 are for Module 1 that was periodically used for

Table 2.9 Flux and Percent Removal of Methanol from Nitrogen at Different Gas Flow Rates for Various High Inlet Methanol Concentrations Using the Membrane Containing Thin ILM*

VOC	Feed Composition (ppmv)	Feed Flow Rate (cc/min)	Product Flow Rate (cc/min)	Product Composition (ppmv)	Permeate Composition (ppmv)	Permeate Pressure (torr)	VOC Flux (gmol/ s cm^2)	VOC Percent Removal (%)
Methanol	137 000	52	48	16 000	N.A.	3.0	9.23 E-09	89.0
Methanol	89 000	53	50	1 200	N.A.	2.0	6.78 E-09	98.7
Methanol	109 000	53	49	1 300	N.A.	2.0	8.31 E-09	98.9
Methanol	129 000	104	101	3 100	N.A.	2.0	7.7 E-09	77.8

* Module 1 with ILM

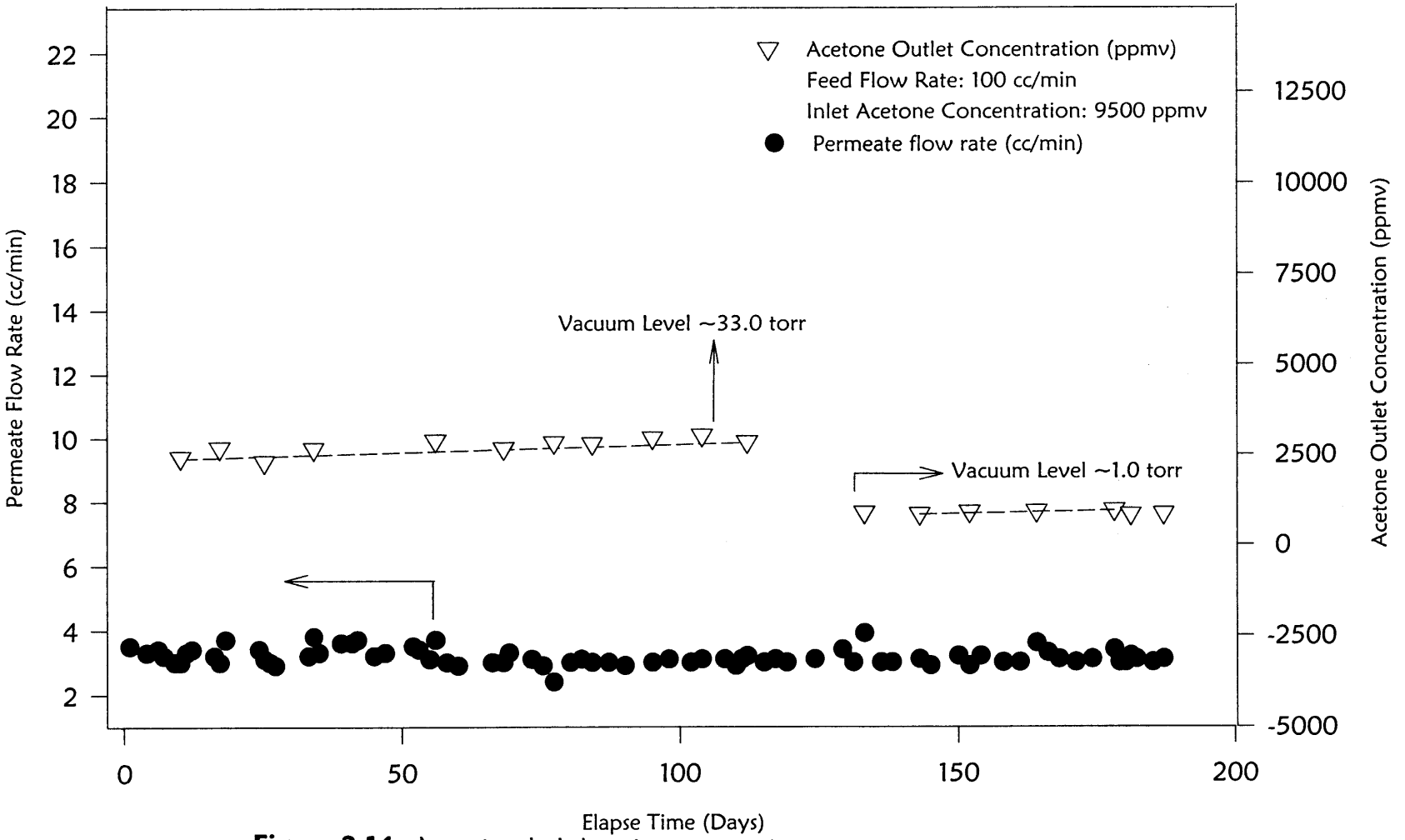

Figure 2.14 An extended duration run to determine membrane stability.

Table 2.10 Stability of Thin ILM Immobilized in Module 1 Periodically Used over Period of 2 Years

VOC	Feed Composition (ppmv)	Feed Flow Rate (cc/min)	Product Composition (ppmv)	Permeate Flow Rate (cc/min)	Permeate Pressure (torr)	Date
Acetone	11 000	100	3 570	2.4	19.9	4/29/99
Acetone	9 500	100	2 770	2.0	16.6	5/16/00
Acetone	9 500	100	910	2.7	2.2	4/26/01

* Module 1 with ILM

the VOC removal over a period of 2.0 years. Beside the extended run, a stable performance of the thin ILM was confirmed once more.

As one can see, the nitrogen permeate flow rate was always around 3 cc/min and it stayed at that level throughout the whole duration of the experiment which indicates that this thin ILM was not deteriorating. In the same figure, the VOC outlet concentration was plotted versus the elapsed time. The level of VOC purification for a given module, the inlet concentration and the flow rate was always the same. A higher purification of the VOC was accomplished only when the oil lubricated vacuum pump was used since a much higher vacuum level was achieved (~ 1 torr) which created a higher driving force for the VOC removal.

Experimental results were also used to compare the results of these runs with those obtained by numerically simulating the mathematical model of the permeator. The procedure adopted to determine all parameters needed for the simulation have been described previously. The values of various parameters used for the simulations of VOC separation are given in Table 2.11. Experimental results for determination of VOC permeance through the oil are summarized in Table 2.12. Results for the medium and low ranges of VOC inlet gas concentrations from experimental data obtained with Module 1 with and without the ILM (Tables 2.4, 2.5, 2.6) were simulated using the same values for $\left(\frac{Q}{\delta}\right)_{VOC_i}$ and overall VOC permeance and in both cases the VOC outlet concentrations were well anticipated. The results of numerical simulations are plotted along with the

Table 2.11 Description and Values of Parameters used in Simulation of VOC Permeation with Thin ILM of Silicone Oil

Description of the parameter, unit	Value
Feed: Toluene/N_2, MeOH/N_2, Acetone/N_2	
Length of the fibers, cm	20.5
Experimental Temperature, °C	25.0
"a" of (Q_{voc})=a*exp(b*p_{voc}), gmol/cm²cmHg s	200.0 E-10 Toluene; 80.0 E-10 MeOH; 155.0 E-10 Acetone
"b" of the above equation, 1/atm	50.0 Toluene; 25.0 MeOH; 22.0 Acetone
"a(N_2)" of (Q_{N2})=a(N_2)*exp(b*p_{N2}), gmol/cm²cmHg s	6.0 E-10
"b(N_2)" of the above equation, 1/atm	0.0
VOC permeance through full ILM δ_{lFull} no coating, gmol/cm²cmHg s	Toluene 4.3E-8 Methanol 1.0E-9 Acetone 1.5E-9
N_2 permeance through full ILM δ_{lFull} no coating, gmol/cm²cmHg s	1.3 E-11
VOC permeance through thin ILM δ_l no coating, gmol/cm²cmHg s	Toluene 2.0 E-7 Methanol 5.3E-9 Acetone 7.7E-9
N_2 permeance through thin ILM δ_l no coating, gmol/cm²cmHg s	9.0 E-11
Pressure of the feed inlet, cmHg	Atmospheric
Pressure on the vacuum side, cmHg	Experimental value
Viscosity of the N_2 at 25°C, poise (g/cm s)	1800.0 E-7
Flow rate of the gas, cm³/min	Experimental value
Mol fraction of VOC at the feed inlet	Experimental value
i.d. of the fiber, cm	240.0 E-4
o.d. of the fiber, cm	290.0 E-4
*Number of fibers	300

* Module 1

Table 2.12 Experimental Results for VOC Removal using Module 2 for Determination of VOC Permeance through the Silicone Oil

VOC	Feed Composition (ppmv)	Feed Flow Rate (cc/min)	Product Composition (ppmv)	Product Flow Rate (cc/min)	Permeate Pressure (torr)	Percent Removal (%)
Methanol	292	51.8	213	51.4	7.0	27.6
Toluene	548	103.4	35	103.0	2.0	93.6
Acetone	9500	102.0	7079	101.6	0.1	25.7

experimental values in Figures 2.15 to 2.17. The results from the model are shown as dashed lines in the same figures. It is clear that the experimental results are described reasonably well by the simulated results from the mathematical model. The same holds true also for the results of Figure 2.14.

2.4.2 Experimental Results for Steady State Removal of Methanol Containing Water Vapor using Thin ILM

The results for water vapor permeation measurements with or without a silicone oil-based immobilized liquid membrane (ILM) are presented and discussed here. Removal of methanol (MeOH) from the humidified nitrogen stream via steady state vapor permeation through the full ILM was also tested. Module 5 (Table 2.2) prepared in the laboratory from plasmapolymerized silicone coated fibers obtained from Applied Membrane Technology (AMT Inc., Minnetonka, MN) was used to determine the water permeance through the silicone skin. Also, the same module was used to determine the MeOH and acetone permeances.

To characterize the membrane, N_2 and CO_2 permeation flow rates across the bare membrane having only a silicone skin on the OD were measured to determine their permeances through the silicone skin $(Q/\delta)_c$, and the CO_2/ N_2 separation factor (Table 2.3). The extents of VOC removal from the $MeOH/N_2$ gas mixture and $acetone/N_2$ gas mixture were studied using the bare membrane (Module 5). The feed gas flow rate was varied in the range of 50-323 cc/min; the

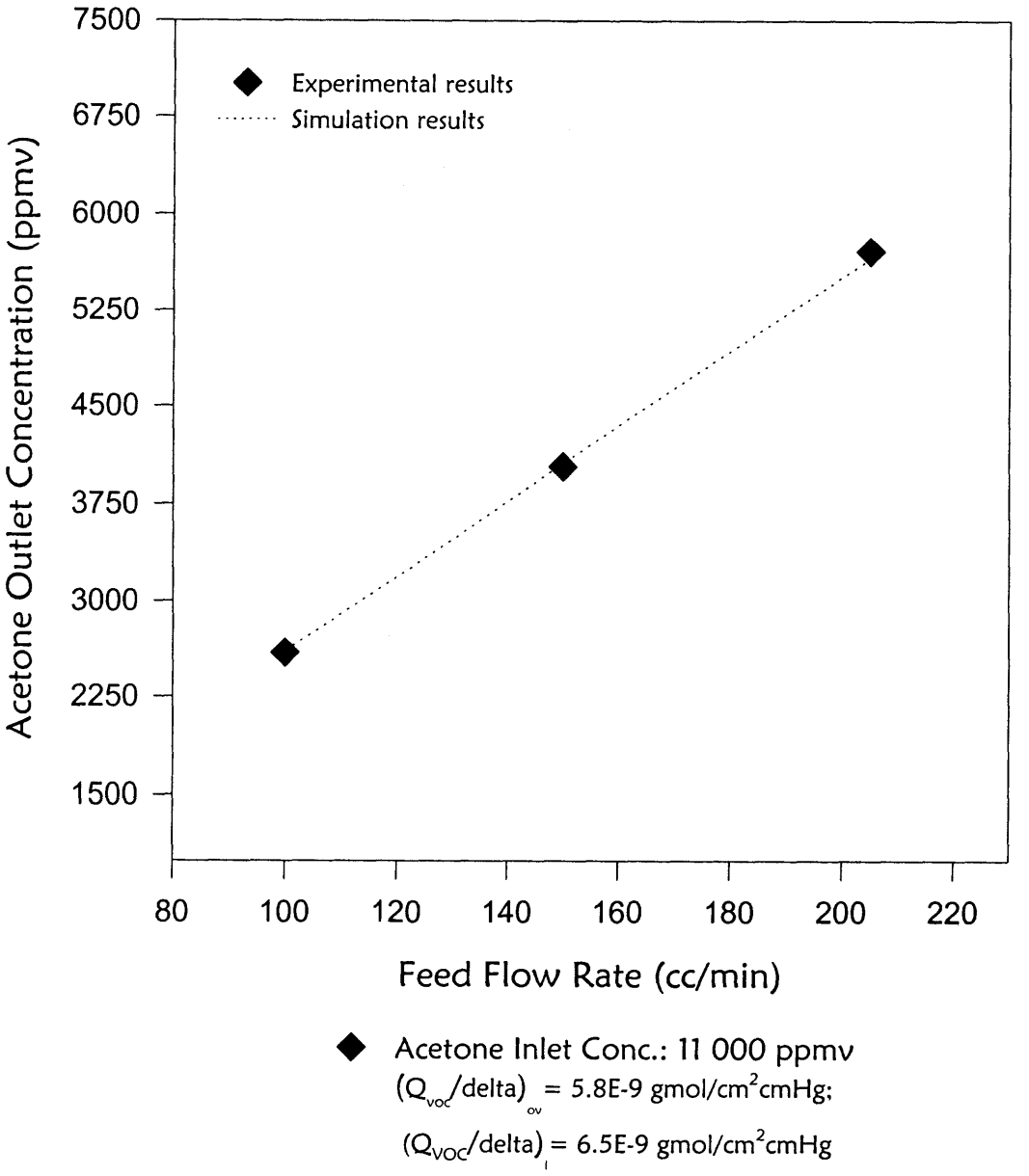

Figure 2.15 Variation of Acetone outlet concentration with feed inlet flow rate and comparison of experimental and simulation results.

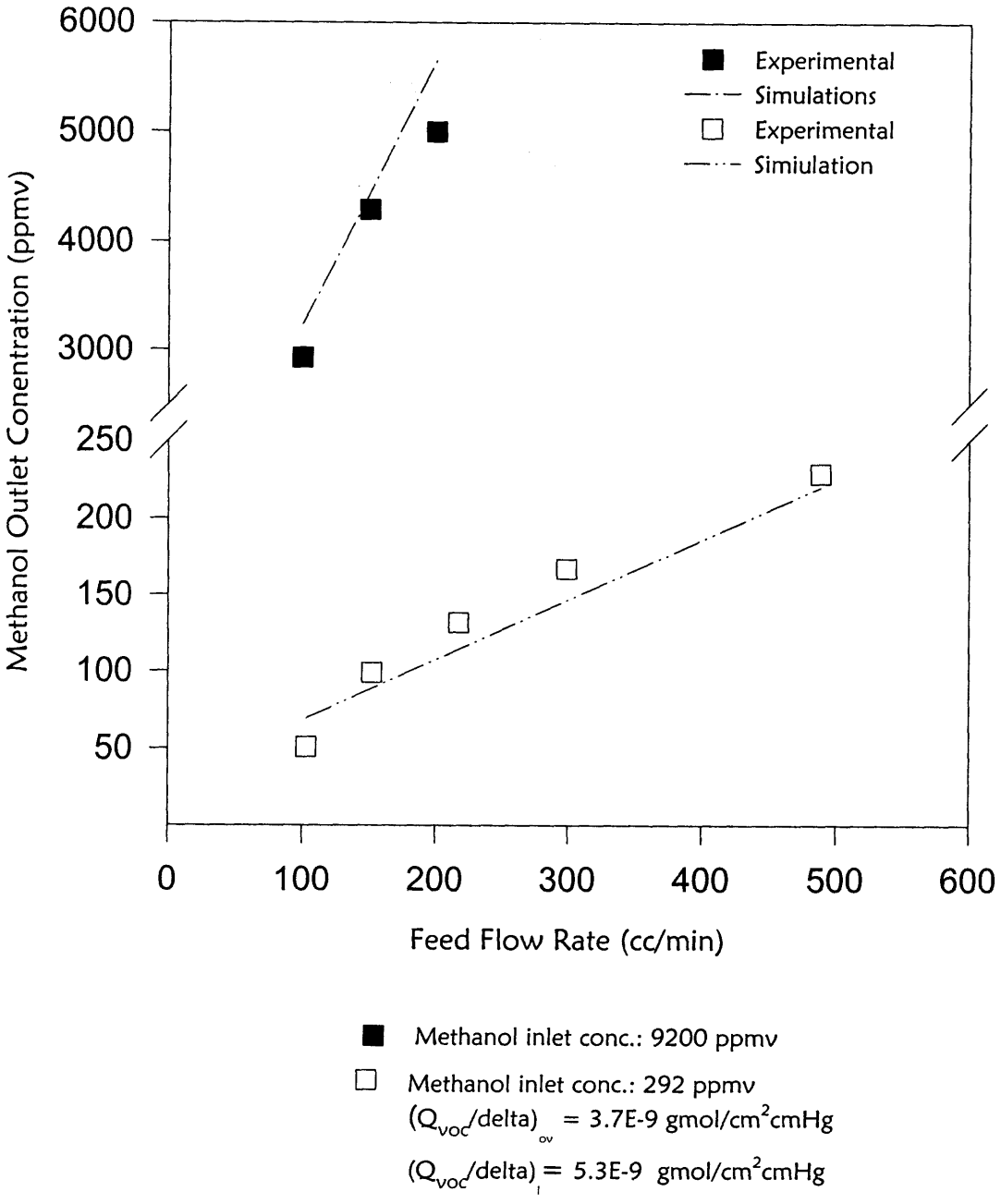

Figure 2.16 Variation of Methanol outlet concentration with feed inlet flow rate and comparison of experimental and simulation results.

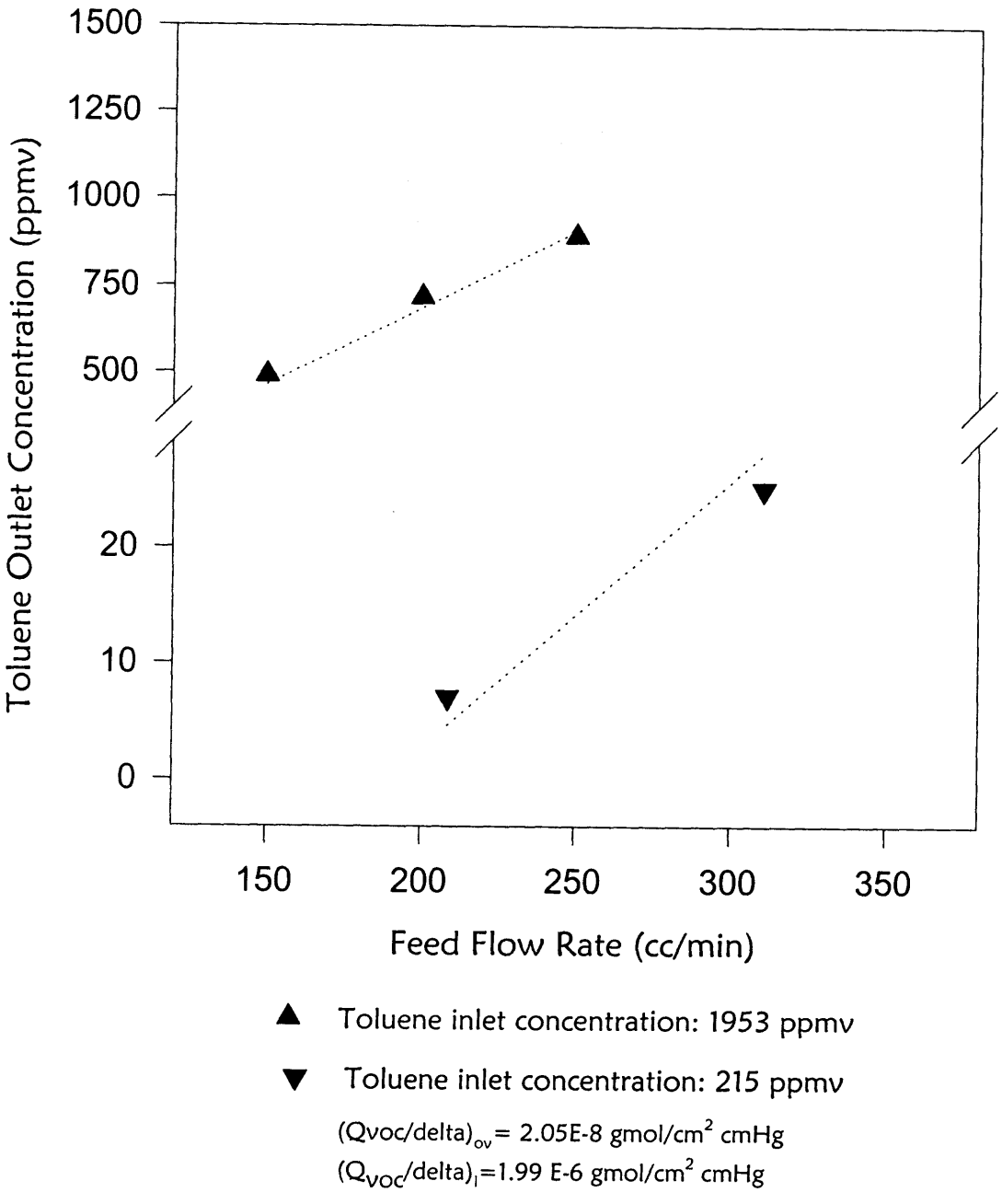

Figure 2.17 Variation of Toluene outlet concentration with feed inlet flow rate and comparison of experimental and simulation results.

acetone and methanol inlet concentrations used were 5900 ppmv and 292 ppmv respectively. Based on these measurements, it appears that the fibers in Module 5 have a somewhat thicker silicone skin than those in the Module 1 without the thin ILM. These results are summarized in Table 2.13.

Water vapor permeance through the silicone skin was measured using Module 5 (Table 2.14). Water vapor transport measurements were conducted using either the vacuum pump on the shell side or passing dry N_2 as a sweep gas. Water vapor permeances through the silicone skin under the vacuum condition were in the range of 2.4-4.5*10^{-4} cm^3/cm^2 s cmHg. When the sweep gas technique was used, under the constant feed flow rate and different feed gas pressures water permeance values varied between 2.7-7.5*10^{-5} cm^3/cm^2 s cmHg.

In order to determine any benefit of the silicone oil for MeOH removal from the humid N_2 stream, water vapor transport across the fully immobilized ILM of silicone oil was determined using Module 2. Humidified N_2 gas was passed through the bore of the hollow fibers while vacuum or dry N_2 gas on the shell side was passed as a sweep gas. Water vapor effective permeance through the fully immobilized silicone-oil membrane values varied from 6.7*10^{-5} to 1.9*10^{-4} cm^3/cm^2 s cmHg depending on the feed pressure and experimental conditions. For similar experimental conditions, e.g. shell side exposed to vacuum and feed gas is under atmospheric conditions, water vapor permeance through the silicone skin is much higher than that through the full ILM. When a dry sweep gas was used along with the similar experimental conditions, water vapor effective

Table 2.13 Flux and Percent Removal* of VOCs from Nitrogen at Different Feed Flow Rates and VOC Concentrations for Module 5**

VOC	Feed Composition (ppmv)	Feed Flow Rate (cc/min)	Product Flow Rate (cc/min)	Product Composition (ppmv)	Permeate Composition (ppmv)	Permeate Pressure (torr)	VOC Flux (gmol/ s cm^2)	VOC Percent Removal (%)
Methanol	292	51	39	~ 0	1 270	31.0	9.1 E-12	99.9
Methanol	292	102	89	~ 0	2 350	31.3	9.8 E-12	99.9
Methanol	292	323	311	10	7 790	31.0	8.7 E-12	96.8
Acetone	5 900	32	18.3	2 150	10 720	18.3	3.9 E-10	79.5
Acetone	5 900	56	43	3 690	13 210	20.8	4.4 E-10	52.0
Acetone	5 900	114	99	4 765	13 390	18.3	5.2 E-10	29.8

* Feed pressure in all experiments was atmospheric

** Module 5 without any ILM

Table 2.14 Water Vapor Flux in Module 5 without a Thin ILM

Experimental Conditions	RH_{in} (%)	RH_{out} (%)	Feed Flow Rate (cc/min)	Water Vapor Flux (cc/cm^2 sec)	Water Vapor Permeance (cc/cm^2 sec cmHg)
Shell side: vacuum 29 in Hg Feed side: atmospheric Product flow rate: 303 cc/min t= 21.3°C	99.5	4.6	325	4.4 E-4	4.5 E-4
Shell side: vacuum 28.9 in Hg Feed side: atmospheric Product flow rate: 149 cc/min t= 20.5°C	99.7	0.0	167	2.2 E-4	2.4 E-4
Shell side: dry N_2 sweep gas Sweep flow rate: 40 cc/min Feed side: atmospheric Product flow rate: 58 cc/min t= 25.1°C	98.5	58.6	58	4.2 E-5	2.7 E-5
Shell side: dry N_2 sweep gas Sweep flow rate: 42.8 cc/min Feed side: 5 psig Product flow rate: 55 cc/min t= 23.8°C	97.0	38.6	58	4.1 E-5	7.1 E-5

Table 2.14 Water Vapor Flux in Module 5 without a Thin ILM (Continued)

Experimental Conditions	RH_{in} (%)	RH_{out} (%)	Feed Flow Rate (cc/min)	Water Vapor Flux (cc/cm^2 sec)	Water Vapor Permeance (cc/cm^2 sec cmHg)
Shell side: dry N_2 sweep gas Sweep flow rate: 47.0 cc/min Feed side: 10 psig Product flow rate: 51.3 cc/min t= 22.3°C	99.2	30.0	58	3.2 E-5	6.2 E-5
Shell side: dry N_2 sweep gas Sweep flow rate: 48.6 cc/min Feed side: 13 psig Product flow rate: 49.7 cc/min t= 23.2°C	99.5	26.8	58	4.0 E-5	7.5 E-5

permeances determined are not far apart, e.g. silicone skin $2.7*10^{-5}$ cm^3/cm^2 s cmHg and for full ILM is $4.2*10^{-5}$ cm^3/cm^2 s cmHg.

The extent of MeOH removal along with the water vapor transport across the composite membrane was measured through the full ILM. For this experiment, humidified nitrogen gas stream was mixed with the dry $MeOH/N_2$ feed gas mixture. The $MeOH/N_2$ humidified gas mixture was analyzed with the GC in order to determine the inlet gas composition. The feed gas mixture was passed through the tube side of the hollow fiber module while vacuum was applied to the shell side. Inlet and outlet relative humidities were measured to determine water vapor permeance. The product stream was analyzed with the GC to determine the MeOH permeance and percent removal. Water vapor and MeOH permeances were $3.8*10^{-5}$ cm^3/cm^2 s cmHg and $2.2*10^{-5}$ cm^3/cm^2 s cmHg respectively. The experimental results are provided in Table 2.15.

Water vapor flux was calculated based on the temperature and the relative humidities of the inlet and outlet feed gas streams. The saturation vapor pressure (p_{sat}) for water vapor was obtained from Perry (1984) at a given temperature. The mole fraction of water vapor at saturation is given as

$$y_{H_2O}^{sat} = \frac{P_{sat}}{P_f} \tag{2.47}$$

where P_f is the total pressure of the feed side.

Mole fractions of water at the feed inlet and feed outlet of the module are:

$$\begin{aligned} y_{H_2O}^{in} &= RH_{in} \times y_{H_2O}^{sat} \\ y_{H_2O}^{out} &= RH_{out} \times y_{H_2O}^{sat} \end{aligned} \tag{2.48}$$

Table 2.15 Water Vapor Flux Using Module 2 with Full ILM without Silicone Skin

Experimental Condition	RH_{in} (%)	RH_{out} (%)	Feed Flow Rate (cc/min)	Water Vapor Flux (cc/cm^2 sec)	Water Vapor Permeance (cc/cm^2 sec cmHg)
Shell side: vacuum 29.5 in Hg Feed side: atmospheric Product flow rate: 10.4 cc/min t= 18.1°C	97.6	20.3	11.9	1.7 E-5	1.4 E-5
Shell side: vacuum 29.4 in Hg Feed side: 1.0 psig Product flow rate: 20.7 cc/min t= 21.0°C	91.2	34.9	22.2	2.8 E-5	6.7 E-5
Shell side: vacuum 29.4 in Hg Feed side: 2.5 psig Product flow rate: 42.6 cc/min t= 21.0°C	91.9	45.4	43.9	3.9 E-5	1.1 E-4
Shell side: vacuum 29.3 in Hg Feed side: 4.0 psig Product flow rate: 82.7 cc/min t= 23.3°C	97.0	53.1	84.3	7.1 E-5	1.9 E-4

Table 2.15 Water Vapor Flux Using Module 2 with Full ILM without Silicone Skin (Continued)

Experimental Condition	RH_{in} (%)	RH_{out} (%)	Feed Flow Rate (cc/min)	Water Vapor Flux (cc/cm^2 sec)	Water Vapor Permeance (cc/cm^2 sec cmHg)
Shell side: dry N_2 sweep gas Sweep flow rate: 30.0 cc/min $RH(\%)_{sweep}$: 30.9, t= 16.2°C Feed side: 2.0 psig Product flow rate: 41.5 cc/min t_{in}= 17.8°C, t_{in}= 17.1°C	98.6	52.9	43.0	3.2 E-5	4.5 E-5
Shell side: dry N_2 sweep gas Sweep flow rate: 30.0 cc/min $RH(\%)_{sweep}$: 18.6, t= 17.5°C Feed side: atmospheric Product flow rate: 11.0 cc/min t_{in}= 17.4°C, t_{in}= 17.4°C	99.6	29.9	12.5	1.5 E-5	1.6 E-5
Shell side: vacuum 29.4 inHg $RH(\%)_{sweep}$: 30.9, t= 16.2°C Feed side: 2.0 psig Product flow rate: 36.0 cc/min t_{in}= 16.8°C, t_{in}= 16.4°C % Removal MeOH: 38 C_{in}: 214 ppmv, C_{out}: 141ppmv MeOH:2.2E-5 cc/cm^2sec cmHg	22.5	7.6	37.5	8.2 E-6	3.8 E-5

Finally, water flux can be calculated using following expression

$$\text{Water Flux} = \frac{V_f\left(y_{H_2O}^{in} - y_{H_2O}^{out}\right)}{A} \tag{2.49}$$

where V_f is the feed side flow rate. Water permeance is obtained by dividing the equation 2.49 with the driving force

$$\text{Driving Force} = \begin{pmatrix}\text{Feed}\\ \text{Pressure}\end{pmatrix} \times \begin{pmatrix}\text{Mole fraction of i}\\ \text{in feed stream}\end{pmatrix} - \begin{pmatrix}\text{Peremate}\\ \text{Pressure}\end{pmatrix} \times \begin{pmatrix}\text{Mole fraction of i}\\ \text{in permeate stream}\end{pmatrix} \tag{2.50}$$

In calculating the driving force when the shell side was exposed to the relatively high vacuum, the permeate pressure was assumed to be close to zero. Therefore, the driving force is calculated based on the feed side conditions only. When the sweep gas technique was used, the driving force was calculated based on the feed side and/or sweep side measurements. A sample calculation is provided in Appendix C.

2.4.3 Experimental Results for Cyclic Mode of Operation for Removal of VOCs

The experimental results for the cyclic process are presented here. After Module 1 was immobilized with a thin layer of silicone oil in the porous structure, the hollow fiber module was used to study the effect of the cyclic mode of separation. The cycle time, T_{cycle}, was varied from 1.6 to 20 seconds. A number of experiments were carried out using Module 1 in the steady state mode of operation to investigate the benefit of the cyclic process. The product flow rate, which fluctuates due to the cyclic mode of operation, was calculated based on the

average value of all flow rates measured at the product surge drum outlet. Due to the change in the cycle times, it was quite difficult to maintain constant inlet feed gas flow rate or atmospheric condition on the bore side. Therefore, the feed side pressure was changing from 1.0 - to 4.0 psig. In order to avoid problems due to unsteady operations, later, two apparently identical hollow fiber modules were prepared and studied.

Table 2.16 illustrates the results obtained from a cyclic mode of separation of methanol, toluene and acetone from the feed N_2 stream. Initially, the separation performance was studied with T_{cycle}=20 seconds, e.g. $t_{abs/reg}$=10 seconds. The VOC inlet feed gas mixture flow rate was varied from 100 cc/min to 250 cc/min. As the feed gas flow rate was decreased, the VOC concentration in the treated surge drum was reduced also to different concentrations depending on the type of the VOC and inlet feed gas concentration. In all cases, the feed gas flow rate was set to various values (100-250 cc/min), whereas the actual inlet gas flow rate was more then 50% lower than the set value. This discrepancy occurred due to a difference in pressures on the feed side and the bypass line.

During the absorption part of the cycle, the feed gas was under a certain pressure (1.0-4.0 psig). Once the regeneration part of the cycle was started, feed flow was directed to the bypass line, which was open to the atmosphere. Therefore, once the feed gas was sent again through the bore of the fiber for the absorption part of the cycle, the surge drum acted as a backpressure regulator. Consequently, the feed gas was repressurized to the initial set value maintained by the surge drum. As a result, more gas was going through the bypass line than

Table 2.16 Experimental Results for Constant Cycle Time and Variable Inlet Gas Flow Rate for Removal of VOC Using Module 1 with an ILM

VOC	Cycle Time abs/reg (sec)	Feed Composition (ppmv)	Product Composition (ppmv)	Set Feed Flow Rate (cc/min)	Product Flow Rate (cc/min)	Feed Pressure (psig)	Permeate Pressure (torr)
Methanol	10/10	9 200	444	100	41	1.0	17.9
Methanol	10/10	9 200	1 470	150	64	2.0	17.9
Methanol	10/10	9 200	2 210	200	86	3.0	17.9
Toluene	10/10	1 953	16	150	66	1.0	17.4
Toluene	10/10	1 953	80	250	111	4.0	17.6
Acetone	10/10	11 000	490	100	47	2.0	17.6
Acetone	10/10	11 000	1 470	150	63	3.0	17.4
Acetone	10/10	11 000	2 560	200	91	4.0	17.6

through the lumen of the fiber module. In the case where one hollow fiber module was used, it was not feasible to measure the actual inlet gas flow rate. The estimate of the actual feed flow rate would be the sum of the measured product flow rate and permeate flow rate. This discrepancy is due to the surge drum pressure, which was maintained in order to draw a constant product flow for the GC analysis. Methanol product concentration increased from 444 ppmv to 2210 ppmv as the set inlet feed gas flow rate was increased from 100 to 200 cc/min maintaining the same cycle time (T_{cycle}=20 seconds). As the set gas flow rate was increased, the surge drum pressure was also increased from 1.0-3.0 psig. The same was observed for toluene, where the gas flow rate was set at 150 cc/min and 250 cc/min and accordingly the product concentration changed from 16 ppmv to 83 ppmv. For 1.1% acetone inlet concentration, the product composition changed from 490 ppmv to 2560 ppmv as the gas flow rate was increased from 100-200 cc/min.

Experimental results for acetone and methanol where the cycle time was varied for a constant feed gas flow rate are presented in Table 2.17. This table illustrates that an increase in t_{abs} from 0.8 seconds to 1.6 seconds (correspondingly T_{cycle} from 1.6 seconds to 3.2 seconds) increases the acetone concentration from 260 ppmv to 445 ppmv in the treated gas while the surge drum pressure was close to atmospheric. When the surge drum pressure was around 2 psig and t_{abs} was changed from 2.0 seconds to 10 seconds the product concentration increased from 140 ppmv to 490 ppmv. One can notice that the increased surge drum pressure and t_{abs}=2 seconds improved the acetone removal despite the fact that at

Table 2.17 Experimental Results for Different Cycle Times and a Constant Inlet Gas Flow Rate for Removal of Acetone and Methanol Using Module 1 with Thin ILM

VOC	Cycle Time abs/reg (sec)	Feed Composition (ppmv)	Product Composition (ppmv)	Set Feed Flow Rate (cc/min)	Product Flow Rate (cc/min)	Feed Pressure (psig)	Permeate Pressure (torr)
Acetone	0.8/0.8	11 000	260	100	38	Atmospheric	17.9
Acetone	1.6/1.6	11 000	445	100	41	Atmospheric	17.6
Acetone	2/2	11 000	140	100	32	2.0	17.6
Acetone	10/10	11 000	490	100	47	2.0	17.6
Methanol	1.6/1.6	9 200	410	100	38	Atmospheric	17.4
Methanol	2.0/2.0	9 200	425	100	39	Atmospheric	17.4

atmospheric conditions the absorption cycle time was lower (t_{abs}=0.8 seconds) which corresponds to the product composition of 140 ppmv and 260 ppmv. This is because the partial pressure driving force for VOC removal was higher for the elevated surge drum pressures. In the case of methanol, the feed pressure was maintained close to atmospheric, t_{abs} cycle times of 1.6 and 2.0 seconds gave the product composition of 410 to 425 ppmv respectively for a gas flow rate of 100 cc/min.

In order to study the benefit of the cyclic process, a set of steady state experiments was also performed with Module 1 and the results are given in Table 2.18. As one can see, the feed gas pressure for different inlet gas flow rates was atmospheric whereas in the cyclic process it was varied from 1.0 to 4.0 psig. Therefore, one experiment under steady state conditions was done at a feed gas pressure of 3.5 psig. The benefit of the increased partial pressure driving force was apparent as better purification of the product stream was achieved. Difficulties of measuring and matching the actual feed gas flow rates and maintaining the feed pressure at the same level in both modes of operations, made comparison of the potential advantage of a cyclic over a steady state process in terms of the product purification much harder (comparing Table 2.17 and Table 2.18).

Therefore, to overcome these problems, two identical modules (Modules 3 and 4) were prepared for the cyclic mode experiments and their characteristics are given in Table 2.2. Initially both modules were tested in a steady state mode of operation in order to get a base line of their performances. These results are presented in Table 2.19. Nitrogen permeation rate for Module 3 was around 10

Table 2.18 Experimental Results for Steady State Runs and Various Inlet Gas Flow Rates for Removal of Acetone, Toluene and Methanol Using Module 1 with Thin ILM

VOC	Cycle Time abs/reg (sec)	Feed Composition (ppmv)	Product Composition (ppmv)	Set Feed Flow Rate (cc/min)	Product Flow Rate (cc/min)	Feed Pressure (psig)	Permeate Pressure (torr)
Acetone	none	9 500	226	39	35	Atmospheric	17.9
Acetone	none	9 500	230	40	36	Atmospheric	17.4
Acetone	none	11 000	661	50	46	Atmospheric	18.0
Acetone	none	11 000	1 976	75	71	Atmospheric	18.0
Acetone	none	11 000	3 310	100	96.0	Atmospheric	19.1
Acetone	none	11 000	2 196	100	94.0	3.5	18.1

Table 2.18 Experimental Results for Steady State Runs and Various Inlet Gas Flow Rates for Removal of Acetone, Toluene and Methanol Using Module 1 with Thin ILM (Continued)

VOC	Cycle Time abs/reg (sec)	Feed Composition (ppmv)	Product Composition (ppmv)	Set Feed Flow Rate (cc/min)	Product Flow Rate (cc/min)	Feed Pressure (psig)	Permeate Pressure (torr)
Toluene	none	1 852	50	75	72	Atmospheric	17.9
Toluene	none	1 852	370	125	121	Atmospheric	17.96
Toluene	none	1 953	490	152	148	Atmospheric	17.9
Toluene	none	1 953	1 976	241	237	Atmospheric	17.4
Methanol	none	9 200	590	50	46	Atmospheric	17.5
Methanol	none	9 200	2 930	101	97	Atmospheric	19.1

Table 2.19 Experimental Results for Steady State Runs at Different Inlet Gas Flow Rates for Removal of Acetone and Methanol Using Modules 3 and 4

VOC/Module Number	Feed Composition (ppmv)	Product Composition (ppmv)	Feed Flow Rate (cc/min)	Product Flow Rate (cc/min)	VOC Permeate Flux ($gmol/cm^2s$)	Permeate Pressure (torr)	Percent Removal (%)
Acetone 3	3 000	1 370	50	40	2.4 E-10	20.5	63
Acetone 3	3 000	2 170	100	90	2.5 E-10	20.5	35
Acetone 3	3 000	2 630	150	140	2.0 E-10	20.4	18
Acetone 4	9 500	4 460	50	36	7.8 E-10	12.2	65
Acetone 4	9 500	6 730	100	85	9.5 E-10	12.2	40
Methanol 3	292	~ 0	53	44	3.9 E-11	0.01	99.9
Methanol 3	292	~ 0	100	91	7.4 E-11	0.01	99.9
Methanol 3	292	33	156	148	1.0 E-10	0.01	89

cc/min and for Module 4 around 15 cc/min. This indicated thicker silicone skin on the outer diameter of the hollow fibers in the case of Modules 3 and 4 than in Module 1. In addition, lower acetone permeate flux was observed for Modules 3 and 4 than it was for Module 1.

In order to demonstrate the potential benefit of the cyclic process, Modules 3 and 4 were studied in parallel and in series during the steady state operation. For the same inlet acetone containing gas flow rate of 100 cc/min. product compositions of 1060 ppmv and 1030 ppmv were achieved in the two cases of parallel and series connections. In addition to the two different connections of Modules 3 and 4, the effect of the different cycle time was studied. Results obtained under steady state and cyclic mode of operation after a considerable number of cycles (after 2-3 hours) are reported in Table 2.20. For the same gas flow rate of 50 cc/min, as cycle time was changed from 2 to 4 seconds, product concentration increased from 350 ppmv to 410 ppmv. Similarly, as cycle time was increased from 4 to 10 seconds while gas flow rate was set at 100 cc/min, acetone concentration increased from 1100 ppmv to 1160 ppmv at the outlet. As one can see, lower cycle time offer lower product concentration, but the obvious benefit of cyclic process over the steady state was hard to conclude since product concentrations differ only by 40 ppmv.

Table 2.20 Comparison of the Steady State and Cyclic Process Using Modules 3 and 4 in Series or Parallel for Removal of Acetone

VOC/Module Number	Cycle Time abs/reg (sec)	Feed Composition (ppmv)	Product Composition (ppmv)	Feed Flow Rate (cc/min)	Product Flow Rate (cc/min)	Permeate Pressure (torr)
Acetone 3 + 4 (in parallel)	none	1 810	1 060	100	78	29.2
Acetone 3 + 4 (in series)	none	1 810	1 025	100	77	25.8
Acetone 3 + 4 (in series)	none	1 810	1 030	100	76	18.5
Acetone 3 + 4 (in parallel)	2	1 810	350	50	27	26.7
Acetone 3 + 4 (in parallel)	4	1 810	410	50	27	27.3
Acetone 3 + 4 (in parallel)	4	1 810	1 100	100	78	26.5
Acetone 3 + 4 (in parallel)	10	1 810	1 160	100	81	26.0

2.5 Conclusions

The following conclusions were drawn from this study on the effect of immobilizing silicone oil in part of the porous substrate of the hollow fibers for VOC separation from N_2, water permeation and a cyclic process configuration:

- The separation factor of each VOC over nitrogen was increased 5- 20 times depending on the VOC and the feed gas flow rate.
- Nitrogen flux was reduced 7-12 times whereas the VOC flux was marginally reduced resulting in more VOC-enriched permeate stream.
- The thin ILM based hollow fiber can remove 99.9% of methanol and toluene for moderate flow rates (50-100 cc/min) and low inlet concentrations (200-300 ppmv). High percent removal (98.9%) was also achieved for very high inlet methanol concentrations and a gas flow rate of 50 cc/min. This gas flow rate corresponds to 0.166 cc/min/fiber.
- The thin ILM based hollow fiber membrane showed an extraordinary stability over an extended period of time (6 months - 2 years); this provides a basis for its potential larger-scale application in VOC-N_2/air separation.
- A numerical model for VOC separation describes the VOC removal from a N_2 stream satisfactorily when using experimentally determined parameters e.g. effective permeances through thin silicone oil, PDMS coating and overall permeance for N_2 and VOC for low and moderate VOC levels in the feed gas stream.

- Under similar experimental conditions, the effective water vapor permanence of silicone skin and full ILM are quite close. Although the thickness of the full ILM is much higher than the plasmapolymerized skin, silicone oil appeared quite permeable to the water vapor. This is considered possible due to the larger diffusion coefficient though the oil.
- The effect of the cyclic time on the product purity was studied. Lower cyclic times offer better product purification. The limited data did not allow any conclusion to be drawn regarding the benefit of cyclic process over steady state vapor permeation.

CHAPTER 3

SELECTIVE REMOVAL OF CARBON DIOXIDE FROM NITROGEN GAS STREAM USING IMMOBILIZED LIQUID MEMBRANES (ILMs)

3.1 Introduction

Large amounts of carbon dioxide (CO_2) are generated when fossil fuels/natural gases are burnt or used in chemical processes. Emissions from these sources are potential cause for global warming. Therefore, one of the main objectives of environmental control is the elimination and/or control of CO_2 emissions into the atmosphere. Besides the environmental concerns, highly CO_2- selective membrane is also needed for space applications where CO_2 has to be selectively removed from the crew compartments in order to regenerate the breathing air. For the space application, it is especially important to develop new membranes with higher CO_2 permeances which however must possess very high CO_2-N_2, CO_2-O_2 selectivities.

The most common device to remove CO_2 from such gas streams is the conventional absorption column using reactive liquids in order to increase the absorption rate and capacity. An aqueous solution of say, sodium hydroxide, sodium carbonate, monoethnolamine (MEA) or diethanolamine (DEA) (Danckwerts, 1970) is typically used in contacting columns for absorption and removal of CO_2. These conventional processes are energy intensive; in addition, they often have numerous operational problems (e.g. foaming, flooding etc.).

One of the alternatives to the conventional absorption process is a hydrophobic microporous membrane based gas-liquid contacting device where the absorption liquid flows on one side of the membrane and the gas flows on the other. Membrane-based contactors have several advantages over conventional packed columns: very larger interfacial area per unit volume (as much as 10-50 times larger) and independent control of liquid and gas flow rates without flooding, foaming etc.. They have been studied extensively by several authors for absorption of various gases in different applications (Qi and Cussler, 1985; Karoor and Sirkar, 1993; Rangwala, 1996).

Traditionally thin nonporous membranes are used for gas separations by permeation where the transport mechanism through such a membrane is based on solution-diffusion. A gas species dissolves in a membrane and diffuses across due to the concentration gradient. In the case of a synthetic polymeric membrane, selectivity and permeability are in general inversely related. Ideally, the membrane should not only be highly permeable to the species of interest, but it should maintain a high selectivity to be economically competitive.

The gas species mass flux and permeability can be increased if a liquid solvent is immobilized in a microporous membrane substrate. This immobilized liquid membrane (ILM) may have an added advantage since gaseous species have higher diffusivities through a liquid than through a solid. Further, an increase of mass flux and selectivity can be achieved if the liquid reversibly reacts with the species to be removed. This phenomenon in membranes is known as the facilitated transport mechanism and the membranes are called facilitated transport

membrane (FTM). The complexation reaction is another transport mechanism in addition to the solution-diffusion mechanism. The basic reaction mechanism between the carrier and the permeating species (e.g. CO_2) can be written as

$$\text{permeant} + \text{carrier} \xleftrightarrow{K_{eq}} \text{complex} \qquad (3.1)$$

The equilibrium of the complexation reaction must provide a balance between the complexation and the reverse reaction to recover the permeate and the carrier. The FTMs can offer high carbon dioxide (CO_2) permeances along with high selectivities. Therefore they have a good potential for industrial and space applications if one can overcome the liquid membrane stability problem.

Facilitated transport membranes (FTM) have few basic configurations:

- emulsion liquid membranes (ELM)
- ion - exchange membrane (IEM)
- immobilized liquid membrane (ILM)
- fixed-site carrier membranes.

Among these basic configurations of FTMs, immobilized liquid membrane (ILM) is the least stable form. Since, the advantage of ILM is that of a simple process design, increasing the membrane stability is of considerable interest. The standard way of preparing a facilitated transport membrane in the form of an ILM is to impregnate the porous membrane matrix with the liquid solution containing the carrier of interest. Microporous supports are selected based on pore size, porosity, thickness and surface properties. It is desirable that the liquid membrane solution easily wet the membrane to prevent gas leakage. The tortuosity of the membrane,

the membrane porosity and the membrane support thickness will strongly influence the permeant flux.

Facilitated transport of carbon dioxide across the ILM containing a primary amine as the carrier is shown in Figure 3.1. The CO_2, which is dissolved on the feed side boundary reacts with the carrier and diffuses across the ILM as a carbamate ion along with the dissolved CO_2 due to their concentration gradients. Once both species reach the sweep side boundary, the complexation reaction is reversed and free CO_2 is released from the liquid membrane. The amine diffuses back to the feed side boundary to form a complex again.

One of the earliest studies on facilitated transport started with a biological system and it was conducted by Scholander (1960) for selective separation of oxygen (O_2)/air gas mixture using a hemoglobin solution. In the beginning, removal of CO_2 across an aqueous bicarbonate film was studied by Langmuir et al. (1966). Many more studies on facilitated CO_2 transport using aqueous based ILMs containing various carriers were conducted e.g. bicarbonate (Ward and Robb, 1967; Otto and Quinn, 1971), diethanolamine (DEA) (Guha et al., 1990; Teramoto et al., 1996) and ethylenediamine (EDA) (Matsuyama et al., 1994). An earlier review paper is by Meldon et al. (1982).

However, for industrial applications, these membranes lack stability due to evaporation of the carrier and/or the solvent. In addition, allowable transmembrane pressure difference is limited since the liquid is held only by capillary forces in the pores of the porous substrate.

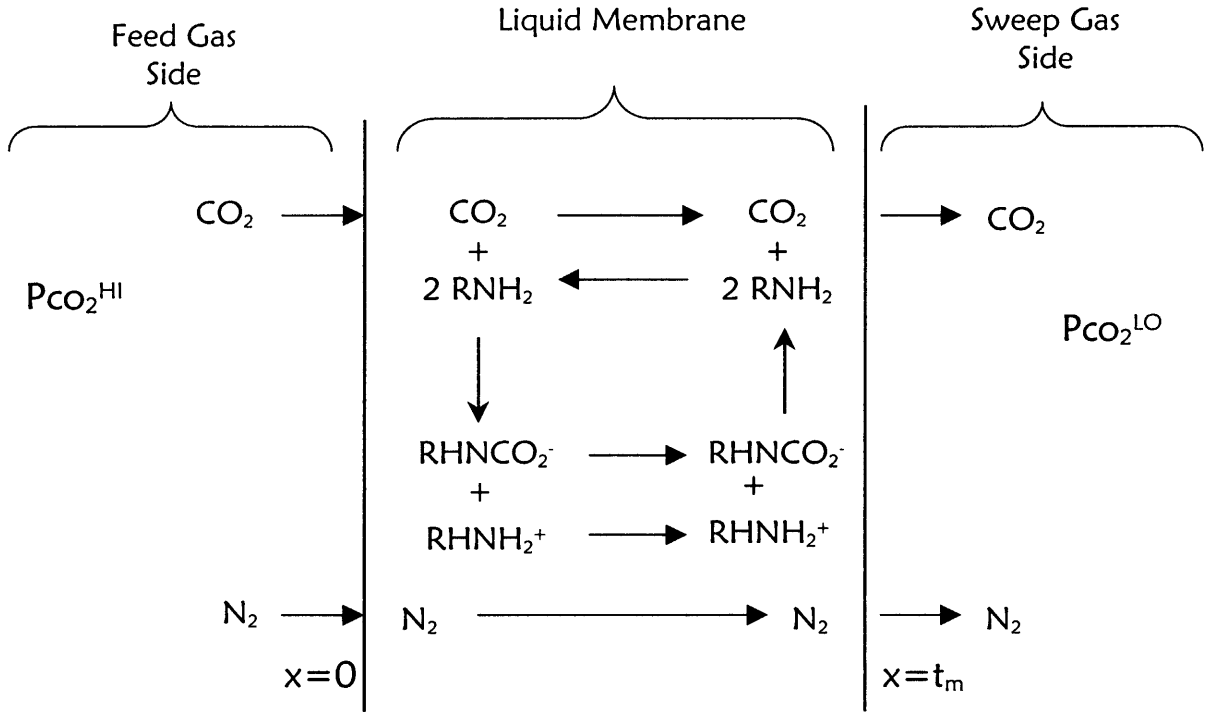

Figure 3.1 Facilitated transport of Carbon Dioxide through an immobilized liquid membrane.

Many efforts were made to overcome the stability problem of the ILM membranes for CO_2 removal. In order to increase the ILM stability, different low volatility and hygroscopic liquids were investigated. Polyethylene glycol (PEG) (Meldon et al., 1986; Saha and Chakma, 1995; Kim et al., 2001) and in the most recent studies, , glycerol (Chen et al. 1999, 2000, 2001), glycerol carbonate (Kovvali and Sirkar, 2002) were tested as the ILM solvent. In addition, molten salt hydrates were studied to improve the ILM stability (Quinn et al., 1995). Use of nonvolatile carriers like sodium bicarbonate (Otto et al., 1971), sodium carbonate (Chen et al., 1999), sodium glycinate (Chen et al., 2000, 2001) instead of volatile carriers e.g. (EDA, MEA etc.) increased ILM stability. Kovvali et al. (2000) studied the possible application of generation zero polyamidoamine (PAMAM) dendrimer as a carrier or pure liquid membrane in order to further increase the ILM stability and CO_2 permeance. The study showed that when pure PAMAM dendrimer is used as the liquid membrane, an 82-100% inlet relative humidity (RH) feed gas is needed for a stable ILM. On the other hand, PAMAM-glycerol based ILM overcomes the higher inlet RH requirements.

Glycerol as an ILM solvent showed very good performance in terms of stability and high CO_2 permeance for different inlet relative humidities. This solvent is highly viscous, has a vanishingly low vapor pressure and it is hygroscopic. This highly viscous liquid has advantages and disadvantages. The advantage is that the non-reacting species, (e.g. nitrogen and oxygen), have a low solubility and quite low permeability through this ILM. Therefore, this ILM can give a high selectivity if CO_2 transport is augmented by reversible reactions.

However, due to the high viscosity, the transport rate of the carrier through the ILM membrane is reduced, giving lower CO_2 permeability. Glycerol-based ILMs were studied with different carriers e.g. sodium carbonate or Na-glycinate (NH_2CH_2COONa) immobilized in a variety of the hydrophilic microporous substrates in the form of flat sheet or hollow fibers. These membranes showed good stability under various humidity levels and CO_2 partial pressures.

The glycerol based ILMs were initially studied as a potential application for removal of CO_2 from a breathing gas mixture. For the space suit application, the required CO_2 permeance has to be of the order of $4*10^{-4}$ cc/cm^2 s cmHg and has to have a CO_2-O_2 selectivity of 2800. The glycerol-based ILM study using sodium-glycinate as a carrier by Chen et al. (2001) achieved, however, an effective CO_2 permeance value of $3.5*10^{-5}$ cc/cm^2 s cmHg. The selectivity required was easily exceeded.

There are many variables that affect the CO_2 facilitated transport e.g. carrier concentration, feed gas relative humidity and ILM thickness. As the carrier concentration increases, initially CO_2 transport increases due to higher concentration of complexation agent available to move CO_2 across the ILM. Initially the CO_2 permeance reaches a maximum and then it starts to decrease as the increased carrier concentration inhibits the complex mobility due to higher solution viscosity and decreased free CO_2 solubility. Chen et al. (1999, 2000) studied the effect of the initial Na_2CO_3 and Na-glycinate concentration in the ILM on CO_2 and N_2 permeabilities and selectivity. Their study showed that sodium glycinate has higher solubility in glycerol than sodium carbonate. Glycerol-based

solution with high Na-glycinate concentration (up to 5M) could be easily prepared.

Therefore, most of the facilitatied transport experiments in this study will be done using glycerol-based ILM containing Na-glycinate salt as a carrier. Sodium glycinate is very soluble in glycerol and reacts rapidly with CO_2, which is very important for rapid CO_2 transport across the ILM. The reaction mechanism between sodium-glycinate and CO_2 is given below. Dissociation of soldium-glycinate in the presence of water can be written as

$$H_2NCH_2COONa \Leftrightarrow H_2NCH_2COO^- + Na^+ \quad (3.2)$$

Like other primary amines (e.g ethanolamine) glycinate reacts with CO_2 to form carbamate

$$CO_2 + RNH_2 \Leftrightarrow RHNCOO^- + H^+ \quad (3.3)$$

$$RNH_2 + H^+ \Leftrightarrow RNH_3^+ \quad (3.4)$$

The overall reaction is given as

$$CO_2 + 2RNH_2 \Leftrightarrow RHNCOO^- + RNH_2^+ \quad (3.5)$$

Feed relative humidity (RH) influences the water content needed for the CO_2 reaction mechanism (Chen et al. (1999, 2000)). The permeances of CO_2 and N_2 increase with increasing RH and with decreasing membrane thickness. In order to increase the CO_2 permeability, higher carrier concentrations are used or thinner liquid membranes are prepared. An effort to prepare a thinner ILM in a flat sheet membrane was made by Chen et al. (2000) by controlled coating method. Efforts

to reduce the thickness of ILM in the same substrate in order to increase CO_2 permeance succeeded; however, the selectivities were affected.

A recent study (Matsuyama and Teramoto, 1996), has indicated that new types of cation-exchange membranes prepared by grafting acrylic acid to microporous polypropylene (PE), polytetrafluoroethylene (PTFE) or poly[1-(trimethylsilyl)-1-propyne] (PTMSP) microporous substrates by plasma graft polymerization technique showed considerable increase of CO_2 permeance when immobilized with water-amine solutions. This improved performance and stability is most probably due to high ion-exchange capacity since the cationic carrier was immobilized in a cation-exchange membrane by strong electrostatic forces. These membranes were stable only when both feed and sweep gases were completely humidified, since the liquid membrane was a water/EDA solution. In terms of carbon dioxide permeance ($1*10^{-4}$ cc/cm^2 s cmHg) and 4700 selectivity, the requirements for the space vehicle application are met; however, EDA will be lost with time since it is a volatile compound and it is not an environmentally friendly carrier. These two aspects are still to be resolved.

The focus of this study is to enhance the CO_2 permeance in hollow fiber membrane modules by reducing the ILM thickness either by immobilization of the liquid membrane into thin acrylic acid (AA) grafted layers on top of the porous hollow fibers or by pressurization technique.

In the first approach, immobilization of the solvent/solution on the AA grafted part of the porous hollow fibers will produce the thinner ILM. In this manner, the thickness of the ILM will be equal to the thickness of the grafted part

of the hollow fiber, which is much smaller than the thickness of a fully immobilized liquid membrane.

Another way to create a thin film was explored by Kovvali (2001) using the pressurization technique on ceramic tubes. A purely physical solvent e.g. glycerol carbonate was used. The solvent previously showed a good CO_2/N_2 selectivity (90-130); the selectivity was not dependent on the inlet relative humidity and CO_2 concentration. The same study showed that the true CO_2 permeability is essentially independent on the substrate thickness and the CO_2-N_2 selectivity can be easily retained. Therefore, if the ILM thickness can be drastically reduced to say, less than 10 μm, it would increase the effective CO_2 permeance.

The pressurization technique will be tested here with asymmetric polymeric hollow fiber membranes and membrane formed from ceramic materials. Most asymmetric membranes consist of an open structural support at the bottom, which provides mechanical stability and a dense film layer at the top where separation is taking place. The thickness of the separating layer is only 1-10% of the total membrane wall thickness. However, alumina-based ceramic membranes were made using two kinds of particles. The support layer was made by deposition of larger α-alumina particles and the surface or separating layer was made by deposition of smaller γ-alumina particles. Therefore, once the membrane is fully immobilized with the solvent/solution, a progressively increasing applied pressure $\Delta P=(P_1-P_2)$ across the membrane will correspondingly expel parts of the solvent/solution from the pore. Figure 3.2 describes the principle of making the

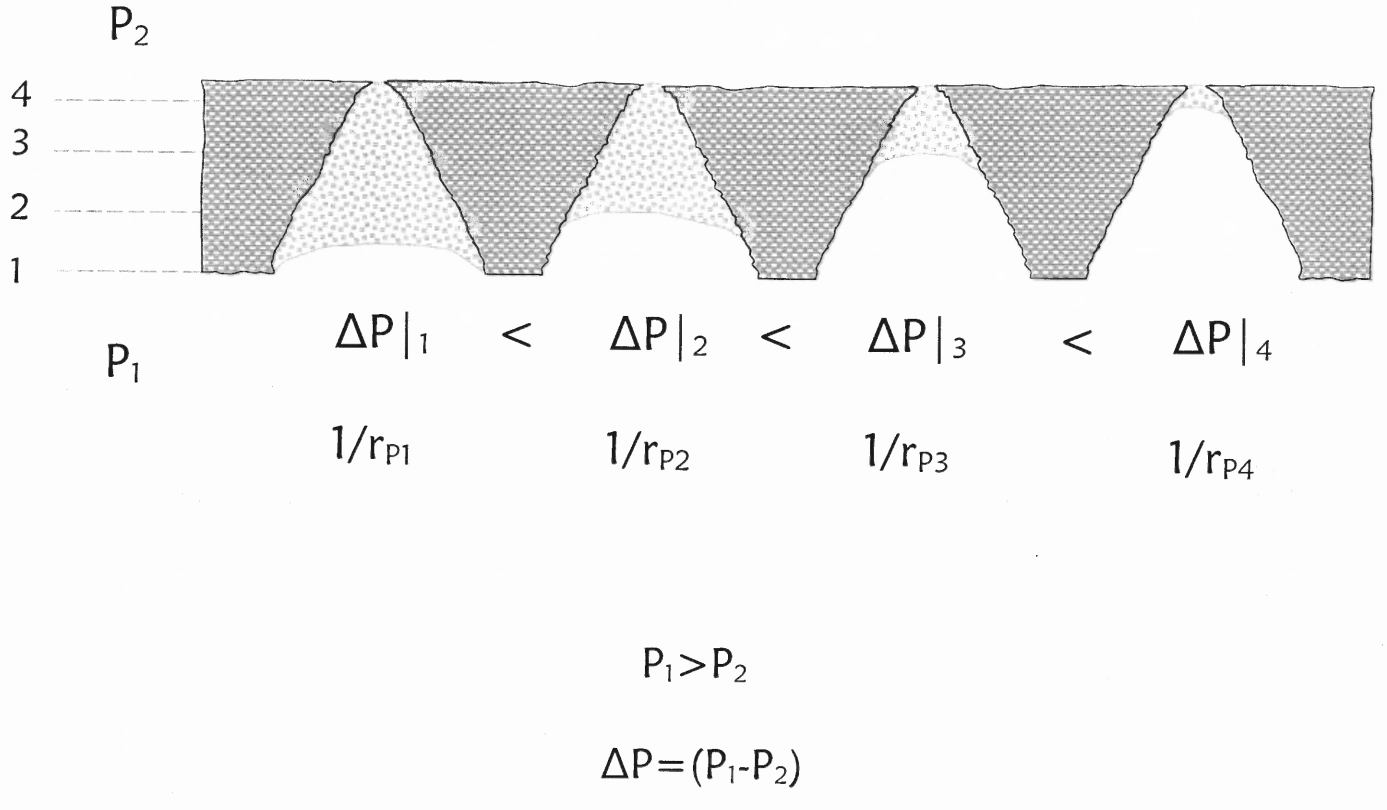

Figure 3.2 Preparation of a thin ILM in an asymmetric membrane by pressurization technique.

thin ILM by progressively increasing the applied $\Delta P = (P_1-P_2)$ in an asymmetric polymeric/ceramic membrane. In the first step of pressurization, the liquid from the largest pore region will be expelled first. As $\Delta P=(P_1-P_2)$ is gradually increasing, liquid from the smaller pore regions will be displaced subsequently. The excess liquid that is displaced from the pores has to be removed from the membrane surface. If the applied ΔP pressure across the membrane is large enough, a thin ILM with a thickness equal of close to the thickness of the separation layer can be made. Hence, ceramic membrane tubes are inherently a better choice for a pressurization technique, since they are able to withstand very high trans-membrane pressures imposed. As a result, a very thin ILM could be prepared if an appropriate ceramic support is available.

In this study, the focus of the facilitated transport ILMs will be on making thinner films either by using the AA-grafted fiber or by the pressurization technique. Preparation of thinner ILMs is studied in order to increase the CO_2 permeance to the desirable levels for the space application, while preserving the stability of the liquid membrane and creating a nontoxic and environmentally friendly ILM.

3.2 Experimental

3.2.1 Types of Experiments

1. For determination of CO_2/N_2 permeances across the full/thin ILM, hydrophilized and hydrophilic polymeric hollow fiber membrane substrates

were used. Feed CO_2/N_2 mixture having an appropriate relative humidity was passed either through the bore side or the shell side, while dry He as a sweep gas was passed on the opposite side. The separation factor between CO_2 and N_2 was estimated based on the permeance measurements of both species.

2. To study the change of the CO_2/N_2 permeances due to reduced thickness ILMs, hollow fibers of hydrophilic polymeric membranes and ceramic substrates were used.
3. To study the effect of different CO_2/N_2 inlet composition on CO_2 permeance and facilitated transport, hydrophilic hollow fiber membranes were used.

3.2.2 Chemicals, Gases, Membranes and Modules

Most experiments using hydrophilized hollow fiber membranes were conducted using 0.5% CO_2/N_2 balance mixtures. To study the effect of the different feed gas CO_2 concentration on the facilitated transport of CO_2 across the membrane, inlet CO_2 concentration was varied between 0.5% -25% balance nitrogen. Hydrophilized polymeric hollow fiber membrane substrates were immobilized with glycerol based ILM containing Na-glycinate as a carrier, water based ILM containing Na-glycinate or EDA as a carrier or a glycerol-water based ILM containing Na-glycinate as a carrier. Hydrophilized polymeric hollow fiber membrane and ceramic substrates were used to study the thinning of the ILM via

pressurization when glycerol carbonate was used as a physical solvent for a liquid membrane.

The CO_2/N_2 gas mixture and pure gases used in this study are listed below (Matheson, E. Rutherford, NJ:

1. Certified standard gas mixture containing CO_2/nitrogen balance:

   CO_2 0.5%; CO_2 1.98%; CO_2 25.0%.

2. Pure gases:

   nitrogen zero; helium zero; air zero.

Solvents used for ILM preparation were glycerol GC 99% (Sigma Chemical Co., St. Louis, MO); and glycerol carbonate (Huntsman, Austin, TX). Carriers studied: Na-glycinate (Sigma Chemical Co., St. Louis, MO); EDA was purchased from Fisher Scientific (Somerville, NJ).

Deionized water used for the humidifier and for the preparation of the ILMs was obtained from Barnstead E-Pure system (Model D4641, Dubuque, IA). Plastic PTFE 1/4" and 3/8" tubing and fittings for module making were obtained from Cole-Palmer (Vernon Hills, IL).

Two types of hydrophilized hollow fiber membranes were studied: polyacrylic acid grafted microporous polypropylene membranes and asymmetric poly(vinylidene flouride) (PVDF) hollow fibers.

Six different batches of loose hollow fibers as well as fibers already potted in modules with stainless steel casing of the polyacrylic acid grafted microporous polypropylene membranes were obtained from Applied Membrane Technology,

Inc. (AMT) (Minnetonka, MN). These membranes were prepared by grafting acrylic acid onto the outside surface of hydrophobic polypropylene hollow fiber substrate (Mitsubishi Rayon Co., Tokyo, Japan) by plasma graft polymerization technique under different conditions and grafting solution concentrations. Table 3.1 summarizes the types and sources of such hollow fiber membranes and modules used.

Asymmetric PVDF hollow fibers having the integrated skin on the inner diameter (I.D.) of the fiber were obtained from Koch Membrane Systems, Inc. (Wilmington, MA). Detailed characteristics of the PVDF hollow fiber membrane modules are given in Table 3.2.

Ceramic tubes were obtained from Media and Process Technology Inc. (Pittsburgh, PA); the module characteristics are given in Table 3.3. The ceramic tube 1 structure is substrate/support (α Al_2O_3) with the substrate pore size being 500 Å. The skin/coating (γ Al_2O_3) thickness is 3-5 μm placed on the inner diameter of the ceramic tube having a pore size of 100 Å. The ceramic tube 2 has a more porous substrate, while the skin/coating pore size and thickness are the same.

3.2.3 Experimental Setup for ILM Based Separation of CO_2 from CO_2/N_2 Gas Mixtures

The experimental setup used for the permeation studies of CO_2 from CO_2/N_2 mixtures using hollow fiber membrane modules is shown in Figure 3.3. Hollow fiber membrane modules immobilized with glycerol-based, water-based or

Table 3.1 Grafted Hollow Fiber Membrane Substrates* and Modules Used for ILM Preparation

Batch/Module** Number		Batch/Module Description
Batch 1		Minimal Plasma/Minimal Vapor Time
	Module 1-1	A= 20.8cm², L= 13.0cm, N=20
	Module 2-1	A= 20.5cm², L= 12.8cm, N=20
	Module 3-1	A= 15.6cm², L= 13.0cm, N=15
Batch 2		Minimal Plasma/Max Vapor Time
	Module 1-2	A= 20.9cm², L= 13.1cm, N=20
	Module 2-2	A= 21.3cm², L= 13.3cm, N=20
	Module 3-2	A= 16.4cm², L= 13.5cm, N=15
Batch 3		Modest Graft Exposure Time
	Module 1-3	A= 20.6cm², L= 12.9cm, N=20
Batch 4		High Graft Exposure Time
	Module 1-4	A= 20.8cm², L= 13.0cm, N=20
	Module 2-4	A= 21.3cm², L= 13.3cm, N=20
	Module 3-4	A= 15.8cm², L= 13.2cm, N=15
Batch 5		Low Graft Concentration/Solution
	Module 1-3	A= 20.8cm², L= 13.0cm, N=20
Batch 6		High Graft Concentration/Solution
	Module 1-6	A= 20.8cm², L= 13.0cm, N=20
	Module 2-6	A= 20.8cm², L= 13.0cm, N=20
Module 6**		Stainless steel casing
		A= 30.0cm², N=25
Module 4**		Stainless steel casing
		A= 30.0cm², N=25
Module 8**		Stainless steel casing
		A= 30.0cm², N=25

* Mitsubishi polypropylene hollow fibers; OD: 255μm, ID: 205μm obtained from Mitsubishi Rayon Co., (Tokyo, Japan)

** Applied Membrane Technology, Inc. (AMT) (Minnetonka, MN) supplied hollow fiber substrates and hollow fiber modules with stainless steel casing.

Table 3.2 Geometrical Characteristics of PVDF Hollow Fiber† Modules Used

Module No.	Type of fiber	Fiber ID (cm)	Fiber OD (cm)	Effective length (cm)	No. of fibers	Mass transfer area (cm^2)*
1	PVDF**	0.118	0.226	21.0	4	29.9
2	PVDF**	0.118	0.226	21.5	4	31.3
3	PVDF**	0.118	0.226	21.5	4	31.3

† Skin molecular weight cutoff 100,000; ultrafiltration membrane with the skin on the I.D.
* Calculation based on inner diameter of the fiber
** Koch Membrane Systems, Wilmington, MA

Table 3.3 Geometrical Characteristics of Ceramic Membrane† Modules Used

Module No.	Type of fiber	Fiber ID (cm)	Fiber OD (cm)	Effective length (cm)	No. of fibers	Mass transfer area (cm^2)*
1	Ceramic**	0.35	0.60	25.4	N.A.	26.0
2	Ceramic**	0.35	0.60	25.8	N.A.	26.0

† γ Al_2O_3 skin placed on the I.D.; has 100 Å pore size
* Calculation based on inner diameter of the fiber
** Media and Process Technology Inc., Pittsburgh, PA

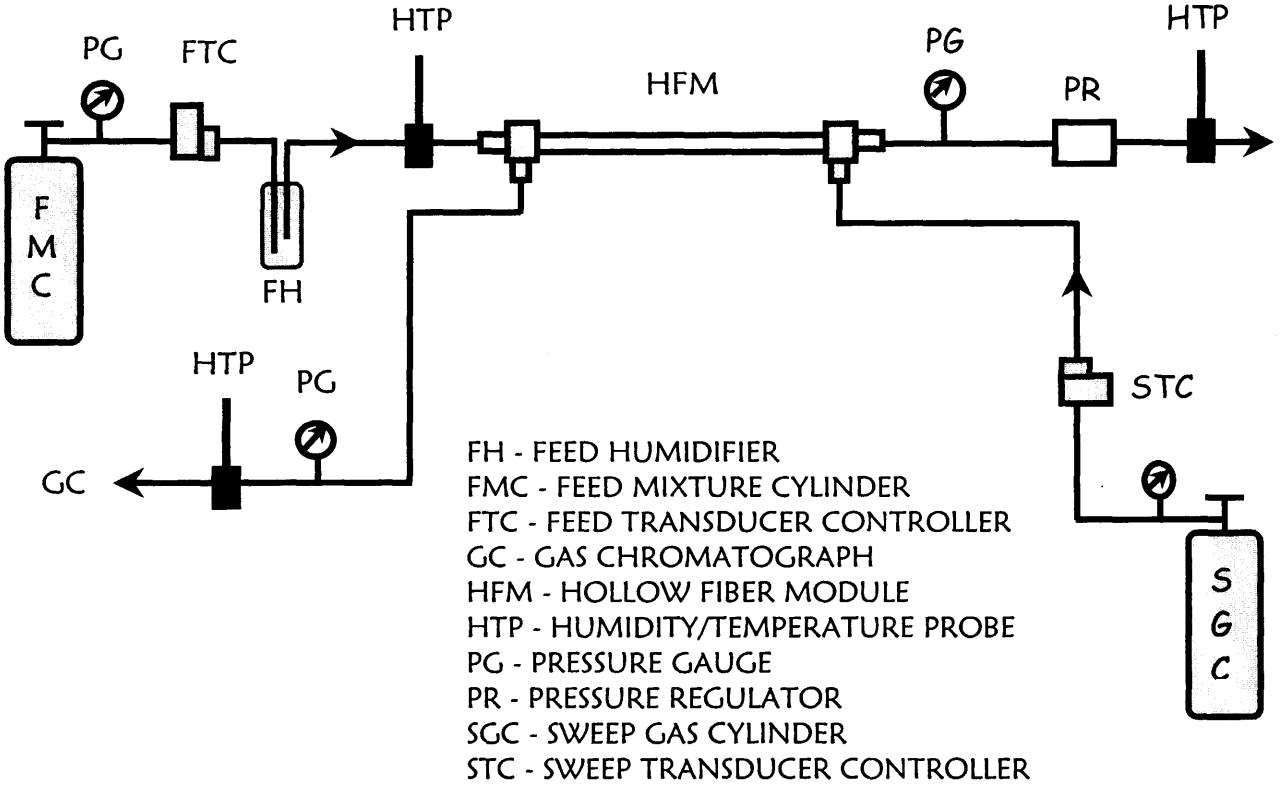

Figure 3.3 Setup for evaluating ILMs for Carbon Dioxide removal in a hollow fiber module.

glycerol-carbonate based solutions/solvents were connected to the system for testing. The humidified feed gas mixture was flowing either through the tube side or through the shell side; dry or humidified sweep gas was passed on the opposite side. The total exposed membrane area varied between 16 cm^2 and 30 cm^2 depending on the number of fibers used for module preparation.

Inlet feed gas streams were completly humidified by passing the gas stream through a water bubbler. Inlet and outlet relative humidities were measured using humidity probes (HMP 31UT; Vaisala, Woburn, MA). The level of humidity was not monitored on the sweep side, although in a few cases, humidified sweep gas was required.

Evaluation of the performance (CO_2/N_2 selectivity and CO_2 permeance) of hollow fiber membrane modules was done using the flow cell technique (Bhave and Sirkar, 1986; Chen et al., 1999; Chen et al., 2001). In this technique, the small amounts of gases which diffused through the membrane were carried away by the sweep gas (e.g. helium) which flowed on the permeate side of the membrane. The flow rate and composition of the permeate side (e.g. sweep gas) were constantly monitored and measured.

The gas flow rates on the feed and the sweep side were controlled using mass flow controllers and Matheson Digital Control Box (Matheson, Horsham, PA). Feed gas pressure was maintained using a pressure regulator (Fairchild Model 10182 BP, Towaco, NJ). The feed pressure was measured with a pressure gage (Matheson, E. Rutherford, NJ). The sweep gas was sampled and analyzed with a Hewlett-Packard Model 5890 series II Gas Chromatograph (GC) having a thermal

conductivity detector (TCD) for CO_2 and N_2 analysis. All experiments were done at room temperature. The GC conditions used are listed below:

- column: Poropack Q 80/100
- carrier gas: helium (He)
- column temperature: 50 °C
- injector temperature: 200 °C
- detector temperature: 200 °C.

3.2.4 Preparation of the ILMs

The general method of preparing the ILMs is to impregnate the membrane matrix with the pure liquid solvent or liquid solution containing the carrier of interest. In most cases, the prepared ILMs using the hydrophilized hollow fiber membrane substrates had a thickness equal to the thickness of the fully or partially hydrophilized substrates. The time required for immobilization varied and depended on the membrane structure, the membrane thickness and the liquid solvent/solution properties. After full immobilization, the polymeric membrane support was removed from the liquid solution and the excess fluid was wiped from the membrane surface.

3.2.4.1 Preparation of the ILMs with Grafted Hollow Fibers Membranes and Modules. The liquid was immobilized onto the grafted layer, placed on the outer diameter (O.D.) of the fiber, by the immersion technique. The hollow fiber membrane was immersed into the solution for an extended period of time to

ensure proper immobilization of the liquid membrane. The hollow fiber membrane was then removed from the glycerol-based liquid solution and the excess fluid was wiped from the surface with the paper napkin. In some cases, the membrane was prewetted with water first and then wetted with Na-glycinate-glycerol or EDA-glycerol solution following the technique previously described.

Water-EDA solution or water- Na-glycinate solution was immobilized in the fibers that were already potted in a module. The shell side was filled with an aqueous solution and after the membrane was wetted, the aqueous solution was drained from the shell side of the hollow fiber module and the module was ready for testing.

The thickness of such prepared ILMs will be equal to the thickness of the acrylic acid grafted section, which varies from batch to batch and depends on the grafting conditions and exposure time.

3.2.4.2 Preparation of the ILMs with PVDF Hollow Fiber Membranes and Modules. Experiments using hydrophilic PVDF asymmetric hollow fiber membrane substrate and preparation of the ILMs with such fibers will be described here. Initially, the ILMs were immobilized in already potted modules. Since the PVDF integrated skin is located on the ID of the hollow fiber, the immobilization takes place from the shell side. The shell side was filled with a solution and after the membrane was completely wetted, the shell side was drained. When glycerol-based or glycerol carbonate solution/solvent were immobilized in already potted modules, in order to remove the excess liquid from the fibers, the following procedure was applied. Either high flow rate of N_2 gas was passed over the fibers

or vacuum was applied on the shell side usually overnight in order to remove excess solution from the fibers. In some cases, both steps were implemented following each other to ensure complete removal of liquid from the outside surface of the fibers and casing walls. When PVDF loose fibers were used, the same procedure of immobilization was followed as described above for the loose grafted hollow fibers case. Thickness of such prepared liquid membranes will be equal to the thickness of the substrate and it is referred to as a full ILM.

3.2.4.3 Preparation of thin ILMs with PVDF Hollow Fibers and Ceramic Membrane Modules using Pressurization Technique. In order to prepare thinner, glycerol carbonate-based or glycerol-based ILMs, pressurization technique was applied in the following manner. One end of the shell side casing was connected to the N_2 gas and the other end was kept closed. The applied shell side pressure will expel a certain amount of the liquid from the asymmetric pore corresponding to the applied pressure difference across the membrane. Maximum applied pressure will be close to the maximum operational membrane pressure. This value is provided by the manufacturer and it is characteristic of a given membrane material, the porous structure and the pore and the tube diameter.

3.2.1 Preparation of the Modules

The first step in module making was matting of the fibers. Each fiber either prewetted with the glycerol- based solution or used as a bare membrane was attached to a vinyl sheet using scotch tape at the ends. Hollow fiber modules

prepared out of the grafted fibers had either 15 or 20 fibers; PVDF modules had only 4 fibers. After placing the fibers on the sheet, one end of the fiber bundle was tied with a cotton thread, which was removed later. The fibers were inserted inside the bore of a 1/4" or 3/8" inch plastic PTFE tubing and end run cross fittings (Cole-Palmer, Vernon Hills, IL). Once the ends of the fibers were placed through the fittings, they were potted first with a silicone rubber adhesive RTV11 (General Electric, Waterford, NY). After curing for one day, an epoxy resin mixture with 4:1 ratio of C-4 resin to activator D (Beacon Chemical Co., Mt. Vernon, NY) was used to seal the module. After the potting of both sides of the module was finished and the epoxy layer was completely cured, the module was ready for testing.

To prepare a module with the ceramic tubes, stainless steel casing (McMaster Carr, New Brunswick, NJ) and fittings (R.S. Crum, Mountainside, NJ) were used. Ceramic tubes modules were potted with only one layer of epoxy resin.

3.2.6 GC calibration for CO_2 and N_2

Calibration curves for carbon dioxide and nitrogen were prepared for the lower ranges of concentrations since only a small amount of CO_2 and N_2 will permeate across the ILM. Different concentrations of a CO_2 containing gas (N_2) stream were prepared by diluting a standard 0.5% CO_2/N_2 gas mixture with a pure He or N_2 gas stream. For preparing the low N_2 concentration calibration curve, a standrad

1000 ppmv N_2/He gas mixture was diluted with a pure He gas stream. For each calibration range and curve, at least 4 to 5 different concentrations were utilized. Certified CO_2/N_2 and N_2/He gas mixture were purchased from Matheson Gas Products (Matheson, E.Rutherford, NJ). Sample GC calibration curves for low ranges of concentrations of CO_2 and N_2 are shown in Figures 3.4 and 3.5.

3.2.7 Calculation of CO_2 and N_2 Effective Permeance $(Q/\delta)_{eff}$ and the Separation Factor $\alpha_{CO_2-N_2}$

The effective permeances $(Q_i/t_m)_{eff}$ for CO_2 and N_2 were measured and subsequently the selectivity $\alpha_{CO_2-N_2}$ was determined. For a membrane of thickness t_m, the effective permeance of a permeating species i, $(Q_i/t_m)_{eff}$, is calculated as follows:

$$\left(\frac{Q_i}{t_m}\right)_{eff} = \frac{V_i}{A\ \Delta p_i} \tag{3.6}$$

Here V_i is the volumetric permeation rate of the gas species i, A and Δp_i are the membrane area and the partial pressure difference of species i across the membrane, respectively. The membrane area A in a hollow fiber module containing N fibers of length L and outside radius r_o is obtained from

$$A = 2\pi r_0 NL \tag{3.7}$$

True permeance of a species through the membrane is given by

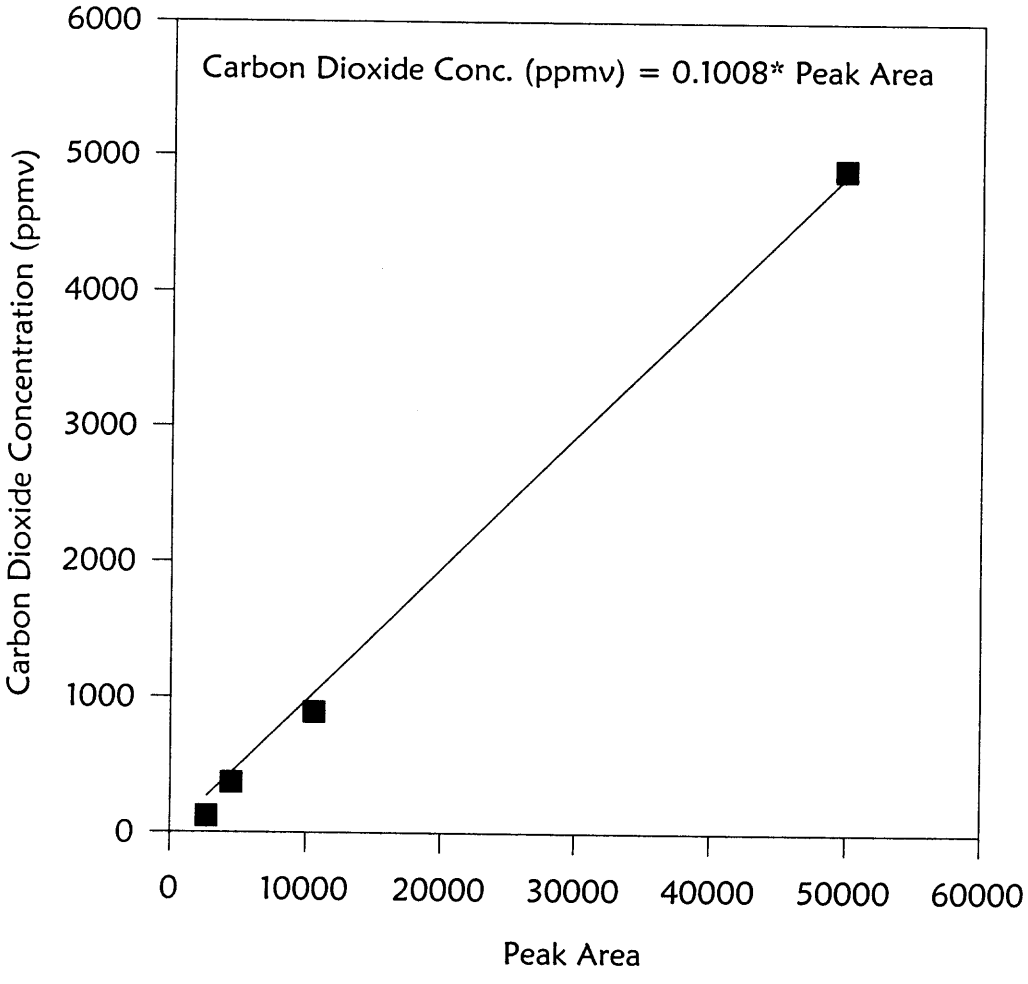

Figure 3.4 Gas chromatograph calibration curve for Carbon Dioxide.

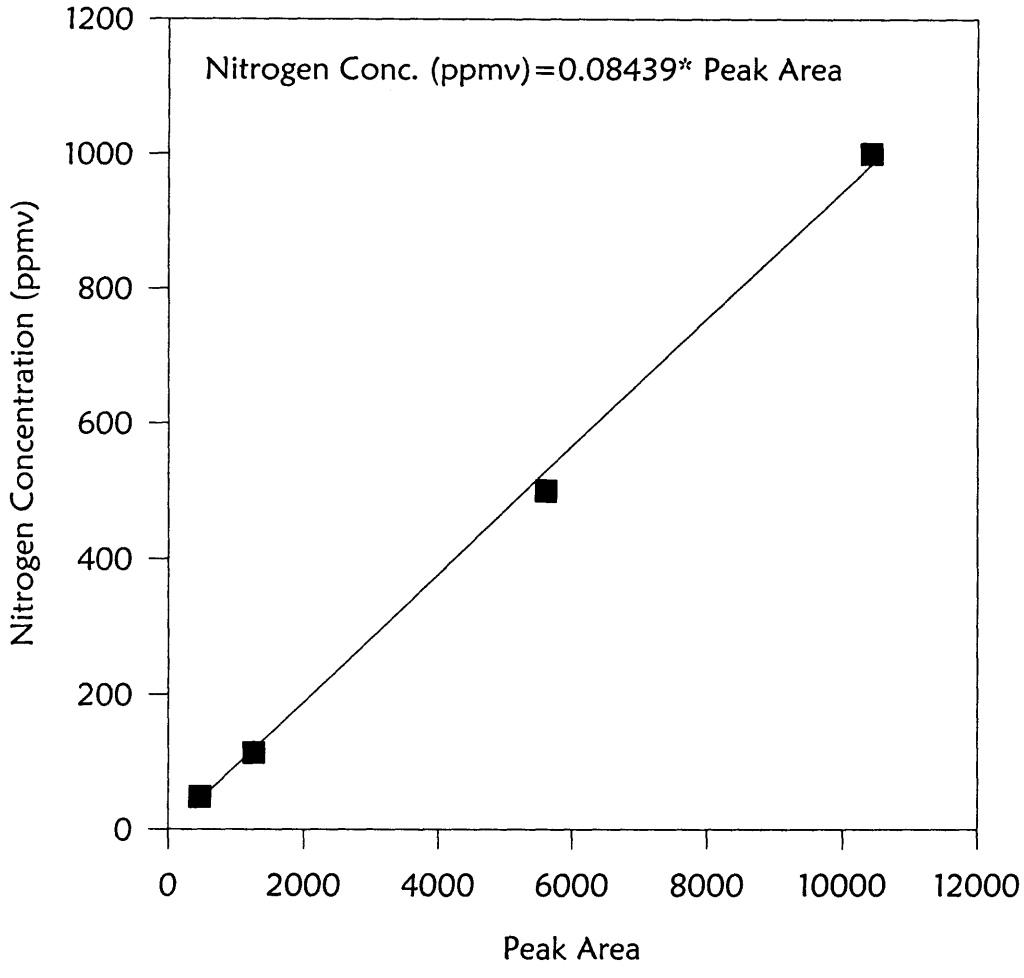

Figure 3.5 Gas chromatograph calibration curve for Nitrogen.

$$\left(\frac{Q_i}{t_m}\right)_{true} = \left(\frac{Q_i}{t_m}\right)_{eff} \frac{\tau_m}{\varepsilon} \tag{3.8}$$

where the permeability of the gas species is

$$Q_i = \left(\frac{Q_i}{t_m}\right)_{true} t_m \tag{3.9}$$

The separation factor α_{i-j} for two gas species i and j is defined by

$$\alpha_{i-j} = \frac{Q_i}{Q_j} = \frac{\left(Q_i / t_m\right)_{eff}}{\left(Q_j / t_m\right)_{eff}} = \frac{\left(Q_i / t_m\right)_{true}}{\left(Q_j / t_m\right)_{true}} \tag{3.10}$$

Sample calculations can be found in Appendix D.

3.3 Results and Discussion

3.3.1 Experimental Results for CO_2 Removal Based on ILMs Using Grafted Hollow Fibers

3.3.1.1 Scanning Electron Micrographs. Six different batches of grafted fibers prepared under different conditions were studied. The membrane structure was checked using a scanning electron microscope (SEM) and the differences between the grafted layers in some batches were compared. Initially fiber samples were simply cut with the razor blade; therefore, in some cases the

difference between the grafted layer and the membrane substrate was not that obvious (Figure 3.6a). Some SEM pictures taken with samples cut with the razor blade (Figure 3.9) show a much clearer image of the AA-grafted layer of approximate thickness of 5-6 μm.

In order to remove the uncertainties of a grafted layer thickness and existence of the same, the new fiber samples were prepared by first immersing them in the liquid nitrogen. Subsequently, fibers were cut and samples were analyzed by a SEM. Figure 3.7 illustrates the cross-sectional views of the AA-grafted fiber from Batch 1 pretreated with liquid nitrogen. Comparing the cross sectional views of the AA-grafted fibers (Batch 1) in Figures 3.6a and 3.7, it appears that treatment with the liquid N_2 affects the grafted layer in such a way that the two different layers are more distinct.

The cross-sectional views of the bare Mitsubishi hollow fiber, and AA-grafted Mitsubishi fiber have been compared (Figure 3.8) in order to assure the presence and the thickness of the AA-grafted layer pretreated with liquid nitrogen. It is clear that the thin (2-3μm) AA-grafted layer is placed on the outside diameter of the hollow fiber.

The SEM picture of the fiber surface indicated whether the fiber surface was properly coated without any defects; the surface of the grafted layer looks quite dense (Figure 3.6b). In order to distinguish and compare the difference in grafting thickness generated by different experimental conditions the SEM pictures from different batches were taken. The cross - sectional views of the Minimal

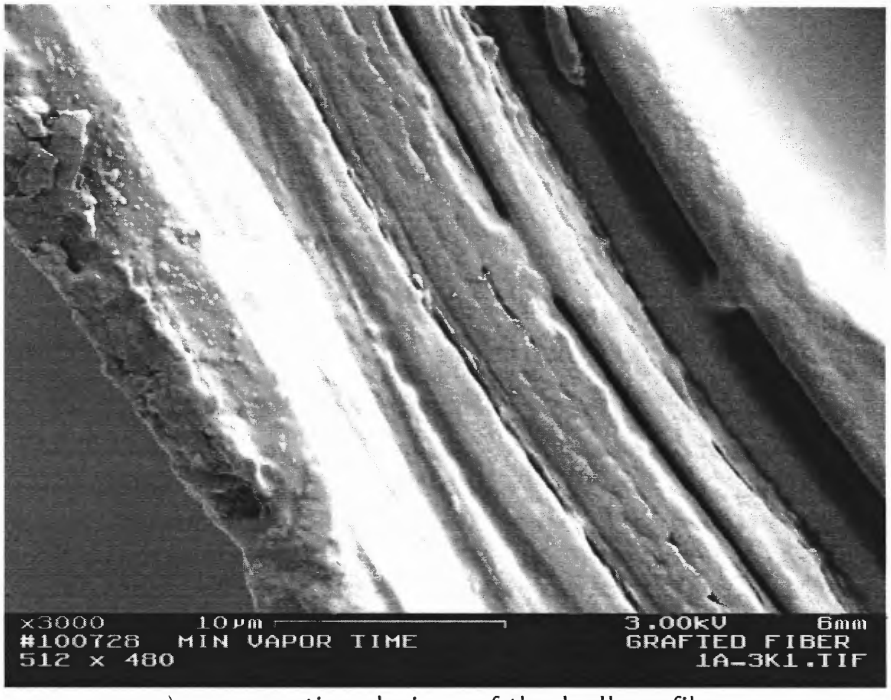

a) cross-sectional view of the hollow fiber

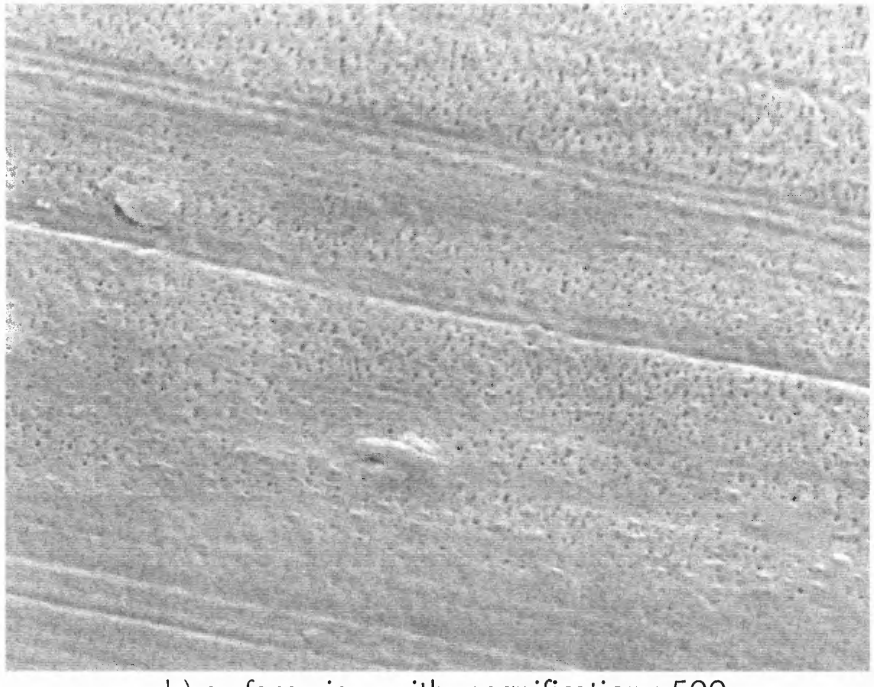

b) surface view with magnification x500

Figure 3.6 Cross-sectional and surface view of the AA-grafted fiber from Batch 1: Minimal Plasma/Minimal Vapor Time.

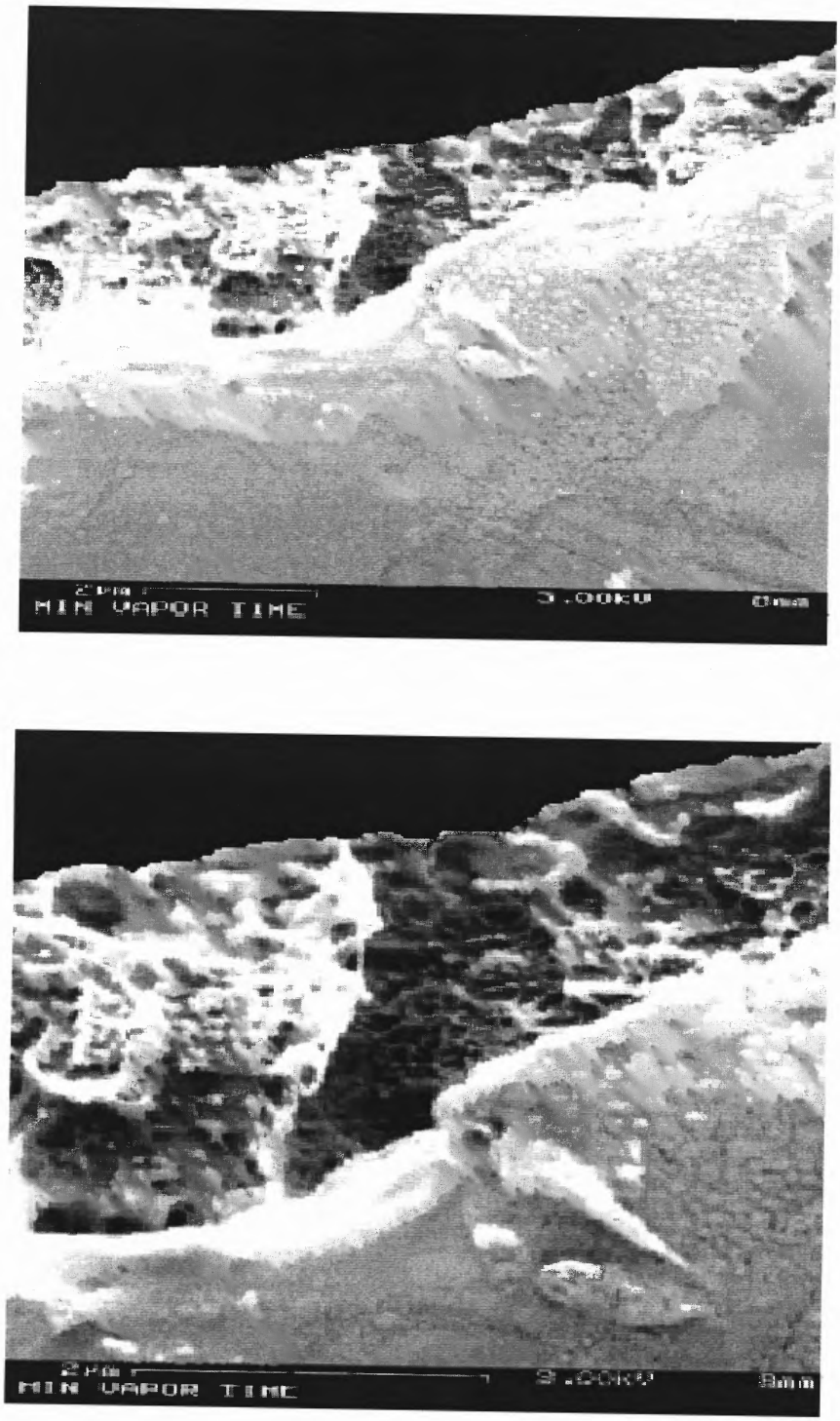

Figure 3.7 Cross-sectional views of the AA-grafted fibers from Batch 1: Minimal Plasma/Minimal Vapor Time treated with liquid nitrogen.

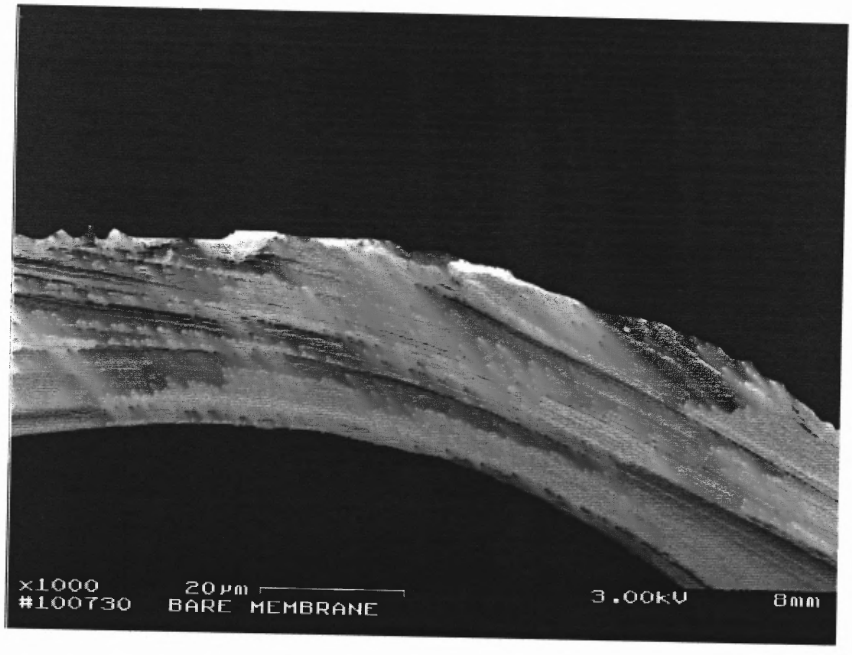

a) cross-sectional view of the bare Mitsubishi hollow fiber

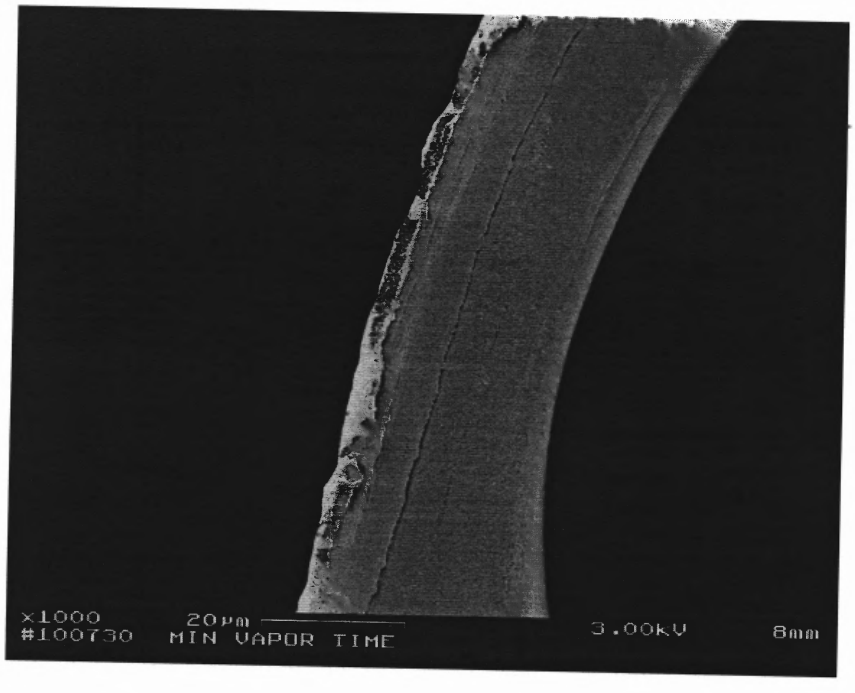

b) cross-sectional view of the grafted Mitsubishi hollow fiber

Figure 3.8 Cross-sectional views of the bare Mitsubishi hollow fiber and Mitsubishi AA-grafted hollow fiber from Batch 1: Minimal Plasma/Minimal Vapor Time.

Plasma/Minimal Vapor Time, Modest Graft Exposure Time and High Graft Exposure Time batches are provided in Figures 3.9, 3.10 and 3.11. It appears that the grafted thickness of the hollow fiber from the minimal plasma/minimal vapor time batch is very small. Details on plasma polymerization conditions and preparation of AA-grafted hollow fibers are provided in Appendix E.

3.3.1.2 ILMs Based on Minimal Plasma/Minimal Vapor Time Grafted Fibers: Batch 1. Table 3.4 lists all results obtained with 3 different modules prepared from Batch 1 fibers. Module 1-1 was prewetted with 3M Na-glycinate-glycerol and was tested with humidified feed gas mixture and dry helium as a sweep gas. After immobilization and potting of the fibers, the module was determined not to be leaking. Experiments in two modes using 0.5% CO_2/N_2 feed gas mixture were done; for shell-side feed and tube-side sweep flow the selectivity was 61; for tube-side feed flow and shell-side sweep flow the selectivity was 94. Low CO_2 effective permeances in the order of 10^{-6} scc/cm^2*s*cmHg were obtained in both cases. This may indicate that the glycerol solution did not penetrate into the grafted part of the membrane. The membrane may have been too dense.

Therefore, Module 2-1 was first prewetted with water and then with 3M Na-glycinate-glycerol solution to make the wetting of the grafted parts easier. This approach reduced both nitrogen as well as CO_2 permeances, but yielded a marginal increase in selectivity since the nitrogen permeance was reduced slightly more than CO_2 permeance. Even in this approach of immobilization, the CO_2 effective permeance remained around 1.6 -2.3*10^{-6} s cc/cm^2*s*cmHg. A possible explanation for this situation is that grafted acrylic acid tends to swell with water.

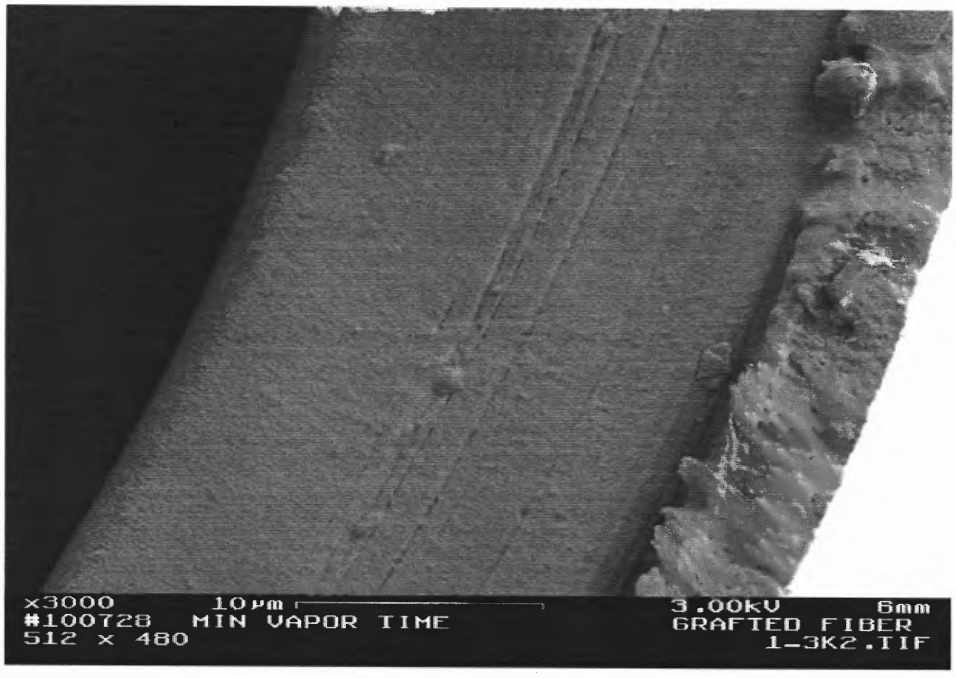

Figure 3.9. Cross-sectional view of the AA-grafted hollow fiber from Batch 3: Modest Graft Exposure Time.

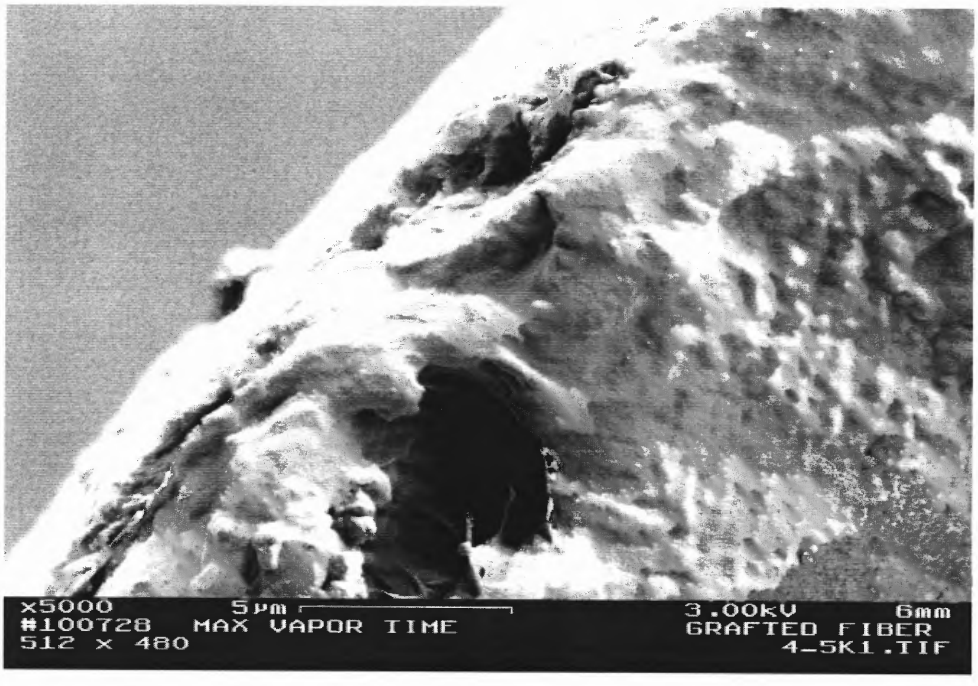

Figure 3.10. Cross-sectional view of the AA-grafted hollow fiber from Batch 4: High Graft Exposure Time.

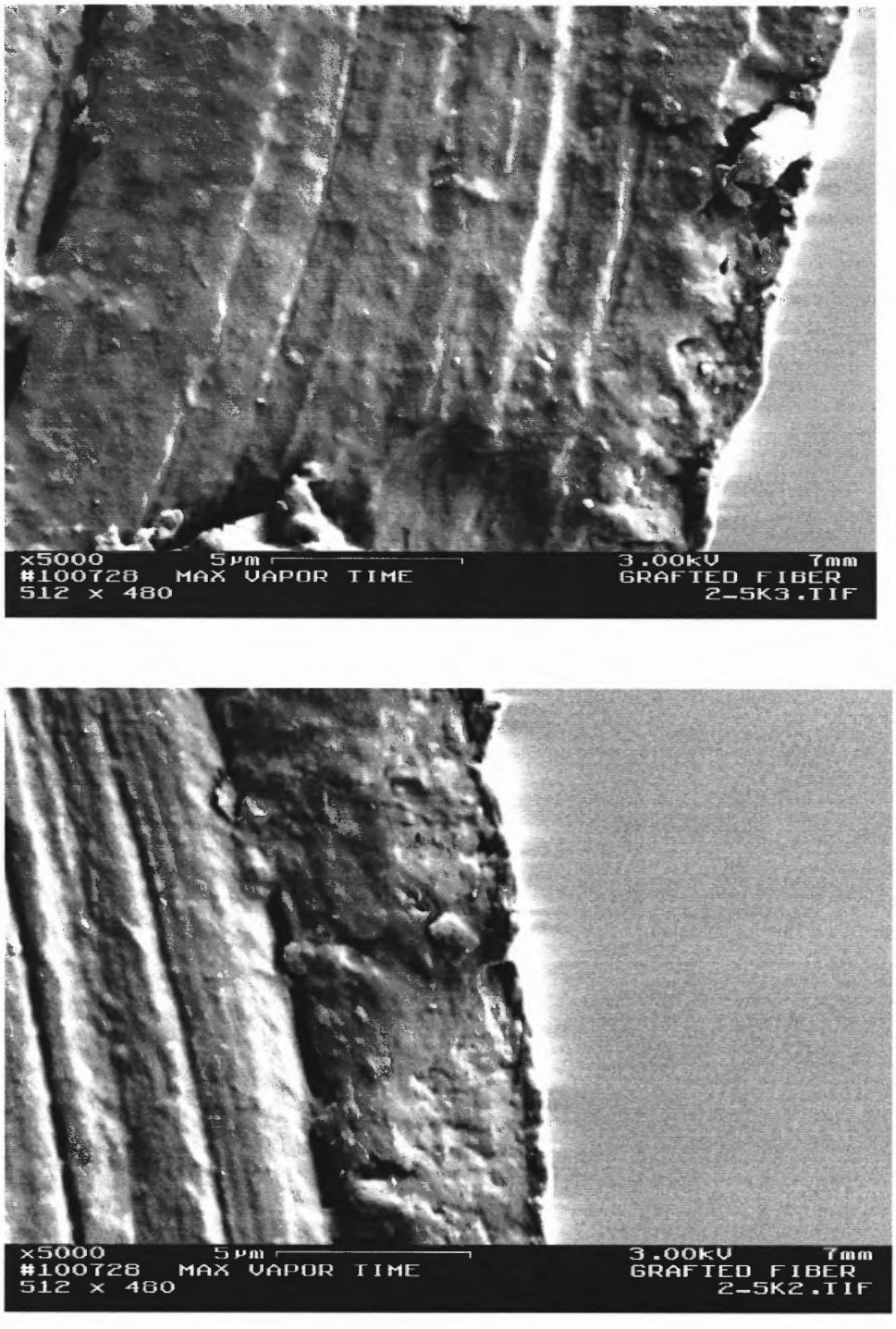

Figure 3.11 Cross-sectional view of the AA-grafted hollow fiber from Batch 2: Minimal Plasma/Max Vapor Time.

Once swollen, the grafted layer may not allow easy penetration of 3M Na-glycinate-glycerol solution into it. As shown in Figure 3.6b, the AA-grafted layer looks quite dense and uniform on the surface, which could be the reason for poor immobilization of glycerol- based solutions.

Since the first experiment, module 2-1 provided an increased CO_2 permeance over an extended period of time; therefore, the experiment was repeated using the same module without reimmobilization in the fibers. Results obtained showed a selectivity of 36 due to an increase in nitrogen permeance by approximately 4 times and a marginal increase of CO_2 permeance. Increased nitrogen permeance is usually an indication of the ILM leakage. Possibly, water evaporation during the time when the module was not used is the basis of this observed behavior.

Module 3-1 was prepared using bare membrane fibers to check if the fibers were grafted properly. This module was immobilized with pure water after potting of the fibers. This experiment using humidified helium sweep stream yielded the expected selectivity of water, namely, 36 although the CO_2 permeance did not show any increase compared to the glycerol immobilization.

Given that previous studies showed good results using grafted membranes with EDA-water solution (Matsuyama and Teramoto, 1996), module 3-1 was immobilized with 3M-EDA-water solution to assure that grafting was present. This experiment yielded the expected results of high selectivity and high CO_2 permeance and reassured that the graft was working. The obtained CO_2 permeances (e.g. 5.9 $*10^{-5}$ s cc/cm^2*s*cmHg) are somewhat lower then that

Table 3.4 Summary of the Permeation Results for Feed Gas Mixture of 0.5% and 0.495% CO_2/N_2 for AMT Grafted Fibers Batch 1: Minimal Plasma/Minimal Vapor Time

Module Number	ILM Preparation	Experimental Conditions	$(Q_i/t_m)_{eff\ N2}$ cc/cm²*s*cmHg	$(Q_i/t_m)_{eff\ CO2}$ cc/cm²*s*cmHg	CO_2-N_2 Selectivity
Module 1-1	prewetted fibers with 3M-Na-glycinate- Glycerol solution	Inlet RH:~100%, Outlet RH:56%. P_h = 4 psig Sweep: dry helium Room Temp: 23°C Shell-side feed flow	$4.36*10^{-8}$	$2.66*10^{-6}$	61
Module 1-1	prewetted fibers with 3M-Na-glycinate- Glycerol solution	Inlet RH:~100%, Outlet RH:56%. P_h = 4 psig Sweep: dry helium Room Temp: 23°C Tube-side feed flow	$3.95*10^{-8}$	$3.72*10^{-6}$	94
Module 2-1	prewetted fibers with water and 3M-Na-glycinate-Glycerol solution	Inlet RH:~100%, Outlet RH:59%. P_h = 4 psig Sweep: dry helium Room Temp: 23°C Tube-side feed flow	$2.14*10^{-8}$	$1.60*10^{-6}$	75
Module 2-1	Same as a above. Experiment continued for 2 days	Inlet RH:~100%, Outlet RH:60.9%. P_h = 4 psig Sweep: dry helium Room Temp: 23°C Tube-side feed flow	$2.14*10^{-8}$	$2.30*10^{-6}$	107

Table 3.4 Summary of the Permeation Results for Feed Gas Mixture of 0.5% and 0.495% CO_2/N_2 for AMT Grafted Fibers Batch 1: Minimal Plasma/Minimal Vapor Time (Continued)

Module Number	ILM Preparation	Experimental Conditions	$(Q_i/t_m)_{eff\ N2}$ cc/cm²*s*cmHg	$(Q_i/t_m)_{eff\ CO2}$ cc/cm²*s*cmHg	CO_2-N_2 Selectivity
Module 3-1	Bare membrane immobilized with pure water	Inlet RH:~100%, Outlet RH:60%. P_h = 4 psig Sweep: humidified helium Room Temp: 23°C Tube-side feed flow	$8.29*10^{-8}$	$3.05*10^{-6}$	36
Module 2-1	prewetted fibers with water and 3M-Na-glycinate-Glycerol solution	Inlet RH:~100%, Outlet RH:65.5%. P_h = 4 psig Sweep: dry helium Room Temp: 22.6°C Tube-side feed flow	$8.54*10^{-8}$	$3.07*10^{-6}$	36
Module 1-1	prewetted fibers with 3M-Na-glycinate- Glycerol solution	Inlet RH:~100%, Outlet RH:64.2%. P_h = 4 psig Sweep: dry helium Room Temp: 22.6°C Tube-side feed flow	$8.88*10^{-8}$	$3.81*10^{-6}$	43
Module 2-1	prewetted fibers with water and 3M-Na-glycinate-Glycerol solution	Inlet RH:~100%, Outlet RH:59%. P_h = 4 psig Sweep: dry helium Room Temp: 23°C Tube-side feed flow	$1.51*10^{-7}$	$3.26*10^{-6}$	21

Table 3.4 Summary of the Permeation Results for Feed Gas Mixture of 0.5% and 0.495% CO_2/N_2 for AMT Grafted Fibers Batch 1: Minimal Plasma/Minimal Vapor Time (Continued)

Module Number	ILM Preparation	Experimental Conditions	$(Q_i/t_m)_{eff\ N2}$ cc/cm²*s*cmHg	$(Q_i/t_m)_{eff\ CO2}$ cc/cm²*s*cmHg	CO_2-N_2 Selectivity
Module 3-1	Bare membrane wetted with 3M-EDA water solution	Inlet RH:~100%, Outlet RH:57.9%. P_h = 4 psig Sweep: humidified helium Room Temp: 23.2°C Tube-side feed flow	$4.25*10^{-8}$	$5.94*10^{-5}$	1 397
Module 3-1	Bare membrane wetted with 3M-Na-glycinate-water solution	Inlet RH:~100%, Outlet RH:76.2%. P_h = 4 psig Sweep: humidified helium Room Temp: 21.4°C Tube-side feed flow	$3.89*10^{-8}$	$3.18*10^{-5}$	818

obtained by Matsuyama and Teramoto (1996); one reason is that the solution concentration reported in that study was approximately 5M.

Module 3-1 was also tested with 3M-Na-glycinate-water solution to assure that similar CO_2 permeance could be achieved. The same module showed that water Na-glycinate solution was also quite effective giving the CO_2 effective permeance in order of $3.2*10^{-5}$ s cc/cm^2*s*cmHg and a CO_2-N_2 selectivity of 818.

Both experiments using immobilized aqueous solutions used humidified helium as the sweep stream to prevent drying of the membrane.

3.3.1.3 ILMs Based on Minimal Plasma/Max Vapor Time Grafted Fibers: Batch 2. Results obtained using this set of fibers are provided in Table 3.5. One module (module 1-2) was immobilized with 3M-Na-glycinate-glycerol solution; the experiment was carried out for an extended period of time till steady state was achieved. This module yielded a low selectivity of 8 with CO_2 permeances in the order of 10^{-5} scc/cm^2*s*cmHg. High CO_2 effective permeance is more likely due to poor immobilization and membrane leakage, rather than facilitated transport of CO_2.

Module 3-2, which was prepared with bare fibers and afterwards immobilized with pure water, gave again very low selectivity.

Module 2-2 preimmobilized with water and 3M-Na-glycinate-glycerol solution again yielded a low selectivity.

Module 3-2 was immobilized with 3M EDA-water solution yielding a selectivity of 287. All previous results indicated poor immobilization of the membrane. The SEM pictures of the fibers from the Batch 2 (Minimal Plasma/Max

Table 3.5 Summary of the Permeation Results for Feed Gas Mixture of 0.5% and 0.495% CO_2/N_2 for AMT Grafted Fibers Batch 2: Minimal Plasma/Max Vapor Time

Module Number	ILM Preparation	Experimental Conditions	$(Q_i/t_m)_{eff\ N2}$ cc/cm²*s*cmHg	$(Q_i/t_m)_{eff\ CO2}$ cc/cm²*s*cmHg	CO_2-N_2 Selectivity
Module 1-2	prewetted fibers with 3M-Na-glycinate- Glycerol solution	Inlet RH:~100%, Outlet RH:56.7%. P_h = 4 psig Sweep: dry helium Room Temp: 23°C Shell-side feed flow	$1.46*10^{-6}$	$1.14*10^{-5}$	8
Module 1-2	prewetted fibers with 3M-Na-glycinate- Glycerol solution	Inlet RH:~100%, Outlet RH:56%. P_h = 4 psig Sweep: dry helium Room Temp: 23°C Shell-side feed flow	$2.30*10^{-6}$	$1.31*10^{-5}$	6
Module 1-2	prewetted fibers with water and 3M-Na-glycinate-Glycerol solution	Inlet RH:~100%, Outlet RH:59%. P_h = 4 psig Sweep: dry helium Room Temp: 23°C Tube-side feed flow	$6.28*10^{-6}$	$1.43*10^{-5}$	2
Module 3-2	Bare fibers wetted with water	Inlet RH:~100%, Outlet RH:60.9%. P_h = 4 psig Sweep: humidified helium Room Temp: 23°C Tube-side feed flow	$1.31*10^{-6}$	$1.46*10^{-5}$	11

Table 3.5 Summary of the Permeation Results for Feed Gas Mixture of 0.5% and 0.495% CO_2/N_2 for AMT Grafted Fibers Batch 2: Minimal Plasma/Max Vapor Time (Continued)

Module Number	ILM Preparation	Experimental Conditions	$(Q_i/t_m)_{eff\ N2}$ cc/cm²*s*cmHg	$(Q_i/t_m)_{eff\ CO2}$ cc/cm²*s*cmHg	CO_2-N_2 Selectivity
Module 2-2	prewetted fibers with water and 3M-Na-glycinate-Glycerol solution	Inlet RH:~100%, Outlet RH:71%. P_h = 4 psig Sweep: dry helium Room Temp: 23°C Tube-side feed flow	$6.57*10^{-7}$	$1.78*10^{-5}$	27
Module 3-2	Bare membrane wetted with 3M-EDA water solution	Inlet RH:~100%, Outlet RH:56%. P_h = 4 psig Sweep: humidified helium Room Temp: 21.4°C Tube-side feed flow	$1.75*10^{-7}$	$5.03*10^{-5}$	287

Vapor Time) somewhat confirmed this conclusion. As shown in Figure 3.11, due to the existence of a very thin layer of grafting on the outer surface of the fiber and possible defects on the fiber surface, immobilization of glycerol-based or water-based solutions were not as successful as in Batch 1.

3.3.1.4 ILMs Based on Modest Graft Exposure Time Grafted Fibers: Batch 3. Table 3.6 shows the results obtained with Modest Graft Exposure Time hollow fiber based ILM module. The observed CO_2/N_2 selectivity was 12 for 3M-Na-glycinate-glycerol and the CO_2 permeance was much lower than the expected range.

Figure 3.9 provides a cross-sectional view of the hollow fiber from this batch having a very distinct layer (~ 5-6 μm) of AA-grafting on the outer surface.

3.3.1.5 ILMs Based on High Graft Exposure Time Grafted Fibers: Batch 4. Table 3.7 provides the permeation results obtained using fibers from Batch 4 e.g. High Graft Exposure Time. Under the same operational conditions, low permeances of CO_2 achieved in this module indicated most probably poor penetration of glycerol based solution into the dense graft layer.

Cross-sectional view in Figure 3.10 indicates that this batch of fibers has a thick AA-grafted layer with an approximate thickness of 12-15 μm.

3.3.1.6 ILMs Based on Low Graft Concentration/Solution Grafted Fibers: Batch 5. A module prewetted with 3M-Na-glycinate-glycerol solution from Batch 5 yielded CO_2 permeance in the range of 10^{-5} scc/cm^2*s*cmHg and selectivity of 36 under the same operational conditions as before (Table 3.8).

Table 3.6 Summary of the Permeation Results for Feed Gas Mixture of 0.495% CO_2/N_2 for AMT Grafted Fibers Batch 3: Modest Graft Exposure Time

Module Number	ILM Preparation	Experimental Conditions	$(Q_i/t_m)_{eff\ N2}$ cc/cm²*s*cmHg	$(Q_i/t_m)_{eff\ CO2}$ cc/cm²*s*cmHg	CO_2-N_2 Selectivity
Module 1-3	prewetted fibers with 3M-Na-glycinate- Glycerol solution	Inlet RH:~100%, Outlet RH:74.3%. P_h = 4 psig Sweep: dry helium Room Temp: 21.4°C Tube-side feed flow	$5.23*10^{-7}$	$6.40*10^{-6}$	12

Table 3.7 Summary of the Permeation Results for Feed Gas Mixture of 0.5% and 0.495% CO_2/N_2 for AMT Grafted Fibers Batch 4: High Graft Exposure Time

Module Number	ILM Preparation	Experimental Conditions	$(Q_i/t_m)_{eff\ N2}$ cc/cm²*s*cmHg	$(Q_i/t_m)_{eff\ CO2}$ cc/cm²*s*cmHg	CO_2-N_2 Selectivity
Module 1-4	prewetted fibers with 3M-Na-glycinate- Glycerol solution	Inlet RH:~100%, Outlet RH:66.6%. P_h = 4 psig Sweep: dry helium Room Temp: 21.7°C Tube-side feed flow	$7.02*10^{-7}$	$1.32*10^{-5}$	19
Module 1-4	prewetted fibers with 3M-Na-glycinate- Glycerol solution	Inlet RH:~100%, Outlet RH:66.6%. P_h = 4 psig Sweep: dry helium Room Temp: 21.5°C Shell-side feed flow	$6.78*10^{-7}$	$1.35*10^{-5}$	20
Module 3-4	Bare membrane immobilized with pure water	Inlet RH:~100%, Outlet RH:72%. P_h = 4 psig Sweep: dry helium Room Temp: 23°C Tube-side feed flow	$7.85*10^{-7}$	$2.31*10^{-6}$	29
Module 2-4	prewetted fibers with water and 3M-Na-glycinate-Glycerol solution	Inlet RH:~100%, Outlet RH:64.2%. P_h = 4 psig Sweep: humidified helium Room Temp: 22.6°C Tube-side feed flow	$9.25*10^{-7}$	$1.49*10^{-5}$	16

Table 3.8 Summary of the Permeation Results for Feed Gas Mixture of 0.495% CO_2/N_2 for AMT Grafted Fibers Batch 5: Low Graft Concentration/Solution

Module Number	ILM Preparation	Experimental Conditions	$(Q_i/t_m)_{eff\ N2}$ cc/cm²*s*cmHg	$(Q_i/t_m)_{eff\ CO2}$ cc/cm²*s*cmHg	CO_2-N_2 Selectivity
Module 1-5	prewetted fibers with 3M-Na-glycinate- Glycerol solution	Inlet RH:~100%, Outlet RH:67.4%. P_h = 4 psig Sweep: dry helium Room Temp: 21.3°C Tube-side feed flow	$4.58*10^{-7}$	$1.65*10^{-5}$	36

3.3.1.7 ILMs Based on High Graft Concentration/Solution Grafted Fibers: Batch 6. Table 3.9 gives the summary of the permeation results obtained with the fibers from Batch 6. Module 2-6 prewetted with water and then with the 3M Na-glycinate-glycerol solution could not reach a steady state immediately. Therefore, the experiment was continued for an extended period of time yielding a selectivity of 26.

Module 1-6 prewetted with 3M-glycinate-glycerol solution only yielded a very low selectivity of 9, which indicated most probably poor immobilization of the solution in the fibers.

Module 3-6 was immobilized with 3M EDA–glycerol solution. This module was tested with humidified 0.495% CO_2/N_2 mixture giving a selectivity of 70 with CO_2 permeance still in the order of 10^{-6} cc/cm^2*s*cmHg.

3.3.1.8 ILM Based on AMT Stainless Steel Module 6. This module already potted in the stainless steel casing was immobilized with 3M-Na-glycinate-glycerol solution from the shell side. Experiments were done in two modes; for shell-side feed flow and tube-side sweep (He) flow, the CO_2/N_2 selectivity was 34; for shell-side sweep (He) flow and tube-side feed gas flow, the selectivity was 44. In both cases, the CO_2 permeance was in the range of 10^{-6} cc/cm^2*s*cmHg (Table 3.10).

3.3.1.9 ILM Based on AMT Stainless Steel Module 4. AMT module 4 was tested first as a bare membrane with dry 0.53% CO_2/N_2 mixture through the shell side as well as through the bore side. Feed gas pressure could be raised to 1 psig. This module was the only module capable of withstanding any pressure as

Table 3.9 Summary of the Permeation Results for Feed Gas Mixture 0.495% CO_2/N_2 for AMT Grafted Fibers Batch 6: High Concentration/Solution

Module Number	ILM Preparation	Experimental Conditions	$(Q_i/t_m)_{eff\ N2}$ cc/cm²*s*cmHg	$(Q_i/t_m)_{eff\ CO2}$ cc/cm²*s*cmHg	CO_2-N_2 Selectivity
Module 2-6	prewetted fibers with water and 3M-Na-glycinate-Glycerol solution	Inlet RH:~100%, Outlet RH:64.7%. P_h = 4 psig Sweep: dry helium Room Temp: 22.6°C Tube-side feed flow	$3.60*10^{-7}$	$1.53*10^{-5}$	43
Module 2-6	Same as above Experiment continued for 3 days	Inlet RH:~100%, Outlet RH:57.9%. P_h = 4 psig Sweep: dry helium Room Temp: 22.5°C Shell-side feed flow	$3.39*10^{-7}$	$1.02*10^{-5}$	30
Module 2-6	Bare membrane immobilized with pure water	Inlet RH:~100%, Outlet RH:57.9%. P_h = 4 psig Sweep: dry helium Room Temp: 23.2°C Tube-side feed flow	$1.71*10^{-7}$	$8.46*10^{-6}$	26

Table 3.9 Summary of the Permeation Results for Feed Gas Mixture 0.495% CO_2/N_2 for AMT Grafted Fibers Batch 6: High Concentration/Solution (Continued)

Module Number	ILM Preparation	Experimental Conditions	$(Q_i/t_m)_{eff\ N2}$ cc/cm²*s*cmHg	$(Q_i/t_m)_{eff\ CO2}$ cc/cm²*s*cmHg	CO_2-N_2 Selectivity
Module 1-6	prewetted fibers with 3M-Na-glycinate- Glycerol solution	Inlet RH:~100%, Outlet RH:64.7%. P_h = 4 psig Sweep: dry helium Room Temp: 22.6°C Tube-side feed flow	$1.71*10^{-7}$	$1.47*10^{-6}$	9
Module 3-6	prewetted fibers with 3M-EDA-Glycerol solution	Inlet RH:~100%, Outlet RH:77%. P_h = 4 psig Sweep: dry helium Room Temp: 22.6°C Shell-side feed flow	$2.31*10^{-8}$	$1.61*10^{-6}$	70

Table 3.10 Summary of the Permeation Results for Feed Gas Mixture 0.5% CO_2/N_2 for AMT Stainless Steel Module 6

Module Number	ILM Preparation	Experimental Conditions	$(Q_i/t_m)_{eff\ N2}$ cc/cm²*s*cmHg	$(Q_i/t_m)_{eff\ CO2}$ cc/cm²*s*cmHg	CO_2-N_2 Selectivity
Module 6	prewetted fibers with water and 3M-Na-glycinate-Glycerol solution	Inlet RH:~100%, Outlet RH:49.7%. P_h = 4 psig Sweep: dry helium Room Temp: 22.4°C Shell-side feed flow	$8.84*10^{-8}$	$1.39*10^{-6}$	16
Module 6	Same as above Experiment continued for 2 days	Inlet RH:~100%, Outlet RH:50.1%. P_h = 4 psig Sweep: dry helium Room Temp: 22.3°C Shell-side feed flow	$5.93*10^{-8}$	$2.06*10^{-6}$	35
Module 6	Bare membrane immobilized with pure water	Inlet RH:~100%, Outlet RH:51.2%. P_h = 4 psig Sweep: dry helium Room Temp: 23°C Tube-side feed flow	$7.31*10^{-8}$	$3.21*10^{-6}$	44

a bare membrane. Sweep side gas mixture was analyzed with the GC giving a selectivity of 24 and an effective CO_2 permeance in the order of 10^{-5} cc/cm^2*s*cmHg (Table 3.11).

Subsequently, this module was immobilized with pure water and tested with humidified feed and sweep gas. Experiments were done in both modes of operations e.g. shell side and tube side feed gas flow. In both cases, N_2 and CO_2 effective permeances were reduced; the achieved selectivity was also low.

AMT module 4, which was previously tested as a bare membrane as well as a wet membrane, was dried out and tested again as a bare membrane. This time, the CO_2 effective permeance was in order of 10^{-4} cc/cm^2*s*cmHg and the CO_2/ N_2 selectivity was 890. This drastic increase of CO_2 effective permeance prompted us to check if the membrane was leaking. The feed gas going out was injected into the GC to verify the gas composition. Analyses gave similar composition for feed out and sweep side composition. Therefore, most probably the high CO_2 permeance was due to leakage through the membrane since once wetted and subsequently dried the grafted layer tended to peel off.

3.3.1.10 ILM Based on AMT Stainless Steel Module 8. One module having stainless steel casing (module 8) with 25 fibers was wetted with 3M water-EDA solution. The shell side was filled with 3M water-EDA solution in order to wet the fibers and subsequently the shell side was drained. The module was tested with humidified 0.495% CO_2/N_2 gas mixture and humidified He as a sweep gas (tube-side feed/shell-side sweep mode). The measured selectivity for tube-side feed

Table 3.11 Summary of the Permeation Results for Feed Gas Mixture 0.5% CO_2/N_2 for AMT Stainless Steel Module 4

Module Number	ILM Preparation	Experimental Conditions	$(Q_i/t_m)_{eff\ N2}$ cc/cm²*s*cmHg	$(Q_i/t_m)_{eff\ CO2}$ cc/cm²*s*cmHg	CO_2-N_2 Selectivity
Module 4	Bare membrane	Inlet RH:~100%, Outlet RH:80.9%. P_h = 4 psig Sweep: dry helium Room Temp: 23.1°C Shell-side feed flow	$1.63*10^{-6}$	$3.92*10^{-5}$	24
Module 4	Immobilized with water	Inlet RH:~100%, Outlet RH:48.9%. P_h = 4 psig Sweep: humidified helium Room Temp: 23°C Shell-side feed flow	$7.03*10^{-8}$	$1.29*10^{-6}$	18
Module 4	Immobilized with water	Inlet RH:~100%, Outlet RH:49.7%. P_h = 4 psig Sweep: dry helium Room Temp: 23°C Tube-side feed flow	$1.43*10^{-7}$	$1.93*10^{-6}$	13

Table 3.11 Summary of the Permeation Results for Feed Gas Mixture 0.5% CO_2/N_2 for AMT Stainless Steel Module 4 (Continued)

Module Number	ILM Preparation	Experimental Conditions	$(Q_i/t_m)_{eff\ N2}$ cc/cm²*s*cmHg	$(Q_i/t_m)_{eff\ CO2}$ cc/cm²*s*cmHg	CO_2-N_2 Selectivity
Module 4	Dried	Inlet RH:~100%, Outlet RH:79.2%. P_h = 4 psig Sweep: dry helium Room Temp: 23°C Tube-side feed flow	$1.81*10^{-7}$	$1.64*10^{-4}$	890
Module 4	Dried	Inlet RH:~100%, Outlet RH:81.5%. P_h = 4 psig Sweep: dry helium Room Temp: 22.7°C Shell-side feed flow	$5.12*10^{-6}$	$4.14*10^{-4}$	80

gas flow was 1435 and the CO_2 permeance was $6.52*10^{-5}$ cc/cm^2*s*cmHg (Table 3.12).

3.3.2 Experimental Results for Full and Thin ILM Based Removal of CO_2 Using PVDF Hollow Fibers

Hydrophilic PVDF hollow fiber based ILMs having an average thickness of 0.108 cm when fully immobilized with pure glycerol carbonate or glycerol-Na-glycinate solution were prepared; subsequently the pressurization technique was applied to prepare thinner ILMs. The originally prepared 3M glycerol-Na-glycinate solution was mixed with pure water to reduce the high viscosity of the solution. Therefore, glycerol-Na-glycinate ILMs studied with these hollow fibers membranes had a carrier concentration of 1 M and 2 M depending on the dilution.

3.3.2.1 Experimental Results Using PVDF Hollow Fibers with Thin Glycerol Carbonate ILMs Prepared Using the Pressurization Technique.

The PVDF hollow fiber module 1 (Table 3.2) was immobilized with pure glycerol carbonate from the shell side. During the immobilization step N_2 gas was passing through the bore side of the hollow fiber in order to remove any excess liquid that is possibly coming to the tube side during the wetting of the substrate. The module was subsequently drained and purged with the N_2 gas to remove excess liquid. Purging of the shell side of the module in order to remove any excess liquid was followed after every pressurization step. This module was tested with 0.49% CO_2/N_2 humidified feed gas mixture passed on the shell side and dry He sweep

Table 3.12 Summary of the Permeation Results for Feed Gas Mixture 0.495% CO_2/N_2 for AMT Stainless Steel Module 8

Module Number	ILM Preparation	Experimental Conditions	$(Q_i/t_m)_{eff\ N2}$ cc/cm²*s*cmHg	$(Q_i/t_m)_{eff\ CO2}$ cc/cm²*s*cmHg	CO_2-N_2 Selectivity
Module 8	Immobilized with 3M-EDA water solution	Inlet RH:~100%, Outlet RH:67.4%. P_h = 4 psig Sweep: dry helium Room Temp: 20.3°C Tube-side feed flow	$3.95*10^{-8}$	$6.52*10^{-5}$	1 435

gas was passed through the bore side resulting in a CO_2 permeance of $8.3*10^{-7}$ $cc/cm^2*s*cmHg$ and a CO_2-N_2 selectivity of 132 (Table 3.13). The same module was initially pressurized at 10 psig for 1 hour from the shell side. After the pressurization step, the shell side was purged with pure N_2 and tested again with 0.49% CO_2/N_2 humidified feed gas mixture. The first pressurization increased the CO_2 permeance from $8.3*10^{-7}$ to $1.4*10^{-6}$ $cc/cm^2*s*cmHg$. When the module was pressurized up to 15 psig, CO_2 permeance did not increase noticeably. After 25 psig applied pressure on the shell side, CO_2 permeance increased approximately 5 times and reached the value of $4.4*10^{-6}$ $cc/cm^2*s*cmHg$ and a selectivity of 400. The highest applied pressure was 30 psig and the final CO_2 permeance value was somewhat lower than the previous one, but the selectivity came back to the value of approximately 167.

Since the result obtained at 25 psig was questionable, the same module (module 1) was reimmobilized with glycerol carbonate and the pressurization technique was repeated again to confirm the measurements. After reimmobilization, the module was incrementally pressurized up to: 0, 15, 25 and 35 psig pressure from the shell side. Corresponding CO_2 permeance values are: $9.1*10^{-7}$, $1.9*10^{-6}$, $2.8*10^{-6}$ and $2.4*10^{-6}$ $cc/cm^2*s*cmHg$. (Table 3.13). For this set of experiments, the selectivity values were between 158-215 as expected. There is a noticeable trend of increasing CO_2 permeability values due to the pressurization technique. The maximum allowable operating pressure for the PVDF hollow fibers is 35 psig. Further increase in CO_2 permeance due to pressurization and thinning of the ILM was not feasible with this type of hollow fibers. Therefore, further

Table 3.13 Summary of the Permeation Results for CO_2/N_2 Gas Mixture Using PVDF Hollow Fiber Module 1 Immobilized with Glycerol Carbonate and Subjected to Pressurization

ILM Preparation	Experimental Conditions	$(Q_i/t_m)_{eff\ N2}$ cc/cm²*s*cmHg	$(Q_i/t_m)_{eff\ CO2}$ cc/cm²*s*cmHg	CO_2-N_2 Selectivity
Wetted with glycerol carbonate from the shell side	C_{in} = 0.49% CO_2/N_2 RH_{in}: 100.0% RH_{out}: 40.7% t = 24.7°C	6.3 E-9	8.3 E-7	132
Wetted with glycerol carbonate from the shell side and pressurized @10psig	C_{in} = 0.49% CO_2/N_2 RH_{in}: 100.0% RH_{out}: 46.6% t = 23.6°C	9.4 E-9	1.4 E-6	149
Wetted with glycerol carbonate from the shell side and pressurized @15psig	C_{in} = 0.49% CO_2/N_2 RH_{in}: 100.0% RH_{out}: 39.4% t = 24.8°C	1.1 E-8	1.2 E-6	109
Wetted with glycerol carbonate from the shell side and pressurized @25psig	C_{in} = 0.49% CO_2/N_2 RH_{in}: 100.0% RH_{out}: 61.4% t = 23.7°C	1.5 E-8	4.4 E-6	400

Table 3.13 Summary of the Permeation Results for CO_2/N_2 Gas Mixture Using PVDF Hollow Fiber Module 1 Immobilized with Glycerol Carbonate and Subjected to Pressurization (Continued)

ILM Preparation	Experimental Conditions	$(Q_i/t_m)_{eff\ N2}$ cc/cm²*s*cmHg	$(Q_i/t_m)_{eff\ CO2}$ cc/cm²*s*cmHg	CO_2-N_2 Selectivity
Wetted with glycerol carbonate from the shell side and pressurized @30psig	C_{in} = 0.49% CO_2/N_2 RH_{in}: 100.0% RH_{out}: 62.6% t = 23.9°C	1.5 E-8	2.5 E-6	167
Reimmobilized with glycerol carbonate from the shell side	C_{in} = 0.51% CO_2/N_2 RH_{in}: 100.0% RH_{out}: 52.9% t = 22.9°C	6.9 E-9	9.1 E-7	132
Reimmobilized with glycerol carbonate from the shell side and pressurized @15psig	C_{in} = 0.51% CO_2/N_2 RH_{in}: 100.0% RH_{out}: 48.7% t = 22.3°C	1.2 E-8	1.9 E-6	158
Wetted with glycerol carbonate from the shell side and pressurized @25psig	C_{in} = 0.51% CO_2/N_2 RH_{in}: 100.0% RH_{out}: 61.4% t = 23.7°C	1.3 E-8	2.8 E-6	215

Table 3.13 Summary of the Permeation Results for CO_2/N_2 Gas Mixture Using PVDF Hollow Fiber Module 1 Immobilized with Glycerol Carbonate and Subjected to Pressurization (Continued)

ILM Preparation	Experimental Conditions	$(Q_i/t_m)_{eff\ N2}$ cc/cm²*s*cmHg	$(Q_i/t_m)_{eff\ CO2}$ cc/cm²*s*cmHg	CO_2-N_2 Selectivity
Wetted with glycerol carbonate from the shell side and pressurized @35psig	C_{in} = 0.49% CO_2/N_2 RH_{in}: 100.0% RH_{out}: 62.6% t = 23.9°C	1.5 E-8	2.4 E-6	160

increase of the CO_2 permeance was only possible by immobilization of the glycerol solution containing carrier species in addition to the thinning of the ILM.

3.3.2.2 Experimental Results Using PVDF Hollow Fibers with Thin Glycerol-Na-Glycinate ILMs Prepared Using the Pressurization Technique.

The new PVDF hollow fiber module 2 (Table 3.2) was prepared and immobilized with 20 cm^3 of 3M glycerol-Na-glycinate solution diluted with 40 cm^3 of pure water yielding an 1M glycerol-Na-glycinate solution with reduced viscosity. The module was subsequently drained and purged with the N_2 gas to remove any excess liquid from the outside of the fiber. The module was tested with 0.51% CO_2/N_2 humidified feed gas mixture passed on the shell side and dry He sweep gas was passed through the bore side. The obtained CO_2 permeance had a high value of $5.1*10^{-5}$ $cc/cm^2*s*cmHg$ and the selectivity was 2550 (Table 3.14). The same module was pressurized from the shell side at 20 psig for one hour. Both N_2 and CO_2 permeances appear to be slightly reduced e.g. $1.4*10^{-8}$ and $3.9*10^{-5}$ respectively with a CO_2-N_2 selectivity of 2785. Module 2 was further pressurized from the shell side up to 30 psig. Unexpectedly, N_2 and CO_2 permeances again decreased further; $1.0*10^{-8}$ and $2.5*10^{-5}$ $cc/cm^2*s*cmHg$ respectively. Since both permeances are decreasing, a likely explanation is that the liquid solution displaced from the pores stayed on the inner surface of the fiber despite an effort to remove it by purging the gas through the bore of the fiber. Therefore, in this case, the prepared ILM with the pressurization technique was not made thinner.

Table 3.14. Summary of the Permeation Results for CO_2/N_2 Inlet Feed Gas Mixture Using PVDF Hollow Fiber Module 2 Immobilized with 1M Na-glycinate Solution and Subjected to Pressurization

ILM Preparation	Experimental Conditions	$(Q_i/t_m)_{eff\ N2}$ cc/cm²*s*cmHg	$(Q_i/t_m)_{eff\ CO2}$ cc/cm²*s*cmHg	CO_2-N_2 Selectivity
Wetted with solution of 20cc 3M Na-glycinate* + 40cc H_2O giving 1M solution	C_{in} = 0.51% CO_2/N_2 RH_{in}: 100.0% RH_{out}: 56.5% t = 21.4°C	2.0 E-8	5.1 E-5	2 550
Wetted with solution of 20cc 3M Na-glycinate* + 40cc H_2O giving 1M solution and pressurize @ 20 psig	C_{in} = 0.51% CO_2/N_2 RH_{in}: 100.0% RH_{out}: 59.2% t = 22.5°C	1.4 E-8	3.9 E-5	2 785
Wetted with solution of 20cc 3M Na-glycinate* + 40cc H_2O giving 1M solution and pressurize @30 psig	C_{in} =0.51% CO_2/N_2 RH_{in}: 100.0% RH_{out}: 53.1% t = 21.2°C	1.0 E-8	2.5 E-5	2 500

* in glycerol

Another attempt to increase the CO_2 permeance was made by increasing the carrier concentration. The new PVDF hollow fiber module 3 (Table 3.2) was prepared and immobilized with 40 cm^3 of 3M glycerol-Na-glycinate solution diluted with 20 cm^3 of pure water to obtain a 2M glycerol-Na-glycinate reduced viscosity solution. The module was tested with 0.51% CO_2/N_2 humidified feed gas mixture passed on the shell side and dry He sweep gas was passed through the bore side. This experiment yielded a CO_2 permeance of $1.0*10^{-5}$ $cc/cm^2*s*cmHg$ and a CO_2-N_2 selectivity of 1493 (Table 3.15). Although the carrier concentration was increased to 2M, the new ILM yielded lower N_2 and CO_2 permeance then previously obtained with module 2 immobilized with 1M glycerol-Na-glycinate solution. These lower permeance values are due to increased viscosity of the 2M solution used for the ILM in module 3. Subsequently, the module was pressurized at 10 psig from the shell side for one hour in order to prepare thinner ILM. The lumen side was purged with N_2 in attempt to remove excess liquid. This time, the CO_2 permeance was decreased to $6.5*10^{-6}$ $cc/cm^2*s*cmHg$, and the N_2 permeance slightly increased (Table 3.15). The lower CO_2 permeance value might be due to the loss of carrier through the pressurization and removal of the excess liquid.

The PVDF hollow fiber wall thickness is quite large and the maximum allowable transmembrane pressure of 35 psig is not big enough to displace an adequate amount of liquid from the pores. Therefore preparation of a sufficiently thin ILM to notice a significant increase of CO_2 permeance due to pressurization technique is not feasible. Hollow fibers that can handle a high pressure are needed.

Table 3.15. Summary of the Permeation Results for Feed Gas Mixture of CO_2/N_2 Using PVDF Hollow Fiber Module 3 and Subjected to Pressurization

ILM Preparation	Experimental Conditions	$(Q_i/t_m)_{eff\ N2}$ cc/cm²*s*cmHg	$(Q_i/t_m)_{eff\ CO2}$ cc/cm²*s*cmHg	CO_2-N_2 Selectivity
Wetted with solution of 40cc 3M Na-glycinate* + 20cc H_2O giving 2M solution	C_{in} = 0.51% CO_2/N_2 RH_{in}: 100.0% RH_{out}: 90.6% t = 23.1°C	6.8 E-9	1.0 E-5	1 493
Wetted with solution of 40cc 3M Na-glycinate* + 20cc H_2O giving 2M solution and pressurized @10 psig	C_{in} = 0.51% CO_2/N_2 RH_{in}: 100.0% RH_{out}: 88.1% t = 24.9°C	8.3 E-9	6.5 E-6	777

* in glycerol

However, this type of the hollow fiber membrane gave the highest CO_2 permeance value of $5.1*10^{-5}$ cc/cm^2*s*cmHg using the glycerol-based ILM. Hence, we studied performance and stability of module 1 immobilized with reduced viscosity 1M glycerol-Na-glycinate solution. The effect of different CO_2 inlet feed gas concentrations on CO_2 and N_2 permeance was summarized in Table 3.16. For 1M glycerol-Na-glycinate based ILM and 100% inlet relative humidity CO_2 permeance decreased from $5.1*10^{-5}$ to $1.6*10^{-6}$ cc/cm^2*s*cmHg with an increase in CO_2 inlet concentration from 0.515 to 25% whereas the N_2 permeance stayed more or less in the same range.

This is a result of the carrier saturation, which is a known fact in the facilitated transport mechanism. At low inlet CO_2 concentrations, the amount of dissolved CO_2 in the liquid membrane is proportionally lower. Therefore, the amount of utilized carrier species is lower. As the CO_2 concentration increases, more and more carrier is used for facilitated transport. This increase in the permeance of the reacting species will occur until all carrier is almost used up and further increase in inlet CO_2 concentration will not affect the CO_2 permeance any more.

The stability of the glycerol-Na-glycinate based ILM in terms of CO_2 permeance and CO_2/N_2 selectivity were studied for a period of 30 days (Figure 3.12). As we can see from the figure, the carbon dioxide permeance fluctuated around $1.0*10^{-5}$ cc/cm^2*s*cmHg for the inlet feed gas mixture concentration of 1.98% CO_2 balance N_2,. The average selectivity was approximately 750. This ILM

Table 3.16. Summary of Permeation Results for Different Inlet Feed Gas Mixtures of CO_2/N_2 for ILMs in PVDF Hollow Fiber Module 1

ILM Preparation	Experimental Conditions	$(Q_i/t_m)_{eff\ N2}$ cc/cm^2*s*cmHg	$(Q_i/t_m)_{eff\ CO2}$ cc/cm^2*s*cmHg	CO_2-N_2 Selectivity
Wetted with solution of 20cc 3M Na-glycinate* + 40cc H_2O giving 1M solution	C_{in} = 0.51% CO_2/N_2 RH_{in}: 100.0% RH_{out}: 56.5% t = 21.4°C	2.0 E-8	5.1 E-5	2 550
Wetted with solution of 20cc 3M Na-glycinate* + 40cc H_2O giving 1M solution	C_{in} = 1.98% CO_2/N_2 RH_{in}: 100.0% RH_{out}: 55.5% t = 22.5°C	1.0 E-8	1.0 E-5	1 000
Wetted with solution of 20cc 3M Na-glycinate* + 40cc H_2O giving 1M solution	C_{in} = 5.0% CO_2/N_2 RH_{in}: 100.0% RH_{out}: 45.2% t = 21.2°C	9.4 E-9	3.5 E-6	372
Wetted with solution of 20cc 3M Na-glycinate* + 40cc H_2O giving 1M solution	C_{in} = 25.0% CO_2/N_2 RH_{in}: 100.0% RH_{out}: 56.5% t = 21.4°C	1.4 E-8	1.6 E-6	114

* in glycerol

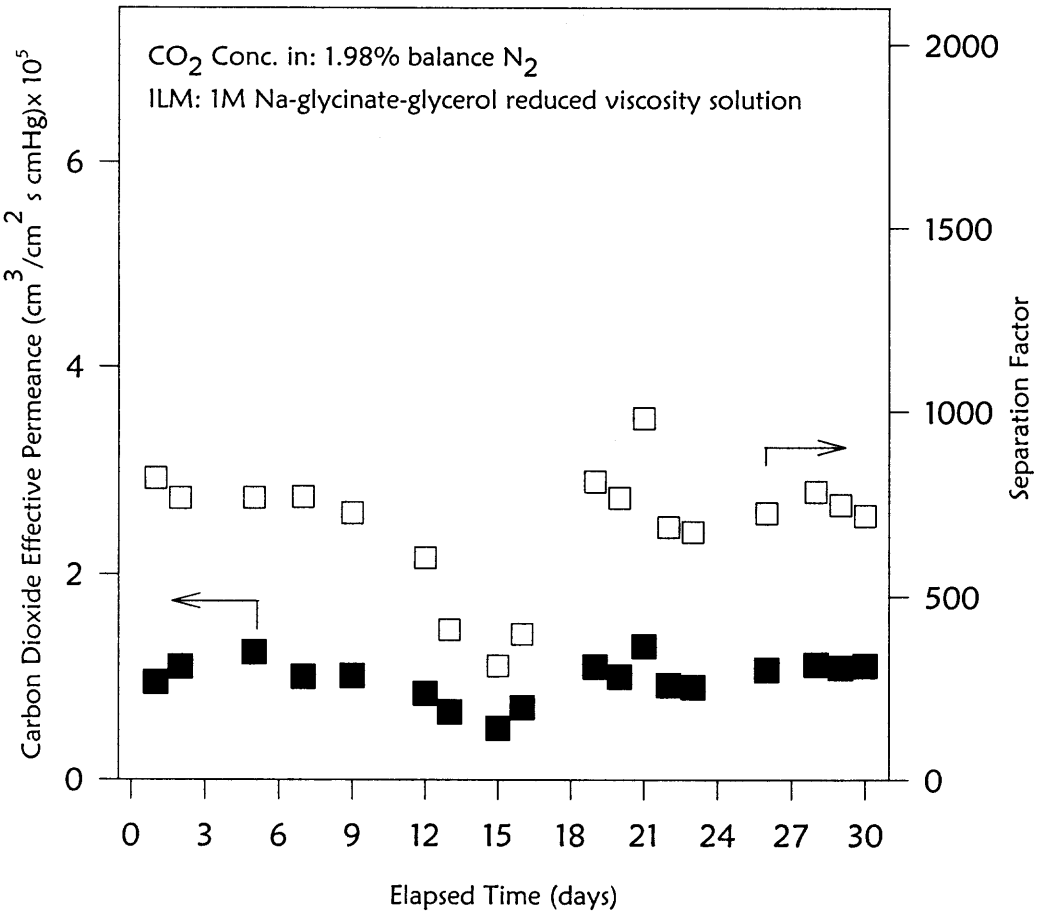

Figure 3.12 PVDF hollow fiber Module 1 stability run using glycerol-Na-glycinate based ILM.

showed good stability using the 100% humidified inlet feed gas mixture and dry He as a sweep gas.

3.3.3 Experimental Results for Full and Thin ILM Based Removal of CO_2 Using Ceramic Membrane Modules

The module was made using the ceramic tube 1 having a substrate/support (α Al_2O_3) with a pore size of 500 Å. The skin/coating (γ Al_2O_3) thickness is 3-5 μm; it is on the inner diameter of the ceramic tube having a pore size of 100 Å. The membrane in this module was immobilized with glycerol carbonate from the shell side. The shell side was drained and purged with pure N_2. The module was tested with 0.49% CO_2/N_2 humidified feed gas mixture passed on the shell side and dry He sweep gas was passed through the bore side. The obtained CO_2 permeance was $5.1*10^{-6}$ cc/cm^2*s*cmHg and a CO_2-N_2 selectivity of ~1050 (Table 3.17). This particular ceramic module was initially tested with a pure dendrimer solution and subsequently washed with methanol. Therefore, this unusually high selectivity obtained for glycerol carbonate is most probably a result of some leftover dendrimer in the module. In order to increase the CO_2 permeance, the module was further pressurized from the shell side first at 20 psig for one hour. Carbon dioxide permeance reached the value of $6.7*10^{-6}$ cc/cm^2*s*cmHg and the selectivity was slightly reduced, since N_2 permeance increased too. Subsequently, the module was pressurized at 50 psig and measured CO_2 and N_2 permeance stayed almost unchanged. After the module was pressurized at 70 psig, N_2

Table 3.17 Summary of the Permeation Results for CO_2/N_2 Gas Mixture for Ceramic Module 1 Immobilized with Glycerol Carbonate Due to Pressurization

ILM Preparation	Experimental Conditions	$(Q_i/t_m)_{eff\ N2}$ cc/cm²*s*cmHg	$(Q_i/t_m)_{eff\ CO2}$ cc/cm²*s*cmHg	CO_2-N_2 Selectivity
Wetted with glycerol carbonate from the shell side	C_{in} = 0.49% CO_2/N_2 RH_{in}: 100.0% RH_{out}: 42.7% t = 23°C	4.9 E-9	5.1 E-6	1 050
Wetted with glycerol carbonate from the shell side and pressurized @20psig	C_{in} = 0.49% CO_2/N_2 RH_{in}: 100.0% RH_{out}: 38.7% t = 23°C	6.1 E-9	6.7 E-6	1 100
Wetted with glycerol carbonate from the shell side and pressurized @50psig	C_{in} = 0.49% CO_2/N_2 RH_{in}: 100.0% RH_{out}: 50% t = 23.2°C	5.5 E-8	6.8 E-6	1 230
Wetted with glycerol carbonate from the shell side and pressurized @70psig	C_{in} = 0.49% CO_2/N_2 RH_{in}: 100.0% RH_{out}: 44.1% t = 24.4°C	7.6 E-8	3.2 E-6	422

Table 3.17 Summary of the Permeation Results for CO_2/N_2 Gas Mixture for Ceramic Module 1 Immobilized with Glycerol Carbonate Due to Pressurization (Continued)

ILM Preparation	Experimental Conditions	$(Q_i/t_m)_{eff\ N2}$ cc/cm²*s*cmHg	$(Q_i/t_m)_{eff\ CO2}$ cc/cm²*s*cmHg	CO_2-N_2 Selectivity
Wetted with glycerol carbonate from the shell side and pressurized @100psig	C_{in} = 0.49% CO_2/N_2 RH_{in}: 100.0% RH_{out}: 44.5% t = 23.9°C	7.3 E-9	2.9 E-6	397
Wetted with glycerol carbonate from the shell side and pressurized @120psig	C_{in} = 0.49% CO_2/N_2 RH_{in}: 100.0% RH_{out}: 44.5% t = 24.6°C	7.4 E-9	2.6 E-6	353
Wetted with glycerol carbonate from the shell side and pressurized @150psig	C_{in} = 0.51% CO_2/N_2 RH_{in}: 100.0% RH_{out}: 44.9% t = 25.1°C	4.5 E-9	2.4 E-6	543
Wetted with glycerol carbonate from the shell side and pressurized @170psig	C_{in} = 0.51% CO_2/N_2 RH_{in}: 100.0% RH_{out}: 61.4% t = 23.7°C	5.4 E-9	2.1 E-6	400

permeance increased from $5.5*10^{-9}$ to $7.6*10^{-9}$ cc/cm^2*s*cmHg whereas the CO_2 permeance was reduced 2 times. As the applied pressure gradually increased from 70 to 170 psig, CO_2 permeance quite unexpectedly decreased from $3.2*10^{-6}$ to $2.1*10^{-6}$ cc/cm^2*s*cmHg (Table 3.17). On the other hand the N_2 permeance was slightly increasing after each pressurization step. Only in the last two pressurization steps, the N_2 permeance decreased from $7.7*10^{-9}$ to $5.4*10^{-9}$ cc/cm^2*s*cmHg. Based on these results it is hard to conclude if the pressurization technique is thinning the ILM. It seems to be that the substrate pore side is too small, and a pressure greater than 170 psig is needed in order to notice any significant changes in N_2 and CO_2 permeance.

Therefore, a new module 2 was prepared with a new ceramic tube having a substrate with a larger pore size. The full thickness glycerol carbonate ILM was prepared in the same manner as described for ceramic tube 1. The module was tested with 0.51% CO_2/N_2 humidified feed gas mixture passing on the shell side and dry He sweep gas passing through the bore side. For a full ILM, N_2 and CO_2 permeance reached the values of $4.5*10^{-9}$ and $1.3*10^{-6}$ cc/cm^2*s*cmHg respectively with the selectivity around 300 (Table 3.18). When the pressure was increased to 20 psig, CO_2 permeance value reached $3.1*10^{-6}$ cc/cm^2*s*cmHg; at 40 psig CO_2 permeance slightly decreased to $1.8*10^{-6}$ cc/cm^2*s*cmHg. The nitrogen permeance for all three runs stayed around $5.5*10^{-9}$ cc/cm^2*s*cmHg. When the pressure was increase to 100 psig, N_2 permeance was drastically increased to $3.7*10^{-7}$ cc/cm^2*s*cmHg while CO_2 permeance value maintained at $3.6*10^{-6}$ cc/cm^2*s*cmHg resulting in very low selectivity of 10. The sudden increase in N_2

Table 3.18 Summary of the Permeation Results for CO_2/N_2 Gas Mixture for Ceramic Module 2 Immobilized with Glycerol Carbonate and Subjected to Stepwise Pressurization

ILM Preparation	Experimental Conditions	$(Q_i/t_m)_{eff\ N2}$ cc/cm²*s*cmHg	$(Q_i/t_m)_{eff\ CO2}$ cc/cm²*s*cmHg	CO_2-N_2 Selectivity
Wetted with glycerol carbonate from the shell side	C_{in} = 0.51% CO_2/N_2 RH_{in}: 100.0% RH_{out}: 42.9% t = 22°C	4.5 E-9	1.3 E-6	283
Wetted with glycerol carbonate from the shell side and pressurized @20psig	C_{in} = 0.51% CO_2/N_2 RH_{in}: 100.0% RH_{out}: 57.6% t = 23°C	5.4 E-9	3.1 E-6	574
Wetted with glycerol carbonate from the shell side and pressurized @40psig	C_{in} = 0.51% CO_2/N_2 RH_{in}: 100.0% RH_{out}: 50% t = 23.2°C	5.9 E-8	1.8 E-6	310
Wetted with glycerol carbonate from the shell side and pressurized @100psig	C_{in} = 0.51% CO_2/N_2 RH_{in}: 100.0% RH_{out}: 44.1% t = 24.4°C	3.7 E-7	3.6 E-6	10

Table 3.18 Summary of the Permeation Results for CO_2/N_2 Gas Mixture for Ceramic Module 2 Immobilized with Glycerol Carbonate and Subjected to Stepwise Pressurization (Continued)

ILM Preparation	Experimental Conditions	$(Q_i/t_m)_{eff\ N2}$ cc/cm²*s*cmHg	$(Q_i/t_m)_{eff\ CO2}$ cc/cm²*s*cmHg	CO_2-N_2 Selectivity
Reimmobilized with glycerol carbonate from the shell side	C_{in} = 0.49% CO_2/N_2 RH_{in}: 100.0% RH_{out}: 44.5% t = 23.9°C	7.3 E-9	2.9 E-6	397
Wetted with glycerol carbonate from the shell side and pressurized @25psig	C_{in} = 0.49% CO_2/N_2 RH_{in}: 100.0% RH_{out}: 44.5% t = 24.6°C	5.4 E-9	3.3 E-6	610
Wetted with glycerol carbonate from the shell side and pressurized @60psig	C_{in} = 0.51% CO_2/N_2 RH_{in}: 100.0% RH_{out}: 44.9% t = 25.1°C	2.5 E-7	3.0 E-6	12

permeance in this would indicate that the ILM is leaking. As we can see in Table 3.18, the module was reimmobilized with glycerol carbonate and gradually pressurized; at 60 psig N_2 permeance drastically increased as result of membrane leakage. This is likely to be the result of some kind of a defect in the membrane material. The role of the expelled liquid on the skin is unclear at this time. A new technique is needed to eliminate this expelled liquid.

3.4 Conclusions

3.4.1 Conclusions Based on AA-Grafted Hollow Fibers Experiments

Facilitated transport of CO_2 through grafted hollow fiber membranes was investigated using glycerol/water based ILM solutions containing either Na-glycinate or EDA as the carrier. Most of the hollow fiber membranes immobilized with 3M-glycerol solution gave very low CO_2 permeance in the order of 10^{-6} cc/cm^2*s*cmHg. Certain batches e.g., batch 4 (High Graft Exposure Time) and batch 5 (Low Graft Concentration/Solution) gave CO_2 permeance of the order of 10^{-5} cc/cm^2*s*cmHg which was the highest observed permeance for glycerol based ILM in these modules. Carbon dioxide permeances in the order of 10^{-5} cc/cm^2*s*cmHg obtained for Batch 2 (Minimal Plasma/Max Vapor Time) were due to leakage and poor immobilization. This was confirmed by the SEM pictures (Figure 3.11) showing a very thin coating on the outer surface of the fibers from Batch 2.

Stainless steel membrane module 8 immobilized with 3M EDA-water solution yielded the highest CO_2 permeance: $6.52*10^{-5}$ cc/cm^2*s*cmHg and a high selectivity of 1648.

Module 3-1 from Batch 1 (minimal Plasma/minimal vapor time) also gave a CO_2 permeance of $5.94*10^{-5}$ cc/cm^2*s*cmHg when immobilized with 3M EDA-water solution. The same module immobilized with 3M Na-glycinate-water solution yielded a permeance value in the same range. This indicates that, most probably low CO_2 permeance obtained so far is due to poor penetration of the glycerol-based solution into the grafted layer or shrinkage in the grafted layer due to glycerol. Also SEM pictures (Figures: 3.6, 3.9 and 3.10) of the cross sections of the grafted fibers show a very dense film on the outer surface of the fibers. Looking at these figures, it is quite difficult to say if the grafted layer was formed inside the porous substrate too; this increased membrane thickness would result in lower CO_2 permeance values. Difficulty in diffusion of the glycerol solution through the grafted layer is confirmed by immobilizing the fibers from Batch 6 with 3M EDA-glycerol solution. This experiment showed low CO_2 permeance in the range of 10^{-6} cc/cm^2*s*cmHg even though EDA was used as a carrier.

In some cases, an attempt was made to loosen up this grafted layer for glycerol solution immobilization by prewetting the fibers with water. This procedure did not show any improvements in the performance of the hollow fiber membrane. The most likely explanation is that, either the time for the glycerol solution exchange was not long enough, or the AA gel layer did not

allow the penetration by glycerol or there was considerable shrinkage in the grafted layer.

3.4.2 Conclusions Based on PVDF Hollow Fibers Experiments

Facilitated transport of CO_2 through PVDF hollow fiber membranes was investigated using glycerol/water based ILM solutions containing Na-glycinate as the carrier or pure glycerol carbonate. Pressurization technique was applied in both cases in order to prepare thinner ILMs.

PVDF module immobilized with glycerol carbonate under the pressurized technique gave an increase of the CO_2 permeance of approximately three times. On an average, the experiment showed the highest CO_2 permeance in the range of 10^{-6} cc/cm^2*s*cmHg.

When this type of the hollow fiber membrane was immobilized with reduced viscosity 1M glycerol/water-Na-glycinate based solution, the ILM gave a CO_2 permeance value of $5.1*10^{-5}$ cc/cm^2*s*cmHg with a selectivity of 2550. This is the highest CO_2 permeance value obtained in a hollow fiber membrane using the glycerol based ILM. The membranes also showed good stability when tested constantly for a period of 30 days, using a 100% humidified feed gas mixture and dry He as a sweep gas.

When the carrier concentration was increased to 2M glycerol/water-Na-glycinate based solution, the CO_2 permeance did not increase any further due to

the reduced diffusivity of the complex and free CO_2 across the ILM since the viscosity of the 2M ILM solution was increased.

It is apparent that the pressurization technique is able to produce a thinner ILM using a PVDF hollow fiber membrane. The maximum allowable transmembrane pressure was not high enough to produce a sufficiently thin ILM. To further increase the CO_2 permanence using the pressurization technique, asymmetric hollow fibers that can withstand higher transmembrane pressures are needed. Also thinner membrane substrates are desirable, since they will have reduced diffusional paths for the transport of carbon dioxide across the membrane.

3.4.3 Conclusions Based on Ceramic Membrane Module Experiments

Increase of CO_2 permeance due to pressurization technique using ceramic tubes immobilized with glycerol carbonate was investigated. This set of experiment resulted in a low CO_2 permeance in the range of 10^{-6} cc/cm^2*s*cmHg even though very high pressures, upto 170 psig was applied. The ceramic module 1, Initially showed an increase of CO_2 and N_2 permeances upto the pressure of 70 psig. As the pressure increased further, quite unexpectedly, both permeances started decreasing. Possibly, removal of the excess liquid from the surface of the ceramic tube on the lumen side was not efficient. Due to limitations in the laboratory equipment limitations, further increase of the applied pressure was not feasible. It

seems that pressure greater than 170 psig is needed in order to prepare sufficiently thin ILM having higher CO_2 permeances.

Ceramic module 2 also maintained the CO_2 permeance in the range of 10^{-6} cc/cm^2*s*cmHg, while due to the pressurization technique N_2 permeance showed a drastic increase from $4.9*10^{-9}$ to $3.7*10^{-7}$ cc/cm^2*s*cmHg. This is most probably due to the defect in the membrane material.

It is very hard to draw any conclusions if the pressurization technique is indeed making a thinner ILM using the ceramic tubes. Most probably, the pore structure of the substrate is more cylindrical in shape than asymmetric. Therefore the pressure needed to displace the liquid from the substrate layer in order to notice any significant change in CO_2 and N_2 permeance is most probably quite high. Further, during the ILM thinning process, the liquid expelled has to be removed from the bore. It would appear that a special technique would be needed to achieve that.

CHAPTER 4

CONCLUSIONS

Based on this experimental work on thin ILMs for different applications, the following conclusions can be drawn; also a number of recommendations can be made.

A thin silicone-oil based ILM for VOC removal resulted in a considerable increase of VOC selectivity over nitrogen and consequently a more concentrated VOC-containing stream on the permeate side. On the other hand, water vapor permeance was not reduced. Therefore, either higher molecular weight silicone oils or other mineral oils should be studied (e.g. Paratherm oil) in order to reduce water vapor permeance.

The cyclic mode of operation for VOC removal should be studied further in order to optimize the experimental conditions and achieve better purification.

Acrylic acid grafted hollow fibers showed good potential for preparation of the thinner ILMs. Optimizing of the grafting conditions and thinner not quite as dense grafted layers should be prepared. Immobilization of the highly viscous solvent and their penetration into the grafted part would thus be made easier.

Further studies on PVDF hollow fibers are highly recommended since these hollow fibers resulted in the highest CO_2 permeances observed with the glycerol-Na-glycinate based ILMs. It would be highly desirable to obtain thinner wall PVDF hollow fibers. This thinner membrane substrate will most probably result in the preparation of a thinner ILMs.

Regarding the pressurization technique, asymmetric hollow fibers, which can withstand the higher transmembrane pressures, are needed. Ceramic tubes have a good stability, but the thinner wall ceramic tubes with more asymmetry in the pore structure in the substrate is needed in order to notice a significant change in the permeances. The long-term chemical stability of the ceramic materials under the alkaline conditions should also be considered.

APPENDIX A

DETERMINATION OF THIN ILM THICKNESS

Sample calculations carried out to determine the thin ILM thickness and nitrogen permeance needed for the mathematical model are provided below.

Module 1 specifications:

Number of fibers, N: 300

Effective module length, L: 20.5 cm

I.D. of the fiber: 240 μm

O.D. of the fiber: 290 μm

Effective surface area based on the logarithmic mean diameter of the fiber, A: 510 cm^2 where $A = \pi D_{lm} LN$ and $D_{lm} = (D_0 - D_i)/\ln(D_0/D_i)$.

From Table 2.3 nitrogen permeate flow rate: $Q_p = 42\ cm^3/min$.

Universal gas constant: $R = 6.234 \times 10^3$ cmHg cm^3/gmolK; T= 293K

Nitrogen permeate molar flow rate (Equation 2.3):

$$F_P = \frac{(76\,cmHg) \times (42\,cm^3/min)}{(6.234 \times 10^3\,cmHg cm^3/gmolK) \times 293K} = 1.74 \times 10^{-3}\,gmol/min$$

Nitrogen permeate flux:

$$N_{N_2} = \frac{F_P}{A} = \frac{1.74 \times 10^{-3}\,gmol/min}{510\,cm^2} = 3.41 \times 10^{-6}\,gmol/cm^2 min$$

Feed side pressure (tube side):

$$P_F = 76\,cmHg + (\frac{76}{14.69} \times 15)\,cmHg = 153.5\,cmHg$$

Permeate side pressure (shell side):

P_P = 76 cmHg

Module average nitrogen permeance:

$$\left(\frac{Q}{\delta}\right)_c = \frac{N_{N_2}}{(P_F - P_P)} = \frac{3.41 \times 10^{-6}\,gmol}{(153.5 - 76)\,cmHg\,cm^2\,60\,s} = 7.3 \times 10^{-10}\,\frac{gmol}{cm^2\,s\,cmHg}$$

$$\left(\frac{Q}{\delta}\right)_c = 1.65 \times 10^{-5}\,\frac{cm^3}{cm^2\,s\,cmHg}$$

Table 2.3 summarizes the measurement results and the calculated nitrogen permeances for three different cases. At this point, one can estimate the liquid membrane thickness knowing all parameters for the overall permeation equation:

$$\frac{1}{\left(\frac{Q}{\delta}\right)_{OV}} = \frac{1}{\left(\frac{Q}{\delta}\right)_c \times \frac{d_0}{d_{lm}}} + \frac{1}{\left(\frac{Q}{\delta_l}\right)_l}$$

In order to determine the thin ILM thickness, the above equation was solved knowing all parameters except (δ_l). The overall nitrogen permeances, $\left(\frac{Q}{\delta}\right)_{OV}$, are obtained measuring the N_2 permeate flow rate with module 1 after immobilization with the thin layer of silicone oil. The values are provided in Table 2.3. The value of Q_l for the silicone oil was estimated from the nitrogen permeate flow measurements made with module 2 in the following manner (Table 2.3):

$$\left(\frac{Q}{\delta}\right)_l = 1.05\times10^{-11}\frac{gmol}{cm^2 s\,cmHg} = 2.36\times10^{-7}\frac{cm^3}{cm^2 s\,cmHg}$$

where full ILM thickness δ_l= 25 x 10 $^{-4}$cm; therefore

$$Q_l = 1.05\times10^{-11}\frac{gmol}{cm^2 s\,cmHg}\times 25\times10^{-4}\,cm = 2.6\times10^{-14}\frac{gmol\,cm}{cm^2 s\,cmHg}$$

$$Q_l = 5.82\times10^{-10}\frac{cm^3}{cm^2 s\,cmHg}$$

Once Q_l was determined; using the already calculated $\left(\frac{Q}{\delta}\right)_c = 1.65\times10^{-5}\frac{cm^3}{cm^2 s\,cmHg}$ and $\left(\frac{Q}{\delta}\right)_{ov} = 1.22\times10^{-6}\frac{cm^3}{cm^2 s\,cmHg}$ values the overall permeation equation was solved for δ_l from equation (2.6). The estimated thickness of the thin ILM is δ_l = 4.7X10^{-4} cm.

APPENDIX B

ESTIMATION OF PARAMETERS

A sample calculation for the estimation of parameters for the mathematical model in terms of VOC permeance through the thin ILM and overall VOC permeance is provided here.

Module 1 specifications:

Number of fibers, N: 300

Effective module length, L: 20.5 cm

I.D. of the fiber: 240 μm

O.D. of the fiber: 290 μm

Effective surface area based on logarithmic mean diameter of the fiber, A: 510 cm^2 where $A = \pi D_{lm} LN$ and $D_{lm} = (D_0 - D_i)/\ln(D_0/D_i)$.

Experimental Data from Table 2.5 for Acetone

Feed flow rate in, Q_{in}: 205 cc/min

Feed flow rate out, Q_{out}: 200 cc/min

Permeate Flow Rate Q_p: $Q_{in} - Q_{out} = 5$ cc/min

Feed pressure in, P_{in}: 78.6 cmHg

Feed Pressure out, P_{out}: 76.0 cmHg

ΔP along the module: 2.6 cmHg

Permeate Pressure, P_{perm}: 1.8 cmHg

Inlet acetone concentration, C_{in}: 11 000 ppmv

Outlet acetone concentration, C_{out}: 5 922 ppmv

Calculations

To calculate molar flow rate using PV=nRT

Pressure is taken to be 76 cmHg since flow rate measurements were made at atmospheric pressure.

R = 6.24x10³ cmHg cm³/gmol°K

Molar flow rate in, F_{in}:

$$F_{in} = \frac{76\ \text{cmHg} \times 205\text{cc/min}}{6.236 \times 10^3\ \text{cmHgcc/gmol°K} \times 293.15\text{°K} \times 60} = 1.421 \times 10^{-4}\ \text{gmol/s}$$

Molar flow rate out, F_{out}:

$$F_{iout} = \frac{76\ \text{cmHg} \times 200\text{cc/min}}{6.236 \times 10^3\ \text{cmHgcc/gmol°K} \times 293.15\text{°K} \times 60} = 1.386 \times 10^{-4}\ \text{gmol/s}$$

Permeate molar flow rate F_p:

$$F_P = F_{in} - F_{out} = 3.5 \times 10^{-6}\ \text{gmol/s}$$

Permeate Mole Fraction of Acetone and Nitrogen

x_{VOC_f}, x_{VOC_w}: mole fraction of acetone in the feed side mixture at the feed inlet and the feed outlet of the permeator

$x_{N_{2f}}, x_{N_{2w}}$: mole fraction of nitrogen in the feed side mixture at the feed inlet and the feed outlet of the permeator

$y_{VOC_w}, y_{N_{2w}}$: mole fraction of acetone and nitrogen in the permeate at the permeate outlet end of the permeator

$x_{VOC_f} = ppmv_{Actone,f}/10^6$ $\quad x_{VOC_f} = 11000/10^6 = 0.011$

$x_{N_{2f}} = 1 - x_{VOC_f}$ $\quad x_{N_{2f}} = 1 - 0.011 = 0.989$

$x_{VOC_w} = ppmv_{Acetone,w}/10^6$ $\quad x_{VOC_w} = 5922/10^6 = 0.005922$

$x_{N_{2w}} = 1 - x_{VOC_w}$ $\quad x_{N_{2w}} = 1 - 0.005922 = 0.994$

$$y_{VOC_w} = \frac{\left(F_{VOC_f} x_{VOC_f} - F_{VOC_w} x_{VOC_w}\right)}{F_{VOC_p}}$$

$$= \frac{\left(1.421\times10^{-4}\times0.011 - 1.386\times10^{-4}\times0.005922\right)}{3.5\times10^{-6}} = 0.21$$

$y_{N_{2w}} = 1 - 0.21 = 0.79$

Acetone and Nitrogen Permeate Flux

Acetone Permeate Flux

$$N_{VOC_p} = \frac{F_P \times y_{VOC_p}}{A} = \frac{3.5\times10^{-6}\,gmol/s\times0.21}{510cm^2} = 1.44\times10^{-9}\,gmol/s\,cm^2$$

$$N_{N_{2p}} = \frac{F_P \times y_{N_{2p}}}{A} = \frac{3.5\times10^{-6}\,gmol/s\times0.79}{510cm^2} = 5.42\times10^{-9}\,gmol/s\,cm^2$$

Percent Removal of Acetone

$$\%Removal = \frac{F_P \times y_{VOC_p}}{F_{in} \times X_{VOC_f}} \times 100 = \frac{3.5\times10^{-6}\,gmol/s\times0.21}{1.421\times10^{-4}\,gmol/s\times0.011} \times 100 = 47.5\%$$

Module Average Permeance of Acetone

P_{VOC_f}, p_{VOC_f}: acetone partial pressure at the feed and the permeate side at the feed inlet of the permeator

P_{VOC_w}, p_{VOC_w}: acetone partial pressure at the feed and the permeate side at the feed outlet of the permeator

$P_{VOC_f} = 78.6\text{cmHg} \times 0.011 = 0.86\text{cmHg}$

$p_{VOC_f} = 1.8\text{cmHg} \times 0.21 = 0.378\text{cmHg}$

$P_{VOC_w} = P_f \times x_f = 76.0\text{cmHg} \times 0.005922 = 0.45\text{cmHg}$

$p_{VOC_w} = 1.8\text{cmHg} \times 0.0 = 0.0\text{cmHg}$

$$\Delta P_{lm} = \frac{(P_{VOC_f} - p_{VOCf}) - (P_{VOC_w} - p_{VOC_w})}{\ln\left(\frac{(P_{VOC_f} - p_{VOCf})}{(P_{VOC_w} - p_{VOC_w})}\right)}$$

$$\Delta P_{lm} = \frac{(0.86\text{cmHg} - 0.39\text{cmHg}) - (0.45\text{cmHg} - 0.0\text{cmHg})}{\ln\left(\frac{(0.86\text{cmHg} - 0.39\text{cmHg})}{(0.45\text{cmHg} - 0.0\text{cmHg})}\right)} = 0.459$$

Acetone overall module average permeance first estimate:

$$\frac{Q_{ov_{VOC}}}{\delta_{ov}} = \frac{N_{VOCP}}{\Delta P_{lm}} = \frac{1.44 \times 10^{-9}\,\text{gmol/scm}^2}{0.459\text{cmHg}} = 3.14 \times 10^{-9}\,\text{gmol/cm}^2\text{s cmHg}$$

Module Average Permeance of Nitrogen

$P_{N_{2f}}, p_{N_{2f}}$ nitrogen partial pressure at the feed and the permeate side at the feed inlet of the permeator

$P_{N_{2w}}, p_{N_{2w}}$ nitrogen partial pressure at the feed and the permeate side at the feed outlet of the permeator

$P_{N_{2f}} = 78.6\text{cmHg} \times 0.989 = 77.73\text{cmHg}$

$p_{N_{2f}} = 1.8\text{cmHg} \times 0.78 = 1.4\text{cmHg}$

$P_{N_{2w}} = P_f \times x_{N_{2f}} = 76.0\text{cmHg} \times 0.994 = 75.54\text{cmHg}$

$p_{N_{2w}} = 1.8\text{cmHg} \times 0.0 = 0.0\text{cmHg}$

$$\Delta P_{lm} = \frac{(77.73cmHg - 1.4cmHg) - (75.54cmHg - 0.0cmHg)}{\ln\left(\frac{(77.73cmHg - 1.4cmHg)}{(75.54cmHg - 0.0cmHg)}\right)} = 75.92cmHg$$

Nitrogen overall module average permeance:

$$\frac{Q_{ov_{N2}}}{\delta_{ov}} = \frac{N_{N2P}}{\Delta P_{lm}} = \frac{5.34 \times 10^{-9} gmol/scm^2}{75.92cmHg} = 7.03 \times 10^{-11} gmol/cm^2 s\, cmHg$$

Separation factor

$$\alpha = \frac{\frac{Q_{ov_{voc}}}{\delta_{ov}}}{\frac{Q_{ov_{N_2}}}{\delta_{ov}}} = \frac{3.24 \times 10^{-9} gmol/cm^2 s\, cmHg}{7.03 \times 10^{-11} gmol/cm^2 s\, cmHg} = 46.06$$

Acetone permeance through the thin ILM

$\left(\frac{Q}{\delta}\right)_c$ acetone permeance through the silicone skin

$\left(\frac{Q}{\delta}\right)_{ov}$ acetone overall permeance

$\left(\frac{Q}{\delta_l}\right)_l$ acetone permeance through the silicone oil

The acetone permeances through the silicone skin was calculated based on the experimental results obtained with module 1 without the thin ILM (Table 2.4). Acetone permeance through the silicone oil is calculated as described in Appendix A. The overall permeance was obtained by solving the flux equation and computer program was developed (Appendix F) to calculate the overall acetone and nitrogen permeance as described in the section 2.3.1.

$$\left(\frac{Q}{\delta}\right)_c = 4.89\times10^{-8}\,\text{gmol/cm}^2\text{s cmHg}$$

$$d_{lm} = 287\times10^{-4}\,\text{cm}$$

$$d_0 = 290\times10^{-4}\,\text{cm}$$

$$\frac{1}{\left(\frac{Q}{\delta}\right)_{OV}} = \frac{1}{\left(\frac{Q}{\delta}\right)_c \times \frac{d_0}{d_{lm}}} + \frac{1}{\left(\frac{Q}{\delta_l}\right)_l}$$

$$\frac{1}{\left(\frac{Q}{\delta_l}\right)_l} = 2.88\times10^{8}\,\frac{\text{gmol}}{\text{cm}^2\text{s cmHg}}$$

$$\left(\frac{Q}{\delta_l}\right)_l = 3.46\times10^{-9}\,\frac{\text{gmol}}{\text{cm}^2\text{s cmHg}}$$

Reevaluation of the Acetone overall permeance

y_{VOC_w} acetone permeate side concentration calculated using a cross flow equation at the feed outlet of the permeator

γ pressure ration

$$\frac{y_{VOC_w}}{(1-y_{VOC_w})} = \frac{\alpha(x_{VOC_w} - \gamma\, y_{VOC_w})}{((1-x_{VOC_w}) - \gamma(1-y_{VOC_w}))}$$

$$\gamma = \frac{p}{P} = \frac{1.8\text{cmHg}}{76.0\text{cmHg}} = 0.023$$

$\alpha = 46.06$

$x_{VOC_w} = 0.005922$

Solving the above equation one can get the first estimate for $y_{VOC_w} = 0.125$ in order to estimate the new driving force.

$$p_{VOC_w} = 1.8\text{cmHg} \times 0.125 = 0.225\text{cmHg}$$

$$\Delta P_{lm} = \frac{(0.86\text{cmHg} - 0.39\text{cmHg}) - (0.45\text{cmHg} - 0.225\text{cmHg})}{\ln\left(\frac{(0.86\text{cmHg} - 0.39\text{cmHg})}{(0.45\text{cmHg} - 0.225\text{cmHg})}\right)} = 0.332\text{cmHg}$$

$$\frac{Q_{ov_{VOC}}}{\delta_{ov}} = \frac{N_{VOC\,P}}{\Delta P_{lm}} = \frac{1.49 \times 10^{-9}\,\text{gmol/scm}^2}{0.332\text{cmHg}} = 4.48 \times 10^{-9}\,\text{gmol/cm}^2\text{s cmHg}$$

$$\alpha = \frac{\frac{Q_{ov_{VOC}}}{\delta_{ov}}}{\frac{Q_{ov_{N_2}}}{\delta_{ov}}} = \frac{4.48 \times 10^{-9}\,\text{gmol/cm}^2\text{s cmHg}}{7.03 \times 10^{-11}\,\text{gmol/cm}^2\text{s cmHg}} = 63.72$$

This result is also provided in Figure 2.11. Reevaluation of the acetone overall permeance is repeated until the acetone permeance parameters used in mathematical model gave good agreement between simulated and experimental results.

Final values are as follows:

$$\left(\frac{Q}{\delta}\right)_l = 6.5 \times 10^{-9}\,\frac{\text{gmol}}{\text{cm}^2\text{s cmHg}}$$

$$\left(\frac{Q}{\delta}\right)_c = 4.89 \times 10^{-8}\,\frac{\text{gmol}}{\text{cm}^2\text{s cmHg}}$$

$$\left(\frac{Q}{\delta}\right)_{ov} = 5.8 \times 10^{-9}\,\frac{\text{gmol}}{\text{cm}^2\text{s cmHg}}$$

In the same manner, VOC permeances for methanol and toluene were estimated. The final estimated values of the overall and silicone oil permeances for all three VOCs are provided in Figures 2.15, 2.16 and 2.17 accordingly.

APPENDIX C

SAMPLE CALCULATION FOR WATER VAPOR TRANSPORT

A sample calculation for water vapor transport across the silicone oil-based ILM in a hollow fiber module is given here. The calculation procedure is the same for all water transport experiments using different substrates.

Experimental conditions (Table 2.15):

Using dry N_2 sweep technique

Feed side:

Feed stream: humidified N_2

Feed inlet RH: 98.6% t=17.8°C ≈ 64°F

Feed outlet RH: 52.9% t=17.1°C ≈ 63°F

Feed side pressure: ~ 2psig = 16.696 psia = 33.8 inHga

Feed inlet flow rate: 43.0 cc/min

Feed outlet flow rate: 41.5 cc/min

Sweep side:

Sweep side: dry N_2

Sweep flow rate: 30.0 cc/min

Sweep side humidity: 30.9% t=16.2°C≈ 61°F

Permeate side pressure: ~ atmospheric

Based on the definition of relative humidity

Relative humidity = $100p/p_s$

p= partial pressure

p_s = vapor pressure at dry bulb temperature (inHg)

Partial pressures are calculated as follows

Feed side:

In: p_s=0.601 inHg @ 64°F; 98.6% =100xp/0.601 inHg $\Rightarrow$ p=0.592 inHg

Out: p_s=0.5805 inHg @ 63°F; 52.9% =100xp/0.5805 inHg $\Rightarrow$ p=0.307 inHg

Sweep side:

Out: p_s=0.541 inHg @ 61°F; 30.9% =100xp/0.541 inHg $\Rightarrow$ p=0.167 inHg

Water vapor permeance is calculated according to the following equation:

$$\left(\frac{Q}{\delta}\right)_{H_2O.eff} = \frac{\text{Flux}}{(\text{Area}) \times (\text{Driving force})}$$

Driving Force (Δp)=(p_{feed} - $p_{permeate}$)

p_{feed} - partial pressure on the feed side

$p_{permeate}$ - partial pressure on the permeate side

Calculation of the water flux

Vapor pressure @ t=17.8 °C is p_s=0.601 inHg

Vapor pressure @ t=17.1 °C is p_s=0.580 inHg

Vapor pressure @ t=16.2 °C is p_s=0.541 inHg

Mole fraction of water vapor at saturation is given as

$$y^{sat}_{H_2O,in} = \frac{p_{sat}}{P_f} = \frac{0.601 inHg}{33.8 inHg} = 0.0177$$

$$y^{sat}_{H_2O,out} = \frac{p_{sat}}{P_f} = \frac{0.580 inHg}{33.8 inHg} = 0.0171$$

$$y^{sat}_{H_2O,sweep} = \frac{p_{sat}}{P_f} = \frac{0.541 inHg}{29.9 inHg} = 0.0180$$

Mole fractions of water at the feed inlet and feed outlet of the module are:

$$y^{in}_{H_2O} = RH_{in} \times y^{sat}_{H_2O} = \frac{98.6}{100} \times 0.0177 = 0.0174$$

$$y^{out}_{H_2O} = RH_{out} \times y^{sat}_{H_2O} = \frac{52.9}{100} \times 0.0171 = 0.0090$$

$$y^{sweep}_{H_2O} = RH_{sweep} \times y^{sat}_{H_2O} = \frac{30.9}{100} \times 0.0180 = 0.00556$$

Water flux based on the feed side conditions can be calculated as follows:

$$\text{Water Flux} = \frac{V_{f,in} \times y^{in}_{H_2O} - V_{f,out} \times y^{out}_{H_2O}}{A}$$

$$= \frac{43 \times 0.0174 - 41.5 \times 0.009}{60 \times 191} = 3.26 * 10^{-5} \frac{cm^3}{cm^2 s}$$

Water Vapor partial pressure differential across the ILM:

Water vapor partial pressure at the inlet and the outlet of the module based on the relative humidity definition:

$$RH = 100 \times \frac{p}{p_s} = 100 \times \frac{\text{partial pressure}}{\text{vapor pressure}}$$

p_{in} = 0.601 x 0.986 = 0.592 inHg=1.50 cmHg

p_{out} = 0.580 x 0.529 = 0.307 inHg = 0.77 cmHg

Feed side average partial pressure

$P_{feed}=(p_{in}+p_{out})/2=(1.5+0.77)/2=1.13$ cmHg

Sweep side partial pressure

p_{sweep} = 0.541 x 0.309 = 0.167 inHg = 0.42 cmHg

Partial pressure driving force:

$$\Delta p_{water} = 1.13 - 0.42 = 0.71 cmHg$$

Water vapor effective permeance calculation:

Based on the membrane area of 191 cm^2 and feed side condition

$$\left(\frac{Q_{H_2O}}{t_m}\right)_{eff} = \frac{Water\,Flux}{\Delta p_{water}} = \frac{3.26 * 10^{-5}}{0.71} = 4.5 * 10^{-5}\,\frac{cm^3}{cm^2 s\,cmHg}$$

$$\left(\frac{Q_{H_2O}}{t_m}\right)_{eff} = 2.0 * 10^{-9}\,\frac{gmol}{cm^2 s\,cmHg}$$

APPENDIX D

SAMPLE CALCULATION FOR THE ILM-BASED CO_2/N_2 SEPARATION

A sample calculation for the ILM-based CO_2-N_2 separation performance in a hollow fiber module is given here. The calculation procedure is same for all CO_2-N_2 separation experiments using different substrates.

Experimental conditions (Table 3.12):

Room temperature: 20.3 °C

Feed stream: 0.495% CO_2-balance N_2

Feed inlet RH: 100%

Feed outlet RH: 67.4%

Feed side pressure: 4psig

Feed inlet flow rate: 21.0 scc/min

Sweep stream: dry helium

Sweep pressure: atmospheric

Sweep outlet flow rate: 8.1 cm^3/min.

Module characteristics:

Module #8 having stainless steel casing: A=30.0 cm^2, N=25

CO_2 and N_2 mole factions calculations:

GC results: N_2 peak area = 10,015; CO_2 peak area = 32,742

From GC calibration results: $K_{N2} = 8.439*10^{-8}$, $K_{CO2} = 1.008*10^{-7}$ where K_{N2} and K_{CO2} represent the values of the GC calibration curve slope (Figures 3.4 and 3.5).

N_2 and CO_2 mole fractions in the sweep outlet can be calculated as follows:

$y_{N2} = 8.439*10^{-8} *10,015 = 8.45*10^{-4}$

$y_{CO2} = 1.008*10^{-7}*32,742 = 3.30*10^{-3}$

N_2 and CO_2 partial pressure differential across the ILM :

$\Delta p_{N2} = [(14.7 + 4.0) \times 0.99505 - 14.7* 8.45*10^{-4}] \times 76/14.7 = 96.1$ cmHg

$\Delta p_{CO2} = [(14.7 + 4.0) \times 0.00495 - 14.7*3.30*10^{-3}] \times 76/14.7 = 0.26$ cmHg

N_2 and CO_2 effective permeances calculations:

Based on the membrane area of 30 cm^2

$(Q_{N2}/t_m)_{eff} = 8.1*8.45*10^{-4} /(60*30*96.1) = 3.95*10^{-8}$ scc/cm^2*s*cmHg

$(Q_{CO2}/t_m)_{eff} = 8.1*3.30*10^{-3} /(60*30*0.26) = 5.67*10^{-5}$ scc/cm^2*s*cmHg

CO_2/N_2 selectivity:

$\alpha_{CO2/N2} = 5.67*10^{-5}/3.95*10^{-8} = 1435$

APPENDIX E

DETAILS ON PLASMA POLYMERIZATION CONDITIONS FOR HOLLOW FIBERS AND PLASMA GRAFT PROCEDURE

All membrane substrates and membrane modules having stainless steel casing were prepared by grafting acrylic acid onto the substrate by plasma graft polymerization technique. The procedure is described in following three steps:

Step 1. Hollow fiber membrane substrate was exposed to the plasma under inert gas atmosphere for a certain amount of time to activate the hollow fiber surface.

Step 2. Once the surface is activated, the fiber is exposed to some vapors of the graft to put some reactive groups onto the outer fiber surface. This swells the fiber dramatically. It is important that fiber does not get exposed to the air, since that will quench the reactive groups.

Step 3. Fiber is introduced into the acrylic acid water solution of fixed concentration. This solution made with degasified distilled water was heated and stirred continuously while under vacuum. Aqueous solution concentration was varied from 1-15%.

Changing plasma polymerization conditions by changing plasma power input, exposure time and/or acrylic acid concentration, different amount of grafting were achieved and fibers were named accordingly:

Batch 1: Minimal Plasma/Minimal Vapor Time

Least power and shortest exposure time to plasma regarding step 1. Also shortest exposure time in step2.

Batch 2: Minimal Plasma./Max Vapor Time

Least power with short plasma exposure time, combined with maximum exposure time regarding step 2.

Batch 3: Modest Graft Exposure Time

Modest exposure time to graft solution in process step 3.

Batch 4: High Graft Exposure Time

Longest time of fiber exposure to graft solution in process step 3.

Batch 5: Low Graft Concentration/Solution

Minimum concentration of acrylic acid in water solution to which the fibers are exposed in step 3.

Batch 6: High Graft Concentration/Solution

Maximum concentration of acrylic acid in water solution to which the fibers are exposed in step 3.

Membrane modules (#4, #6 and #8) having stainless steel casing:

Grafting conditions, for fibers in these modules were moderate for all three steps.

APPENDIX F

PROGRAM FOR MODELING OF THE VOC PERMEATION THROUGH THE HOLLOW FIBER MODULE

PART 1

This part of the program calculates the VOC and N_2 permeance through the silicone skin and the overall permeances. The example program calculation given below calculates the overall permeance for acetone. Parameters used for the calculation are listed in Table 2.11 and experimental conditions are given in Table 2.5.

```
C     ------------------------------------------------------------
C     CALCULATION OF THE VOC AND NITROGEN FLUX, PERMEANCE
C     THROUGH THE SKIN AND OVERALL PERMEANCES: ALFA AND BETA
C     ------------------------------------------------------------
C     1=VOC, 2=NITROGEN
C     ------------------------------------------------------------
C     UNITS OF THE PARAMETERS
C     ------------------------------------------------------------
C     PERMPR = PERMEATE PRESSURE (cmHg)
C     FEEDPR = FEED PRESSURE (cmHg)
C     FEEDCOM = FEED COMPOSITION (mol fraction)
C     PERMCOM = PERMEATE COMPOSITION (mol fraction)
C     PERMOIL = PERMEANCE THROUGH THE OIL (gmol/sec cm2 cmHg)
C     PERMSKIN = PERMEANCE THROUGH THE SKIN (gmol/sec cm2 cmHg)
C     DLOGM = MEAN LOGARITHMIC DIAMETER (cm)
C     D0 = OUTSIDE DIAMETER (cm)
C     A = VOC PERMEANCE PARAMETER (1/(gmol cm2 cmHg))
C     B = VOC PERMEANCE PARAMETER (1/cmHg) FOR P = A*EXP(b*PX)
C     DELL =
C     ALFA = VOC OVERALL PERMEANCE (gmol/sec cm2 cmHg)
C     BETA = NITROGEN OVERALL PERMEANCE (gmol/sec cm2 cmHg)
C     ------------------------------------------------------------
C
C
      INTEGER       ITMAX, N
      PARAMETER (N=1)
      REAL    ERRREL, FCN, FNORM, Z(N), ZGUESS(N)
      COMMON        PERMPR, FEEDPR, FEEDCOM1, PERMCOM1, PERMOIL1, DLOGM, D0
      COMMON        A, B, DELL, FEEDCOM2, PERMCOM2, PERMOIL2, PERMSKIN2
      COMMON        Y3,Y4,Y5
      REAL    ALFA, BETA
      EXTERNAL  FCN, NEQNF
```

```
C
      DATA ZGUESS /1.0E-9/
C
      PERMPR = 3.3
      FEEDPR = 77.0
      FEEDCOM1 = 1.0e4*11000.0*1.0E-6
      PERMCOM1 = 74510*1.0e4*1.0E-6
      FEEDCOM2 = 1.0E4 - FEEDCOM1
      PERMCOM2 = 1.0E4 - PERMCOM1
      PERMOIL1 = 7.7E-9
      PERMOIL2 = 9.0e-11
      PERMSKIN2 = 6.0E-10
      DLOGM = 2.87E-2
      D0 = 290.0E-4
      A = 155.0E-10
      B =22.0/77.0
      DELL = 2.0
C
C
      ERRREL = 0.01
      ITMAX = 100
C
      Y3=FEEDCOM1
      Y4=PERMCOM1
      Y5=FEEDPR

C
      CALL NEQNF (FCN, ERRREL, N, ITMAX, ZGUESS, Z, FNORM)
C
      WRITE(6, *) 'Z1', Z(1) , 'FNORM',  FNORM
      FLUX1 = Z(1)
C
C     --------------
C     CALCULATE P'X'
C     --------------
C
      PXPRIME = FEEDPR*FEEDCOM1 - LUX1/(3.14*DLOGM*DELL*PERMOIL1)
C
      PYPRIME2 = PERMPR*PERMCOM1
      PX = FEEDPR*FEEDCOM1
      PX2 = FEEDPR*FEEDCOM2
      WRITE (6,*) 'PX',  PX, 'PXPRIME', PXPRIME, PYPRIME2,PX2
C
C     ----------------------------------------
C     CALCULATE VOC PERMEANCE THROUGH THE SKIN
C     ----------------------------------------
C
      PERMSKIN1 = A*EXP((B/1.0E4)*PXPRIME)
      ALFA = 1/(1/(PERMSKIN1*D0/DLOGM)+1/PERMOIL1)
      WRITE (6,*) 'PERMSKIN1' , PERMSKIN1, 'ALFA', ALFA
C
C     -----------------------------------
C     CALCULATE NITROGEN OVERALL PERMEANCE
C     -----------------------------------
```

```
C
      BETA = 1/(1/(PERMSKIN2*D0/DLOGM)+1/PERMOIL2)
      FLUX2 = 3.14*DLOGM*DELL*BETA*(FEEDPR*FEEDCOM2-PERMPR*PERMCOM2)
      WRITE (6,*) 'BETA', BETA, 'FLUX2', FLUX2
C
C
C
C
      Y3=FEEDCOM1
      Y4=PERMCOM1
      Y5=FEEDPR
      ALFA2=OVPERM(Y3,Y4,Y5)
      WRITE (6,*) ALFA2
      STOP
      END
C
      FUNCTION OVPERM(R3,R4,R5)
      INTEGER  ITMAX, N
      PARAMETER (N=1)
      REAL ERRREL,FCN,FNORM,Z(N),ZGUESS(N)
      EXTERNAL FCN,NEQNF
      COMMON   PERMPR, FEEDPR, FEEDCOM1, PERMCOM1, PERMOIL1, DLOGM, D0
      COMMON   A, B, DELL, FEEDCOM2, PERMCOM2, PERMOIL2, PERMSKIN2
      COMMON Y3,Y4,Y5
      ERRREL = 0.0001
      ITMAX = 100
      Y3=R3
      Y4=R4
      Y5=R5
      DATA ZGUESS /1.0E-10/
      CALL NEQNF (FCN, ERRREL, N, ITMAX, ZGUESS, Z, FNORM)
      FLUX1 = Z(1)
      PXPRIME = Y5*Y3 - FLUX1/(3.14*DLOGM*DELL*PERMOIL1)
      PERMSKIN1 = A*EXP((B/1.0E4)*PXPRIME)
      WRITE (6,*) PERMSKIN1
      OVPERM = 1/(1/(PERMSKIN1*D0/DLOGM)+1/PERMOIL1)
      RETURN
      END
C
      SUBROUTINE FCN (Z,F,N)
      INTEGER N
      REAL Z(N), F(N)
      REAL PART1, PART2, PART3, PART4, PART5,PART6
      REAL EXP
      INTRINSIC EXP
      COMMON PERMPR, FEEDPR, FEEDCOM1, PERMCOM1, PERMOIL1, DLOGM, D0
      COMMON A,B,DELL,FEEDCOM2,PERMCOM2,PERMOIL2,PERMSKIN2
      COMMON Y3,Y4,Y5
C
      PART1 = 1.0/PERMOIL1
      PART2 = Z(1)/(3.14*DLOGM*DELL*PERMOIL1)
      PART3 = Y5*Y3 - PART2
      PART4 = (A*EXP((B/1.0E4)*PART3))*(D0/DLOGM)
      PART5 = 1/PART4
```

```
      PART6 = 3.14*DLOGM*DELL*(Y5*Y3 - PERMPR*Y4)
C
C
      F(1) = Z(1)*(PART1 + PART5) - PART6
      RETURN
      END
```

PART 2

This program is used for the initial estimate of each dependant variable at the selected grid point. The estimate values are generated by solving the initial value problem for concurrent flow in the permeator. The initial value problem is solved by the IMSL subroutine IVPRK.

```
C     ------------------------------------------------
C     PROGRAM FOR INITIAL ESTIMATE OF EACH
C     DEPENDANT VARIABLE FOR THE COCURRENT FLOW
C     IN THE HOLLOW FIBER MODULE
C     ------------------------------------------------
C     1= VOC, 2=NITROGEN
C     ------------------------------------------------
C     UNITS OF THE PARAMETERS
C     ------------------------------------------------
C     PERMPR = PERMEATE PRESSURE (cmHg)
C     FEEDPR = FEED PRESSURE (cmHg)
C     FEEDCOM = FEED COMPOSITION (mol fraction)
C     PERMCOM = PERMEATE COMPOSITION (mol fraction)
C     FEEDFLOW = FEED FLOW RATE (gmol/sec)
C     PERMFLOW = PERMEATE FLOW RATE (gmol/sec)
C     PERMOIL = PERMEANCE THROUGH THE OIL (gmol/s cm2 cmHg)
C     PERMSKIN = PERMEANCE THROUGH THE SKIN (gmol/s cm2 cmHg)
C     R = UNIVERSAL GAS CONSTANT = 8.314E7(g*cm2/gmol*s2*K)
C     TEMP = TEMPERATURE (K)
C     DO = OUTSID DIAMETER (cm)
C     DI = INSIDE DIAMETER (cm)
C     A = VOC PERMEANCE PARAMETER (1/(gmol cm2 cmHg)
C     B = VOC PERMEANCE PARAMETER (1/cmHg) FOR P=A*EXP(B*P'X')
C     VIS = VISCOSITY OF FEED GAS 1800E-7(g/cm*s)
C     DLOGM = MEAN LOGARITMIC DIAMTER (cm)
C     ALFA = VOC OVERALL PERMEANCE (gmol/sec cm2 cmHg)
C     BETA = NITROGEN OVERALL PERMEANCE (gmol/sec cm2 cmHg)
C     DELL = DIFERENTIAL LENGTH
C     RLENGTH = AVTIVE LENGTH OF THE PERMEATOR (cm)
C     CONST1 = PI*DLOGM
C     CONST2 = (128*R*TEMP*FEEDFLOW*VIS)/(PI*DI**4)
```

```
C     ------------------------------------------------------
C
C     PART 2
C     ---------------------------------------
C     PROGRAM TO GUESS INITAL VALUE OF YINIT
C     USING IMSL IVPRK/DIVPRK SUBROUTINE
C     ---------------------------------------
C
      INTEGER MXPARM, NEQ, NGRID
      PARAMETER (MXPARM=50,NEQ=5,NGRID=10)
C
      INTEGER IDO, ISTEP, NOUT
      REAL FCN,FLOAT,PARAM(MXPARM),T,TEND,TOL,Y(NEQ)
C
      INTRINSIC FLOAT
      EXTERNAL FCN, IVPRK
      COMMON FEEDFLOW,PERMFLOW,FEEDCOM1,PERMCOM1,FEEDPR,PERMPR,
      DLOGM
      COMMON DI,CONST1,CONST2,ALFA,BETA,RLENGTH,FACTOR,R,TEMP,VIS
C
C
      FEEDFLOW=1.0E4*200.0/(22400.0*300.0*60)
      PERMFLOW=0.0
      FEEDCOM1=1.0E4*11000.0*1.0E-6
      FEEDPR=76.0
      PERMPR=1.8
      DLOGM=2.87E-2
      DI=240.0E-4
      R=8.314E7
      FACTOR=7.50E-5
      TEMP=298.0
      VIS=1800.0E-7
      ALFA=5.9E-9
      BETA=7.2E-11
      RLENGTH=20.0
      CONST1=DLOGM*3.14
      CONST2=(128.0*R*FACTOR**2*TEMP*VIS)/(3.14*DI**4)
      PERMCOMA=1.0E4*BETA*FEEDPR+(ALFA-
      BETA)*(FEEDPR*FEEDCOM1+PERMPR*1.0E4)
      PERMCOMB=4.0*ALFA*FEEDPR*PERMPR*FEEDCOM1*(ALFA-BETA)*1.0E4
      PERMCOMC=2.0*PERMPR*(ALFA-BETA)
      PERMCOM1=(PERMCOMA-(PERMCOMA**2-PERMCOMB)**0.5)/PERMCOMC
C     WRITE (6,*) PERMCOMA,PERMCOMB,PERMCOMC,PERMCOM1
C
C      ---------------------
C     SET INITAL CONDITIONS
C     ---------------------
      T=0.0
      Y(1) = FEEDFLOW
      Y(2) = PERMFLOW
      Y(3) = FEEDCOM1
      Y(4) = PERMCOM1
      Y(5) = FEEDPR
C
```

```
C       WRITE(6,*) T,Y
C       ------------------
C       SET ERROR TOLERANCE
C       ------------------
        TOL = 0.01
C       -------------------------
C       SET ABSOLUTE ERROR CONTROL
C       -------------------------
        PARAM(10) = 1.0
C
C
        IDO = 1
        XLEFT = 0.0
        XRIGHT =RLENGTH
        OPEN (2,FILE='YTEMP.DAT',STATUS='NEW')
        DO 10 J= 1,NGRID
          TEND = XLEFT+FLOAT(J-1)*(XRIGHT-XLEFT)/FLOAT(NGRID-1)
          CALL IVPRK (IDO,NEQ,FCN,T,TEND,TOL,PARAM,Y)
          WRITE(2,*) T,Y
 10     CONTINUE
        CLOSE (2,STATUS='KEEP')
C
C       --------------------------------
C       FINAL CALL TO RELEASE WORKSPACE
C       --------------------------------
C
        IDO=3
        CALL IVPRK (IDO,NEQ,FCN,T,TEND,TOL,PARAM,Y)
        CALL REVERSE (NEQ,NGRID)
        END
C
C       --------------
C       SUBROUTINE FCN
C       --------------
C
        SUBROUTINE FCN (NEQ,T,Y,YPRIME)
        INTEGER NEQ
        REAL T,Y(NEQ),YPRIME(NEQ)
        COMMON FEEDFLOW,PERMFLOW,FEEDCOM1,PERMCOM1,FEEDPR,PERMPR,
        DLOGM
        COMMON DI,CONST1,CONST2,ALFA,BETA,RLENGTH,FACTOR,R,TEMP,VIS
C
C       ----------------------------
C       DEFINE DIFFERENTIAL EQUATIONS
C       ----------------------------
C
        Y1P1=CONST1*ALFA*(Y(5)*Y(3)-PERMPR*Y(4))
        Y1P2=CONST1*BETA*(Y(5)*(1.0E4-Y(3))-PERMPR*(1.0E4-Y(4)))
        YPRIME(1)= -(Y1P1+Y1P2)
        YPRIME(2)= -YPRIME(1)
        Y3P1= CONST1*ALFA*(Y(5)*Y(3)-PERMPR*Y(4))*(1.0E4-Y(3))
        Y3P2= CONST1*BETA*Y(3)*(Y(5)*(1.0E4-Y(3))-PERMPR*(1.0E4-Y(4)))
        YPRIME(3)= -(Y3P1-Y3P2)/Y(1)
        YPRIME(5)=-(CONST2/1.0E4)*(Y(1)/Y(5))
```

```
      IF (Y(2).EQ.0.0) THEN
      Y40P1=CONST1*ALFA*(YPRIME(5)*Y(3)+Y(5)*YPRIME(3))*(1.0E4-Y(4))
C     Y40P2=CONST1*ALFA*(1.0E4-Y(4))*(Y(5)*Y(3)-PERMPR*Y(4))
C     Y40P3=CONST1*BETA*Y(4)*(Y(5)*(1.0E4-Y(3))-PERMPR*(1.0E4-Y(4)))
      Y40P4=CONST1*BETA*Y(4)*(YPRIME(5)*(1.0E4-Y(3))-Y(5)*YPRIME(3))
      Y40PD=Y40P1-Y40P4
      Y40P5=CONST1*ALFA*(Y(5)*Y(3)-PERMPR*Y(4))
      Y40P6=CONST1*ALFA*PERMPR*(1.0E4-Y(4))
      Y40P7=CONST1*BETA*(Y(5)*(1.0E4-Y(3))-PERMPR*(1.0E4-Y(4)))
      Y40P8=CONST1*BETA*Y(4)*PERMPR
      Y40PE=YPRIME(2)+Y40P5+Y40P6+Y40P7+Y40P8
      YPRIME(4)=Y40PD/Y40PE
      ELSE
      Y4P1= CONST1*ALFA*(Y(5)*Y(3)-PERMPR*Y(4))*(1.0E4-Y(4))
      Y4P2= CONST1*BETA*Y(4)*(Y(5)*(1.0E4-Y(3))-PERMPR*(1.0E4-Y(4)))
      YPRIME(4)= (Y4P1-Y4P2)/Y(2)
      ENDIF
      RETURN
      END
C
C
C     ---------------------------------------------
C     SUBROUTINE TO REVERSE THE ORDER OF Y VALUES
C     ---------------------------------------------
C
      SUBROUTINE REVERSE(NEQ,NGRID)
      INTEGER NEQ,NGRID
      REAL TT(20),YNEW(10,20)
      OPEN (3,FILE='YTEMP.DAT',STATUS='OLD')
      DO 40 I=1,NGRID
      READ (3,*) T,Y1,Y2,Y3,Y4,Y5
      TT(I)=T
      YNEW(1,NGRID+1-I)=Y1
      YNEW(2,I)=Y2
      YNEW(3,NGRID+1-I)=Y3
      YNEW(4,I)=Y4
      YNEW(5,NGRID+1-I)=Y5
40    CONTINUE
      CLOSE (3,STATUS='KEEP')
      OPEN(4,FILE='YINIT.DAT',STATUS='NEW')
      DO 50 J=1,NGRID
      WRITE (4,*) YNEW(1,J),YNEW(2,J),YNEW(3,J),YNEW(4,J),YNEW(5,J)
50    CONTINUE
      CLOSE (4,STATUS='KEEP')
      RETURN
      END
```

PART 3

This part of the program predicts the VOC permeation through the hollow fiber permeator in a countercurrent mode of operation. The IMSL subroutine BVPFD

was used to numerically solve the set of nonlinear equations using the boundary condition.

```
C     ------------------------------------------------
C     PROGRAM FOR MODELING OF VOC PERMEATION
C     THROUGH THE HOLLOW FIBER MODULE
C     ------------------------------------------------
C     1= VOC, 2=NITROGEN
C     ------------------------------------------------
C     UNITS OF THE PARAMETERS
C     ------------------------------------------------
C     PERMPR = PERMEATE PRESSURE (cmHg)
C     FEEDPR = FEED PRESSURE (cmHg)
C     FEEDCOM = FEED COMPOSITION (mol fraction)
C     PERMCOM = PERMEATE COMPOSITION (mol fraction)
C     FEEDFLOW = FEED FLOW RATE (gmol/sec)
C     PERMFLOW = PERMEATE FLOW RATE (gmol/sec)
C     R = UNIVERSAL GAS CONSTANT = 8.314E7(g*cm2/gmol*s*K)
C     TEMP = TEMPERATURE (K)
C     DI = INSIDE DIAMETER (cm)
C     VIS = VISCOSITY OF FEED GAS 1800E-7(g/cm*s)
C     DLOGM = MEAN LOGARITMIC DIAMTER (cm)
C     ALFA = VOC OVERALL PERMEANCE (gmol/sec cm2 cmHg)
C     BETA = NITROGEN OVERALL PERMEANCE (gmol/sec cm2 cmHg)
C     DELL = DIFERENTIAL LENGTH
C     RLENGTH = AVTIVE LENGTH OF THE PERMEATOR (cm)
C     CONST1 = PI*DLOGM
C     CONST2 = (128*R*TEMP*FEEDFLOW*VIS)/(PI*DI**4)
C     ------------------------------------------------
C
C     PART 3
C     ------------------------------------------------
C     PROGRAM TO MODEL A HOLLOW FIBER PERMEATOR WITH
C     TUBE SIDE FEED AND SHELL SIDE VACUUM
C     USING IMSL BVPFD/DBVFD
C     ------------------------------------------------
C
C
      INTEGER LDYFIN,LDYINI,MXGRID,NEQNS,NINIT
      PARAMETER (MXGRID=100,NEQNS=5,NINIT=10,LDYFIN=NEQNS,
     &  LDYINI=NEQNS)
      INTEGER I,J,NCUPBC,NFINAL,NLEFT
C
      REAL CONST,ERREST(NEQNS),FCNBC,FCNEQN,FCNJAC
      REAL PISTEP,XFINAL(MXGRID),XINIT(NINIT),XLEFT
      REAL XRIGHT,YFINAL(LDYFIN,MXGRID),YINIT(LDYINI,NINIT)
      REAL XIVP(NINIT),YIVP(LDYINI,NINIT)
C
      LOGICAL LINEAR, PRINT
      INTRINSIC FLOAT
```

```
      EXTERNAL BVPFD,CONST,FCNBC,FCNEQN,FCNJAC,SSET,UMACH
      COMMON FEEDFLOW,PERMFLOW,FEEDCOM1,PERMCOM1,FEEDPR,PERMPR,
     &  DLOGM
      COMMON DIAIN,DIAOUT,CONST1,CONST2,BETA,RLENGTH,FACTOR,R,TEMP,VIS
      COMMON A,B,DELL,PERMOIL1
      COMMON ALFA
C
C
      FEEDFLOW=1.0E4*200.0/(22400.0*300.0*60.0)
      PERMFLOW=0.0
      FEEDCOM1=11000.0*1.0E-6*1.0E4
      FEEDPR=77.0
      PERMPR=1.8
      PERMOIL1 =6.0E-9
      DLOGM=2.87E-2
      DIAIN=240.0E-4
      DIAOUT=290.0E-4
      A= 155.0E-10
      B=22.0
      R=8.314E7
      FACTOR=7.50E-5
      TEMP=298.0
      VIS=1800.0E-7
      ALFA=5.3E-9
      BETA=7.0E-11
      RLENGTH=20.0
      DELL=RLENGTH/9.0
      CONST1=DLOGM*3.14
      CONST2=(128.0*R*FACTOR**2*TEMP*VIS)/(3.14*DIAIN**4)
C     PERMCOMA=BETA*FEEDPR+(ALFA-BETA)*(FEEDPR*FEEDCOM1+PERMPR)
C     PERMCOMB=4.0*ALFA*FEEDPR*PERMPR*FEEDCOM1*(ALFA-BETA)
C     PERMCOMC=2.0*PERMPR*(ALFA-BETA)
C     PERMCOM1=(PERMCOMA-(PERMCOMA**2-PERMCOMB)**0.5)/PERMCOMC
C
C     --------------
C     SET PARAMETERS
C     --------------
C
      NLEFT=3
      NCUPBC=0
      TOL=0.1
      XLEFT=0.0
      XRIGHT=RLENGTH
      PISTEP=0.0
      PRINT= .FALSE.
      LINEAR= .FALSE.
C
C     ------------
C     DEFINE XINIT
C     ------------
C
      DO 70 I=1, NINIT
    XINIT(I)=XLEFT+(I-1)*(XRIGHT-XLEFT)/(FLOAT(NINIT-1))
 70   CONTINUE
```

```
C
C       ------------------------
C       GET YINIT FROM YINIT.FOR
C       ------------------------
C
        OPEN (2,FILE='YINIT.DAT',STATUS='OLD')
        DO 10 I=1,NINIT
        READ(2,*) YINIT(1,I),YINIT(2,I),YINIT(3,I),YINIT(4,I),
     &  YINIT(5,I)
        WRITE(*,*) XINIT(I),YINIT(1,I),YINIT(2,I),YINIT(3,I),
     &  YINIT(4,I),YINIT(5,I)
 10     CONTINUE
        CLOSE (2,STATUS='KEEP')
C
C       -------------
C       SOLVE PROBLEM
C       -------------
C
C       ALFA=OVPERM(Y(3),Y(4),Y(5))
C
        CALL BVPFD (FCNEQN,FCNJAC,FCNBC,FCNEQN,FCNBC,NEQNS,NLEFT,
     & NCUPBC,XLEFT,XRIGHT,PISTEP,TOL,NINIT,XINIT,YINIT,
     & LDYINI,LINEAR,PRINT,MXGRID,NFINAL,XFINAL,YFINAL,
     & LDYFIN,ERREST)
C
C       -------------
C       PRINT RESULTS
C       -------------
C
C
C       OPEN (2, FILE =
        DO 75 I=1,NFINAL

        WRITE (*,*) ((XFINAL(I),(YFINAL(J,I),J=1,NEQNS)))
 75     CONTINUE
C
        STOP
        END
C
C
C       ------------------------------------------------
C       SUBROUTINE
C       ------------------------------------------------
C       Y(1),Y(2),Y(3),Y(4) AND Y(5) ARE L,V,X,Y AND P
C       DYDX(1),DYDX(2),DYDX(3),DYDX(4) AND DYDX(5) ARE
C       dL/dl,dV/dl,dx/dL,dy/dl AND dP/dl
C       ------------------------------------------------
C
        SUBROUTINE FCNEQN (NEQNS,X,Y,P,DYDX)
        INTEGER NEQNS
        REAL X,Y(NEQNS),P,DYDX(NEQNS)
        COMMON FEEDFLOW,PERMFLOW,FEEDCOM1,PERMCOM1,FEEDPR,PERMPR,
     &  DLOGM
        COMMON DIAIN,DIAOUT,CONST1,CONST2,BETA,RLENGTH,FACTOR,R,TEMP,VIS
```

```
      COMMON A,B,DELL,PERMOIL1
      COMMON ALFA
C
C     ----------------------------
C     DEFINE DIFFERENTIAL EQUATIONS
C     ----------------------------
C
C
c     ALFA=OVPERM (Y(3),Y(4),Y(5))
      WRITE (*,*) ALFA
      Y1P1=CONST1*ALFA*(Y(5)*Y(3)-PERMPR*Y(4))
      Y1P2=CONST1*BETA*(Y(5)*(1.0E4-Y(3))-PERMPR*(1.0E4-Y(4)))
      DYDX(1)=Y1P1+Y1P2
      DYDX(2)=DYDX(1)
      Y3P1= CONST1*ALFA*(Y(5)*Y(3)-PERMPR*Y(4))*(1.0E4-Y(3))
      Y3P2= CONST1*BETA*Y(3)*(Y(5)*(1.0E4-Y(3))-PERMPR*(1.0E4-Y(4)))
      DYDX(3)=(Y3P1-Y3P2)/Y(1)
      DYDX(5)=(CONST2/1.0E4)*(Y(1)/Y(5))
      IF (Y(2).EQ.0.0) THEN
      Y40P1=CONST1*ALFA*(DYDX(5)*Y(3)+Y(5)*DYDX(3))*(1.0E4-Y(4))
C     Y40P2=CONST1*ALFA*(1.0-Y(4))*(Y(5)*Y(3)-PERMPR*Y(4))
C     Y40P3=CONST1*BETA*Y(4)*(Y(5)*(1.0-Y(3))-PERMPR*(1.0-Y(4)))
      Y40P4=CONST1*BETA*Y(4)*(DYDX(5)*(1.0E4-Y(3))-Y(5)*DYDX(3))
      Y40PD=Y40P1-Y40P4
      Y40P5=CONST1*ALFA*(Y(5)*Y(3)-PERMPR*Y(4))
      Y40P6=CONST1*ALFA*PERMPR*(1.0E4-Y(4))
      Y40P7=CONST1*BETA*(Y(5)*(1.0E4-Y(3))-PERMPR*(1.0E4-Y(4)))
      Y40P8=CONST1*BETA*Y(4)*PERMPR
      Y40PE=DYDX(2)+Y40P5+Y40P6+Y40P7+Y40P8
      DYDX(4)=Y40PD/Y40PE
      ELSE
      Y4P1= CONST1*ALFA*(Y(5)*Y(3)-PERMPR*Y(4))*(1.0E4-Y(4))
      Y4P2= CONST1*BETA*Y(4)*(Y(5)*(1.0E4-Y(3))-PERMPR*(1.0E4-Y(4)))
      DYDX(4)= (Y4P1-Y4P2)/Y(2)
      ENDIF
      RETURN
      END
C
C     --------------------------------
C     SUBROUTINE TO EVALUATE JACOBIAN
C     --------------------------------
C
      SUBROUTINE FCNJAC (NEQNS,X,Y,P,DYPDY)
      INTEGER NEQNS
      REAL X,Y(NEQNS),P,DYPDY(NEQNS,NEQNS),YPRIME(5)
      COMMON FEEDFLOW,PERMFLOW,FEEDCOM1,PERMCOM1,FEEDPR,PERMPR,
     &  DLOGM
      COMMON DIAIN,DIAOUT,CONST1,CONST2,BETA,RLENGTH,FACTOR,R,
     & TEMP,VIS

      COMMON A,B,DELL,PERMOIL1
      COMMON ALFA
c     COMMON R3,R4,R5
C
```

```
c       ALFA=OVPERM(Y(3),Y(4),Y(5))

C       --------------------
C       EVALUATE DERIVATIVES
C       --------------------
C
        DO 100 I=1,NEQNS
        K=I
        YPRIME(I)=FUNC(NEQNS,X,Y,K)
 100    CONTINUE
C
C       ----------------------------------------
C       ESTIMATE PARTIAL DERIVATIVES NUMERICALLY
C       ----------------------------------------
        DELTA=1.0E-1
        DO 30 J=1,NEQNS
C       DELTA=Y(J)*1.0E-2
C       IF (DELTA.EQ.0.0) THEN DELTA=1.0E-7
        Y(J)=Y(J)+DELTA
        DO 20 I=1,NEQNS
        K=I
        DYPDY(I,J)=(FUNC(NEQNS,X,Y,K)-YPRIME(I))/DELTA
 20     CONTINUE
        Y(J)=Y(J)-DELTA
 30     CONTINUE
        RETURN
        END
C
C       -------------------------------------
C       FUNCTION TO CALCULATE JACOBIAN VALUES
C       -------------------------------------
C
        FUNCTION FUNC(NEQNS,X,Y,I)
        REAL Y(NEQNS)
        COMMON
        FEEDFLOW,PERMFLOW,FEEDCOM1,PERMCOM1,FEEDPR,PERMPR,
   &    DLOGM
        COMMON DIAIN,DIAOUT,CONST1,CONST2,BETA,RLENGTH,FACTOR,R,
   &    TEMP,VIS
        COMMON A,B,DELL,PERMOIL1
        COMMON ALFA
c       COMMON R3,R4,R5
c       ALFA=OVPERM (Y(3),Y(4),Y(5))
c       WRITE (*,*)'ALFA IN FUNC', ALFA
        GO TO (1,2,3,4,5),I
   1    Y1P1=CONST1*ALFA*(Y(5)*Y(3)-PERMPR*Y(4))
        Y1P2=CONST1*BETA*(Y(5)*(1.0E4-Y(3))-PERMPR*(1.0E4-Y(4)))
        FUNC=Y1P1+Y1P2
        RETURN
   2    Y2P1=CONST1*ALFA*(Y(5)*Y(3)-PERMPR*Y(4))
        Y2P2=CONST1*BETA*(Y(5)*(1.0E4-Y(3))-PERMPR*(1.0E4-Y(4)))
        FUNC=Y2P1+Y2P2
        RETURN
   3    Y3P1= CONST1*ALFA*(Y(5)*Y(3)-PERMPR*Y(4))*(1.0E4-Y(3))
```

```
      Y3P2= CONST1*BETA*Y(3)*(Y(5)*(1.0E4-Y(3))-PERMPR*(1.0E4-Y(4)))
      FUNC=(Y3P1-Y3P2)/Y(1)
      RETURN
    4 IF (Y(2).EQ.0.0)THEN
      Y3P1= CONST1*ALFA*(Y(5)*Y(3)-PERMPR*Y(4))*(1.0E4-Y(3))
      Y3P2= CONST1*BETA*Y(3)*(Y(5)*(1.0E4-Y(3))-PERMPR*(1.0E4-Y(4)))
      YPRIME5=CONST2*(Y(1)/Y(5))
      YPRIME3=(Y3P1-Y3P2)/Y(1)
      Y40P1=CONST1*ALFA*(YPRIME5*Y(3)+Y(5)*YPRIME3)*(1.0E4-Y(4))
C     Y40P2=CONST1*ALFA*(1.0E4-Y(4))*(Y(5)*Y(3)-PERMPR*Y(4))
C     Y40P3=CONST1*BETA*Y(4)*(Y(5)*(1.0E4-Y(3))-PERMPR*(1.0E4-Y(4)))
      Y40P4=CONST1*BETA*Y(4)*(YPRIME5*(1.0E4-Y(3))-Y(5)*YPRIME3)
      Y40PD=Y40P1-Y40P4
      Y40P5=CONST1*ALFA*(Y(5)*Y(3)-PERMPR*Y(4))
      Y40P6=CONST1*ALFA*PERMPR*(1.0E4-Y(4))
      Y40P7=CONST1*BETA*(Y(5)*(1.0E4-Y(3))-PERMPR*(1.0E4-Y(4)))
      Y40P8=CONST1*BETA*Y(4)*PERMPR
      Y2P1=CONST1*ALFA*(Y(5)*Y(3)-PERMPR*Y(4))
      Y2P2=CONST1*BETA*(Y(5)*(1.0E4-Y(3))-PERMPR*(1.0E4-Y(4)))
      YPRIME2=Y2P1+Y2P2
      Y40PE=YPRIME2+Y40P5+Y40P6+Y40P7+Y40P8
      FUNC=Y40PD/Y40PE
      ELSE
      Y4P1= CONST1*ALFA*(Y(5)*Y(3)-PERMPR*Y(4))*(1.0E4-Y(4))
      Y4P2= CONST1*BETA*Y(4)*(Y(5)*(1.0E4-Y(3))-PERMPR*(1.0E4-Y(4)))
      FUNC=(Y4P1-Y4P2)/Y(2)
      ENDIF
      RETURN
    5 FUNC=(CONST2/1.0E4)*(Y(1)/Y(5))
      RETURN
      END
C
C     ------------------------------------
C     SUBROUTINE TO SET BOUNDARY CONDITIONS
C     ------------------------------------
C
      SUBROUTINE FCNBC(NEQNS,YLEFT,YRIGHT,P,F)
      INTEGER NEQNS
      REAL YLEFT(NEQNS),YRIGHT(NEQNS),P,F(NEQNS)
      COMMON  FEEDFLOW,PERMFLOW,FEEDCOM1,PERMCOM1,FEEDPR,PERMPR,
      DLOGM
      COMMON DI,DO,CONST1,CONST2,BETA,RLENGTH,FACTOR,R,TEMP,VIS
      COMMON A,B,DELL,PERMOIL1
      COMMON ALFA
C     COMMON R3,R4,R5
C
C     -------------------------
C     DEFINE BOUNDARY CONDITIONS
C     -------------------------
C
c     ALFA=OVPERM (YLEFT(3),YLEFT(4),YLEFT(5))
c     WRITE (*,*)'ALFA IN FUNBC', ALFA
      F(1)=YLEFT(2)-0.0
      PARTA=1.0E4*BETA*YLEFT(5)+(ALFA-BETA)*(YLEFT(5)*YLEFT(3)
```

```
     &    +PERMPR*1.0E4)
          PARTB=4.0*ALFA*YLEFT(5)*PERMPR*YLEFT(3)*(ALFA-BETA)*1.0E4
          PARTC=2.0*PERMPR*(ALFA-BETA)
          ZZZ=(PARTA-(PARTA**2-PARTB)**0.5)/PARTC
          F(2)=YLEFT(4)-ZZZ
          F(3)=YLEFT(5)-FEEDPR
C
C         ------------------------------------------
C         BOUNDARY CONDITIONS FOR L AND X AT l=RLENGTH
C         ------------------------------------------
C
          F(4)=YRIGHT(1)-FEEDFLOW
          F(5)=YRIGHT(3)-FEEDCOM1
          RETURN
          END
C
C         ---------------------------------
C         FUNCTION TO CALCULATE ALFAOVERALL
C         ---------------------------------
C
c         FUNCTION OVPERM(Y3,Y4,Y5)
C
C         -----------------------------------
C         CALLING OF NEQNF TO CALCULATE FLUX1
C         -----------------------------------
C
c         INTEGER ITMAX,N
c         PARAMETER (N=1)
c         REAL ERRREL,FCN,FNORM, Z(N),ZGUESS(N)
c         EXTERNAL FCN,NEQNF
c         COMMON FEEDFLOW,PERMFLOW,FEEDCOM1,PERMCOM1,FEEDPR,PERMPR,DLOGM
c         COMMON DIAIN,DIAOUT,CONST1,CONST2,BETA,RLENGTH,FACTOR,R,TEMP,VIS
c         COMMON A,B,DELL,PERMOIL1
C         COMMON Y3,Y4,Y5
c         COMMON R3,R4,R5
C         SAVE ZGUES,JFLAG
C
c         ERRREL = 0.0001
c         ITMAX =100
C         R3=65.13
C         R4=1941.0
C         R5=75.6
C         R3=Y3
C         R4=Y4
C         R5=Y5
c         WRITE (*,*)'Y3,Y4,Y5 IN OVPERM FUNCTION', Y3,Y4,Y5
C
c         DATA ZGUESS /1.0E-9/
C
c         CALL NEQNF (FCN,ERRREL,N,ITMAX,ZGUESS,Z,FNORM)
C
c         WRITE (*,*)'Z1 IN OVPERM',  Z(1)
c         FLUX1=Z(1)
C
```

```
C       --------------
C       CALCULATE P'X'
C       --------------
C
c       PXPRIME=(Y5*Y3)-FLUX1/(3.14*DLOGM*DELL*PERMOIL1)
c       WRITE(6,*)'PXPRIME', PXPRIME
C
C       ----------------------------------------
C       CALCULATE VOC PERMEANCE THROUGH THE SKIN
C       ----------------------------------------
C
C       WRITE (*,*)'A,B', A,B
c       PERMSKIN1=(A*EXP(B/1.0E4*PXPRIME))
C       WRITE (*,*)'PERMSKIN1', PERMSKIN1
C       WRITE (*,*)'PERMOIL1, DO, DLOGM', PERMOIL1, DO, DLOGM
c       OVPERM = 1/(1/(PERMSKIN1*DIAOUT/DLOGM)+1/PERMOIL1)
c       WRITE (6,*)'FINAL PXP,PSK,OVPERM ', PXPRIME,PERMSKIN1,OVPERM
c       RETURN
c       END
C
C       --------------
C       SUBROUTINE FCN
C       --------------
C
c       SUBROUTINE FCN (Z,F,N)
c       INTEGER N
c       REAL Z(N), F(N)
c       REAL PART1,PART2,PART3,PART4,PART5,PART6
c       REAL EXP
c       INTRINSIC EXP
c       COMMON FEEDFLOW,PERMFLOW,FEEDCOM1,PERMCOM1,FEEDPR,PERMPR,DLOGM
c       COMMON DIAIN,DIAOUT,CONST1,CONST2,BETA,RLENGTH,FACTOR,R,TEMP,VIS
c       COMMON A,B,DELL,PERMOIL1
C       COMMON R3,R4,R5
c       COMMON  Y3,Y4,Y5
C
c       PART1 = 1.0/PERMOIL1
c       PART2=Z(1)/(3.14*DLOGM*DELL*PERMOIL1)
c       PART3=(Y5*Y3)-PART2
c       PART4=(A*EXP((B/1.0E4*PART3)*(DIAOUT/DLOGM)))
c       PART5=1.0/PART4
c       PART6=3.14*DLOGM*DELL*((Y5*Y3)-PERMPR*Y4)
C
c       F(1)=Z(1)*(PART1+PART5)-PART6
c       RETURN
c       END
```

REFERENCES

Beaver, E.R., P.V. Bhat and D.S. Sarcia, Integration of Membranes with Other Air Separation Technologies, *AIChE Symp.Ser.* 84 (1988) 118.

Bhave R.R. and K.K. Sirkar, Gas permeation and separation by aqueous membranes immobilized across the whole thickness or in a thin section of the hydrophobic microporous Celgard films, *J. Membrane Sci.*, 27 (1986) 41.

Bhaumik D., S. Majumdar and K. K. Sirkar, Pilot-plant and laboratory studies on vapor permeation removal of VOCs from waste gas using silicone-coated hollow fibers, *J. Membr. Sci.*, 167 (2000) 107-122.

Bhaumik, S., S. Majumdar, and K.K. Sirkar, Hollow-Fiber Membrane Based Rapid Pressure Swing Absorption, *AIChEJ.*, 42 (1996) 409.

Cha J. S., R. Li and K.K. Sirkar, Removal of water vapor and VOCs from nitrogen in a hydrophilic hollow fiber gel membrane permeator, *J. Membr. Sci.*, 119 (1996) 139-153.

Cha J. S., V. Malik, D. Bhaumik, R. Li and K.K. Sirkar, Removal of VOCs from waste gas streams by permeation in a hollow fiber permeator, *J. Membr. Sci.*, 128 (1997) 195-211.

Chen H., G. Obuskovic, S. Majumdar and K.K. Sirkar, Immobilized glycerol-based liquid membranes in hollow fibers for selective CO_2 separation from CO_2-N_2 mixtures, *J. Membr. Sci.*, 183 (2001) 75-88.

Chen H., A.S. Kovvali and K.K. Sirkar, Selective CO_2 separation form CO_2-N_2 mixtures by immobilized glycine-Na-glycerol membranes, *Ind. Eng. Chem. Res.*, 39 (2000) 2447.

Chen H., A.S. Kovvali, S. Majumdar and K.K. Sirkar, Selective CO_2 separation from CO_2-N_2 mixtures by immobilized carbonate-glycerol membranes, *Ins. Eng. Chem. Res.*, 38 (1999) 3489-3498.

Danckwerts, P.V., *Gas Liquid Reactions*, McGraw-Hill:New York, (1970).

Fouda A., J. Bai, S.Q. Zhang, O. Kutowy and T. Matsuura, Membrane separation of low volatile organic compounds by pervaporation and vapor permeation, *Desalination*, 90 (1993) 209-233.

Gales L., A. Mendes and C. Costa, Removal of acetone, ethyl acetate and ethanol vapors from air using a hollow fiber PDMS membrane module, *J. Membr. Sci.*, 197 (2002) 211-222.

Gilleskie, G.L., Parker, J.L. and Cussler, E.L. Gas separations in hollow-fiber adsorbers. *AIChEJ.* 41 (1995) 1413.

Guha A.K., S. Majumdar and K.K. Sirkar, Facilitated transport of CO_2 through an immobilized liquid membrane of aqueous diethanolamine, *Ind. Eng. Chem. Res.*, 29 (1990) 2093.

Guha A.K., Studies on different gas separation modes with the hollow fiber contained liquid membrane, Ph.D. Dissertation, Stevens Institute of Technology, Hoboken, NJ, 1989.

Henis J. M. S. and Tripodi M. K., Composite hollow fiber membranes for gas separation: the resistance model approach, *J. Membr. Sci.*, 8 (1981) 233-246.

Henis J.M. and M.K. Tripodi, Multicomponent membranes for gas separation, US Pat., 4,230,463, 28 October 1980.

Ho W. S. W. and K.K. Sirkar, *Membrane Handbook*, Van Nostrand Reinhold: New York (1992).

Kammermeyer K., Separation of gases by diffusion through silicone rubber, US Pat., 2,966,235, 27 December 1960.

Karoor, S. and K. K. Sirkar, Gas absorption studies in microporous hollow fiber membrane modules, *Ind. Eng. Chem. Res.*, 32 (1993) 674.

Kim J.H., S.Y. Ha, S.Y. Nam, J.W. Rhim, K.H. Baek and Y.M. Lee, Selective permeation of CO2 through pore-filled polyacrylonitrile membrane with poly(ethylene glycol), *J. Membr. Sci.*, 186 (2001) 97-107.

Kimmerle K., C. M. Bell, W. Gudernatsch and H. Chmiel, Solvent recovery from air, *J. Membr. Sci.*, 36 (1988) 477-488.

Khan F.I. and A.K. Ghoshal, Removal of volatile organic compounds from polluted air, *J. Membr. Sci.*, 13 (2000) 527-545.

Klass D.L., and C.D. Landahl, Separation of nitrogen ad methane containing gas mixture, US Pat., 3,616,607, 2 November 1971.

Klug A., P.H. Pfromm, M.E. Rezac and P. Czermak, Selective removal of methanol from humid air streams using a water-vapor-purged membrane separator, *Ins. Eng. Chem. Res.*, 40 (2001) 2685-2692.

Kovvali A.S. and K.K. Sirkar, Carbon dioxide separation with novel solvents as liquid membranes, *Ins. Eng. Chem. Res.*, 41 (2002) 2287-2295.

Kovvali A.S., H. Chen and K.K. Sirkar, Dendrimer membranes: a CO2-selective molecular gate, *J. Am. Chem. Soc.*, 122 (2000) 7594-7595.

Kovvali A.S., Immobilized liquid membranes for facilitated transport and gas separation, Ph.D. Dissertation, New Jersey Institute of Technology, Newark, NJ, 2000.

Langmuir I.S., R.E. Foster and C.Y. Woo., Diffusion of carbon dioxide through thin layers of solution, *Nature*, 209 (1966) 393.

Leemann M., G. Eigenberger and H. Stratmann, Vapor permeation for the recovery of organic solvents from waste air streams: separation capacities and process optimization, *J. Membr. Sci.*, 113 (1996) 313-322.

Loeb S. and S. Surirajan, High flow porous membrane for separating water from saline solutions, US Pat., 3,133,132, 12 May 1964.

Majumdar S., D. Bhaumik, K.K. Sirkar and G. Simes, A pilot-scale demonstration of a membrane-based absorption-stripping process for removal and recovery of volatile organic compounds, *Environmental Progress*, 20 (2001) 27-35.

Majumdar S., A.K. Guha and K.K. Sirkar, A new liquid membrane technique for gas separation, *AIChE J.*, 34 (1988) 1135.

Majumdar S., A new liquid membrane technique for gas separation, Ph.D. Dissertation, Stevens Institute of Technology, Hoboken, NJ, 1986.

Matsuyama H., and M. Teramoto, Facilitated Transport of Carbon Dioxide Through Functional Membranes Prepared by Plasma Graft Polymerization Using Amines as Carrier, Chemical Separations in the Liquid Membranes, R.A. Bartsch and J.D. Way (Eds.), ACS Symposium Series 642, ACS, Washington, DC (1996).

Matsuyama H., M. Teramoto, K. Iwai, Development of new functional cation-exchange membrane and its application to facilitated transport of CO_2, *J. Membr. Sci.*, 93 (1994) 237.

Meldon J.H., P. Stroeve and C.E. Gregorie, Facilitated transport of carbon dioxide: a review, *Chem. Eng. Commun.*, 16 (1982) 263.

Meldon J.H., A. Paboojian and G. Rajangam, Selective CO2 permeation in immobilized liquid membranes, *AIChE. Symp. Ser.*, 248 (1986) 114.

Noble R.D., C.A. Koval and J.J. Pellegrino, Facilitated transport membrane systems, *Chemical Engineering Progress*, (1989) 58-70.

Obuskovic G., T.K. Poddar and K.K. Sirkar, Flow swing membrane-absorption permeation, *Ind. Eng. Chem. Res.*, 37 (1998) 212.

Obuskovic G., Removal of VOCs from waste gas streams by cyclic membrane separation techniques, M.S. Thesis, Department of Chemical Engineering, New Jersey Institute of Technology, Newark, NJ, 1996.

Otto N.C. and J. A. Quinn, The facilitated transport of carbon dioxide through bicarbonate solution, *Chem. Engng. Sci.*, 26 (1971) 949-961.

Paul H., C. Philipsen, F. J. Gerner and H. Strathmann, Removal of organic vapors from air by selective membrane permeation, *J. Membr. Sci.*, 36 (1988) 363-372.

Paul, D.R. Membrane Separation of Gases Using Steady Cyclic Operation. *I&E.C. Proc. Des .Dev.*, 10 (1971) 375.

Perry, R.H., *Chemical Engineer's Handbook*, 6th Ed. McGraw-Hill:New York, 12 (1984) 7.

Poddar T.K., and K.K. Sirkar, Henry's law constant for selected volatile organic compounds in high-boiling oils, *Journal of Chemical and Engineering Data*, 41 n 6 (1996) ACS Washington DC USA 1329-1332.

Poddar T.K., S. Majumdar and K.K. Sirkar, Membrane-Based Absorption of VOCs from a Gas Stream, *AIChEJ.*, 42, (1996a) 3267.

Poddar T.K., S. Majumdar and K.K. Sirkar, Removal of VOCs from air by membrane-based absorption and stripping, *J. Membr. Sci.*, 120 (1996b) 221-237.

Poddar T.K., Removal of VOCs from air by absorption and stripping in hollow fiber devices, Ph.D. Dissertation, New Jersey Institute of Technology, Newark, NJ, 1995.

Qi Z. and E. L. Cussler, Microporous hollow fibers for gas absorption. I. mass transfer in the Liquid, *J. Mem. Sci.*, 23 (1985) 321.

Qi Z. and E. L. Cussler, Microporous hollow fibers for gas absorption. II. mass transfer across the membrane, *J. Mem. Sci.*, 23 (1985) 333.

Quinn R., J. B. Appleby and G. P. Pez, New facilitated transport membranes for the separation of carbon dioxide from hydrogen and methane, *J. Membr. Sci.*, 104 (1995) 139.

Huseni A. Rangwala, Absorption of carbon dioxide into aqueous solutions using hollow fiber membrane contactors, *J. Membr. Sci.*, 112 (1996) 229.

Robb W.L, Thin substantially defect-free organo-polysiloxane films and preparation thereof, US Pat., 3,325,330, 13 June 1967.

Saha S. and A. Chakma, Selective CO_2 separation from CO_2/C_2H_6 mixtures by immobilized diethanolamine/PEG membranes, *J. Membr. Sci.*, 98 (1995) 157-171.

Scholander P.F., Oxygen transport through hemoglobin solution, *Science*, 131 (1960) 585-590.

Sengupta, A., and K.K. Sirkar. 1986. Membrane Gas Separation. In *Progress in Filtration and Separation*, ed. Richard. J Wakerman, 289-415, Amsterdam; Elsevier Scientific Publishing Co.

Simmons V.L., Baker R.W., Kaschemekat J. and Wijmans J.G., Membrane systems for VOC recovery from air streams, *Filtration & Separation*, 31 (1994) 231-235.

Sohn W.I., D. H. Ryu, S. J. Oh and J. K. Koo, A study on the development of composite membranes for the separation of organic vapors, *J. Membr. Sci.*, 175 (2000) 163-170.

Teramoto, M., Nakai K., Ohnishi N., Huang Q., Watari T., Matsuyama H., Facilitated transport of carbon dioxide through supported liquid membrane of aqueous amine solutions, *Ind. Eng. Chem. Res.*, 45 (1996) 538.

Xia, B., S. Majumdar and K.K. Sirkar, Regenerative oil scrubbing of volatile organic compounds from a gas stream in hollow fiber membrane devices, *Ind. Eng. Chem. Res.*, 38 (1999) 3462-3472.

Yamamoto M., M. Hirai and J. Sakata, Gas separating members and a method of making the same, US Pat., 4,410,338, 18 October 1983.

Yasuda H., Method of preparation of composite semipermeable membrane, US Pat., 3,775,308, 27 November 1973.

Ward W.J. and W.L. Robb, Carbon dioxide-oxygen separation: facilitated transport of carbon dioxide across a liquid film, *Science*, 156 (1967) 1481.

Watson. J.M. and M.G. Baron, The behavior of water in poly(dimethylsiloxane), *J. Membr. Sci.*, 110 (1996) 47-57.